4.23 Tracer Test 3 (9/5/76)

The purpose of the third tracer test was to characterize the transport and dispersion associated with the Nighttime meteorological period. SF_6 was released from the Dow site at a steady rate of 9.5 g/sec (0.90 ton/day) from midnight to 0500 PDT.

Average winds at the Dow site and throughout the area were 280^o at 9.3 m/sec and 290^o at 3.3 m/sec, respectively. The average standard deviation of the wind at Dow was 7^o. There were scattered clouds, and stability conditions were considered to be Pasquill classes D-F. This predicted range of stability classes results from the wide range of wind speeds observed in the area. The average mixing height during the test was 860 meters with a maximum of 1300 meters observed near the end of the tracer release. The wind pattern given in Figure 22 agrees with the results of the tracer data. Later patterns showed the sea flow meeting the mountain drainage winds between Lodi and Stockton. Under those conditions, one layer, presumably the sea flow, is pushed aloft by the opposite flow field. However, as will be apparent, the tracer trajectory throughout the night followed the streamlines drawn from 0100 PDT wind data.

Fourteen automobile traverses were conducted from 0100 to 0511 PDT. These traverses indicated that the plume crossed Highway 160 6.9 km north of the Highway 160-Highway 4 junction with an average peak concentration of 4992 ppt. The maximum level observed in these traverses was 8660 ppt. Typical crosswind SF_6 profiles are shown in Figures 23 and 24. Traverses along Highway 99 indicated the tracer trajectory passed through Stockton

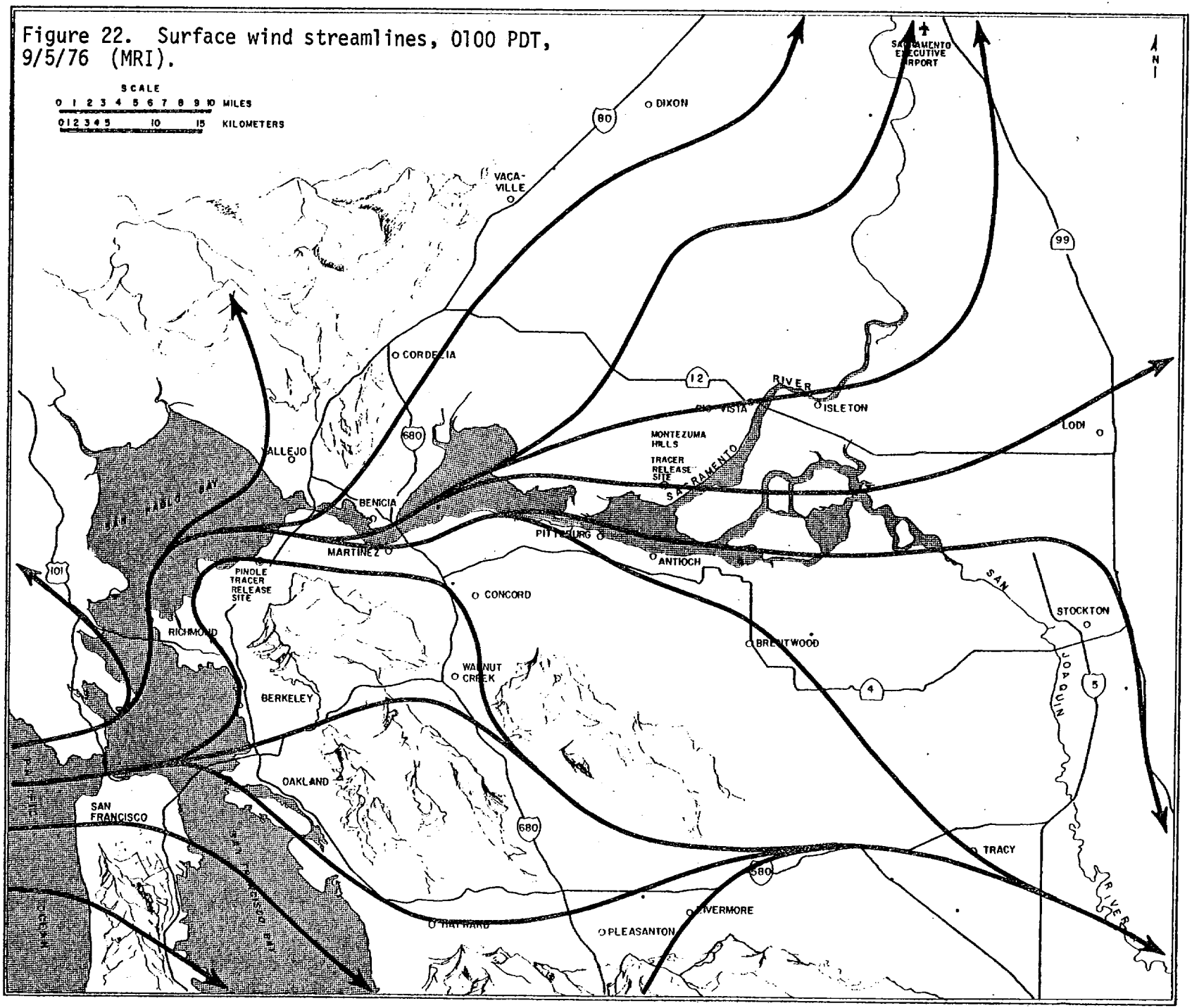

Figure 22. Surface wind streamlines, 0100 PDT, 9/5/76 (MRI).

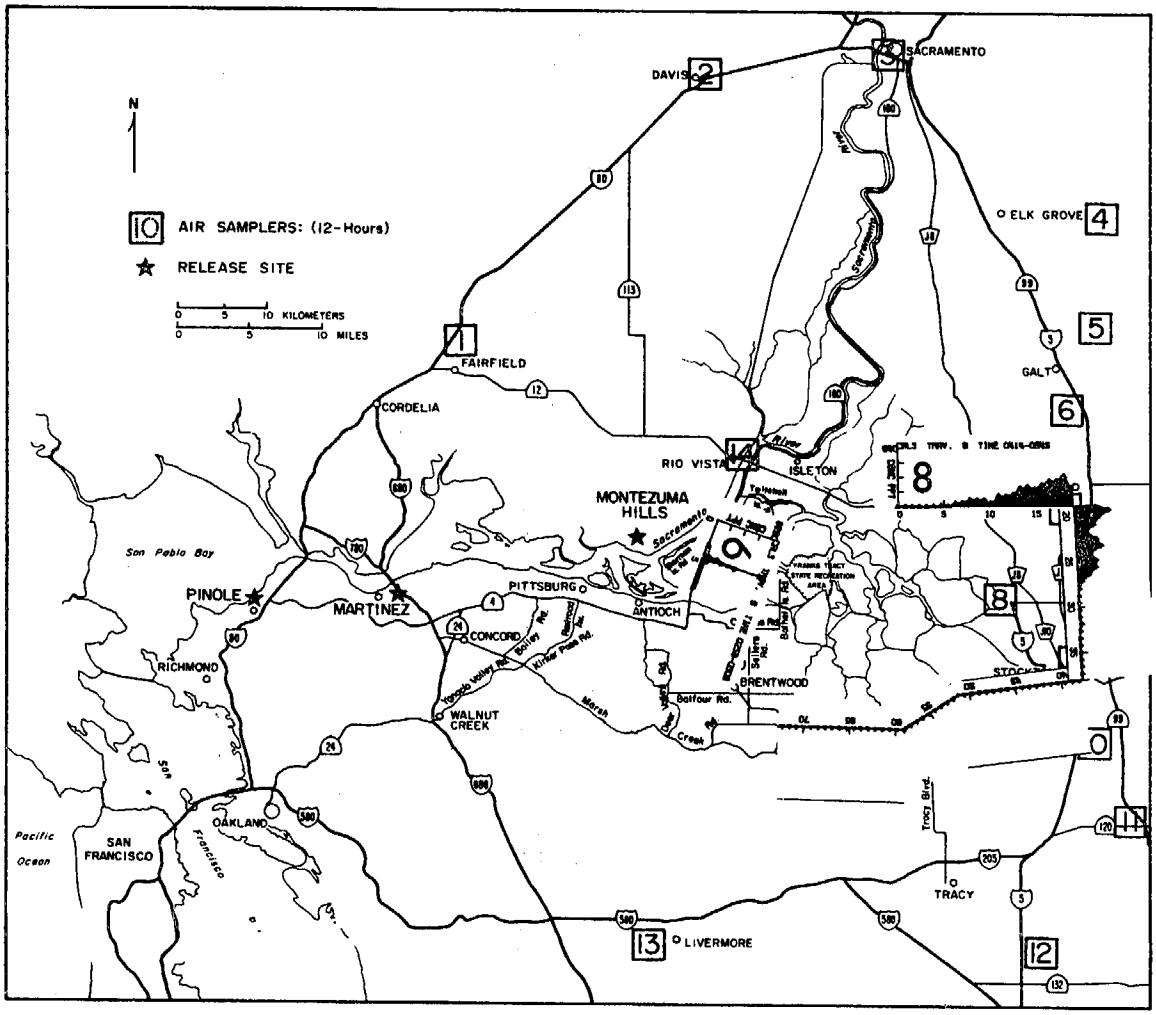

Figure 24. Overview of automobile traverse SF_6 data.

TEST 3

9/5/76

Auto Traverses:

6 0259 - 0306 PDT, SF_6(max) = 8660 ppt

8 0414 - 0545 PDT, SF_6(max) = 370 ppt

SF_6 released from the Montezuma Hills from 0000-0500 PDT.

around 0200 PDT, but shifted north to Lodi by 0400 PDT. These data yield a transport speed of 7 m/sec (25 km/hr). Maximum levels measured in Stockton and near Lodi were 537 ppt and 608 ppt, respectively. During the daytime in Test 1, the plume widths along Highway 99 were 40 km; at night during Test 3, the plume widths along the same route were only 20 km.

The maximum SF_6 concentration observed in the hourly averaged air samples was 918 ppt, which occurred from 0600 to 0700 PDT at Station 8, 6 km north of Stockton. The data in the overview map in Figure 25 suggest that the wind shifted twice during the night. The plume impacted in the Stockton area from 0200 to 0400; it moved north towards Lodi from 0400 to 0600 PDT, and then shifted back towards Stockton and further south for the remaining hours. This shift in winds is more clearly seen in Figures 26-28 where the hourly crosswind tracer profiles are shown. Concentrations as high as 22 ppt were observed in Manteca as late as 1200 PDT.

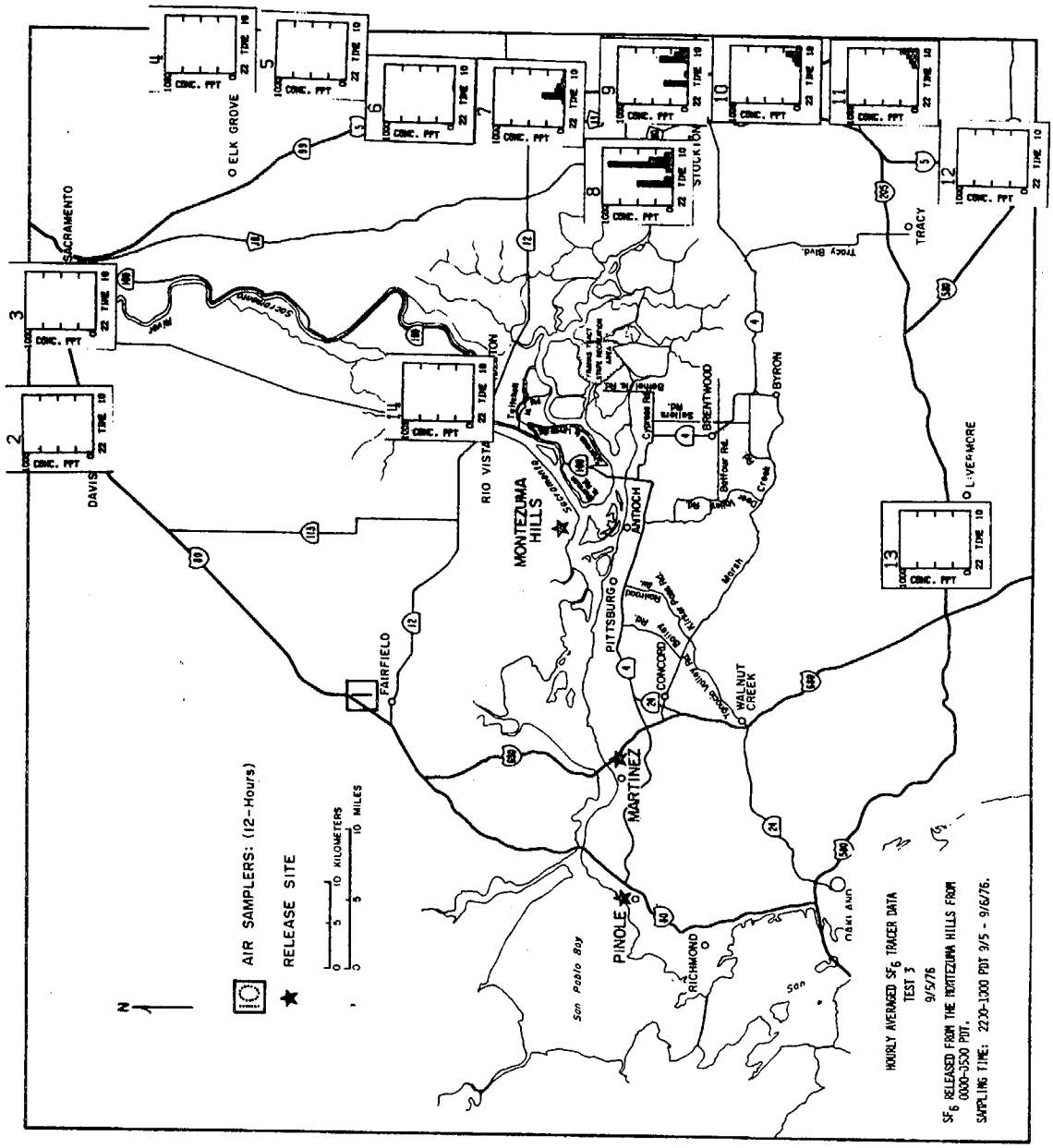

Figure 25. Overview of hourly averaged SF_6 data. Full scale SF_6 = 1000 ppt.

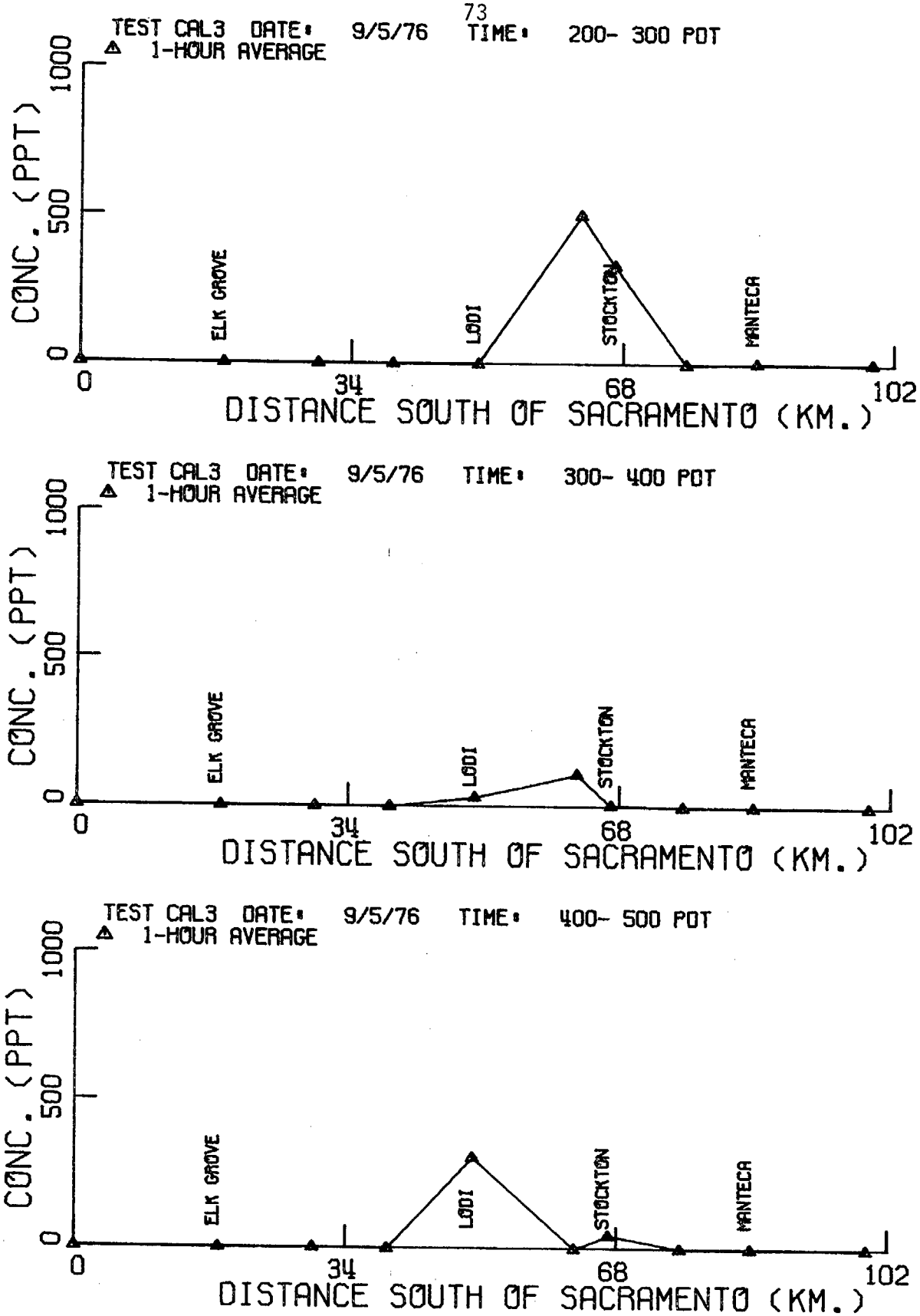

Figure 26. Hourly averaged crosswind. SF_6 profiles measured along Highway 99.

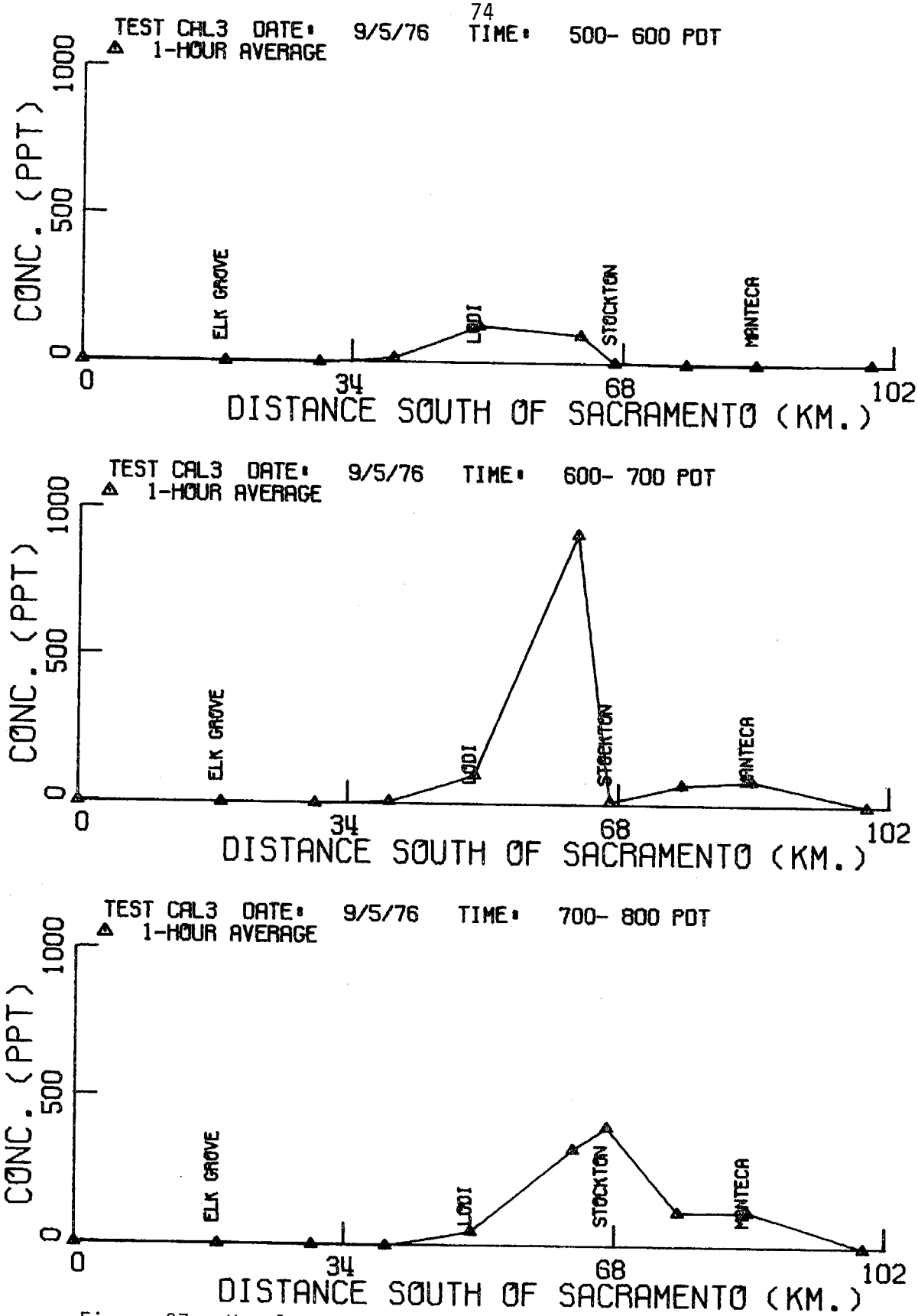

Figure 27. Hourly averaged crosswind SF_6 profiles measured along Highway 99.

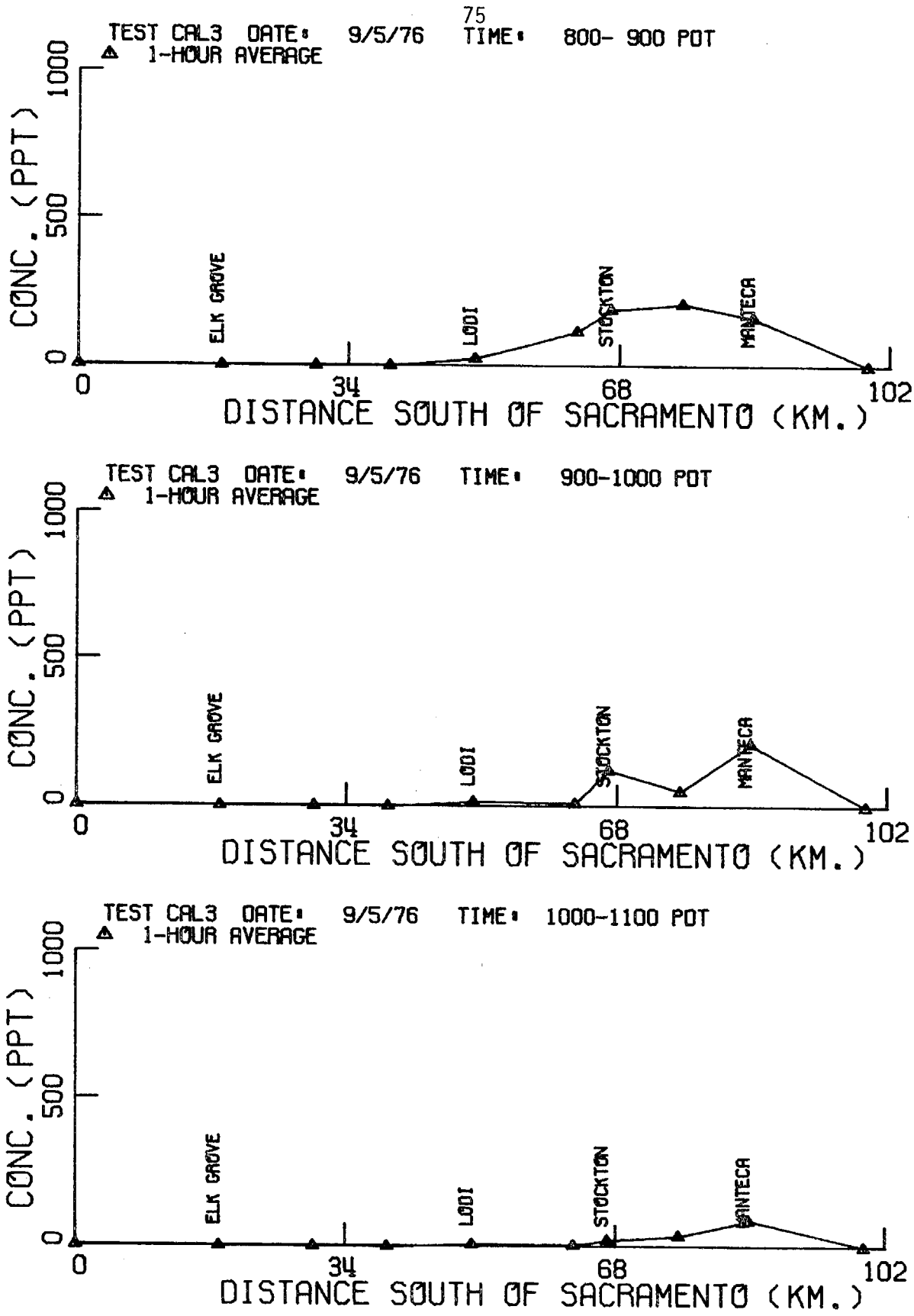

Figure 28. Hourly averaged crosswind SF_6 profiles measured along Highway 99.

4.24 Tracer Test 4 (9/6/76)

The purpose of Test 4 was to determine the characteristics of the transport and dispersion of pollutants emitted from the Montezuma Hills under the Sea Breeze Tail meteorological condition. SF_6 was released at a constant rate of 10.8 g/sec (1.02 tons/day) from 1800 to 2300 PDT.

The average wind vector at the Dow site during the release was 280° at 7.1 m/sec; the overall area average was 290° at 3.3 m/sec. The average value of σ_{θ} at the Dow site during the test was 7°. The cloud cover was broken, with Pasquill classes D-F assumed to exist. The average mixing height during the release was 510 meters with a maximum height of 650 meters measured at 1800 PDT. This was somewhat lower than that observed during the nighttime test. The wind field during the night generally consisted of westerly flow past the Montezuma Hills as shown in Figure 29. However, the tracer data indicate that the streamline over the Dow site curved to the south throughout the night. Ozone concentrations in the area during the day of the test were about .08 ppm.

Three automobile traverses were conducted along Highway 160 from 1928 through 2222 PDT, and four traverses were completed along Highway 99 between 2130 and 2400 PDT. The data obtained along Highway 160, shown in Figure 30, indicated that the plume from the Montezuma Hills, although narrow with high concentrations, appeared to behave similarly to those in previous tests. The maximum concentration observed along HIghway 160 was 11,900 ppt in Traverse 5 shown in Figure 31. The traverses crossed Highway 160 5.7 km north of the Highway 160-Highway 4 junction. The data measured along Highway 99 again showed that emissions from the Dow site curved south on a trajectory through Stockton. The maximum

Figure 29. Surface wind streamlines, 1900 PDT, 9/6/76 (MRI).

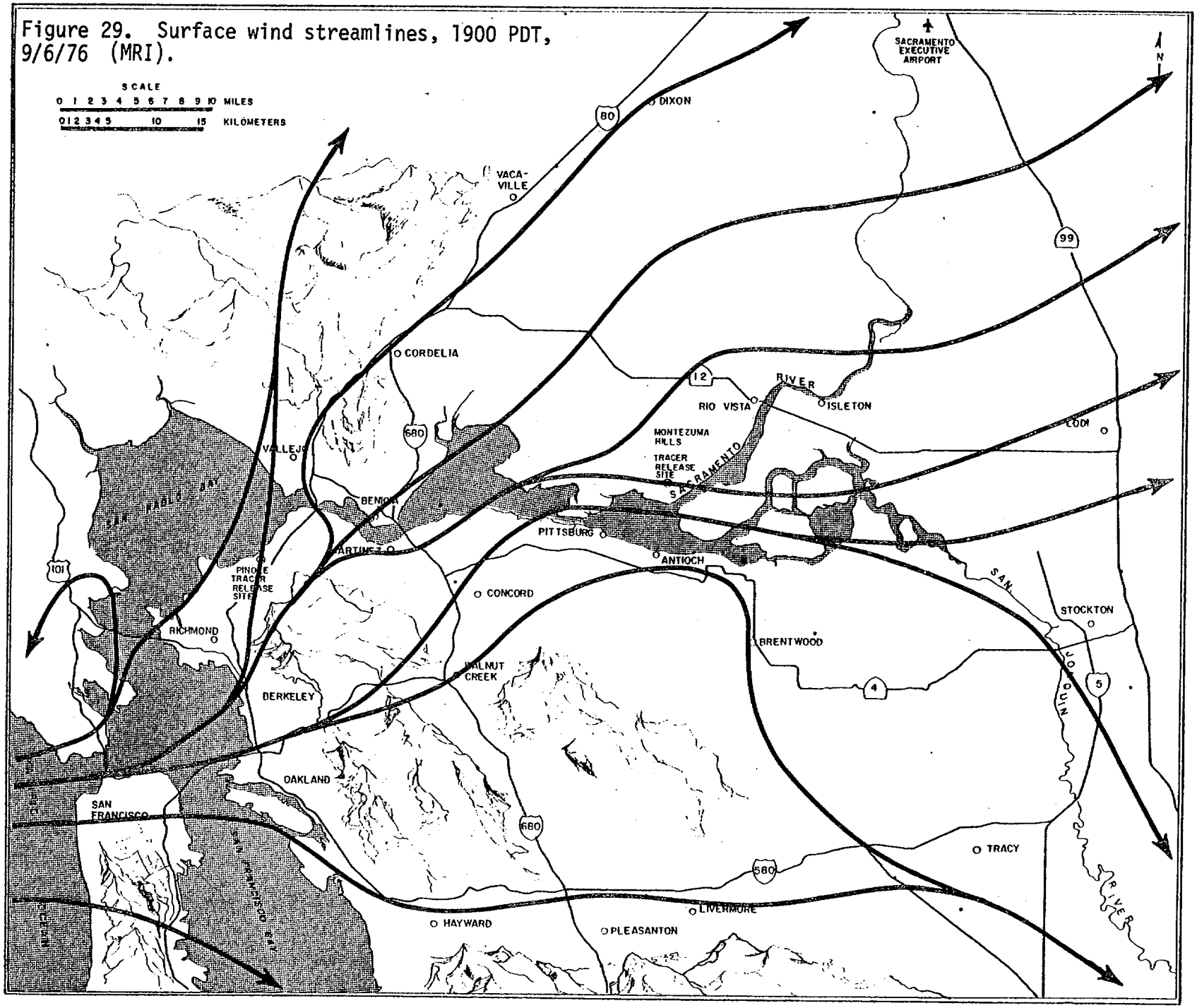

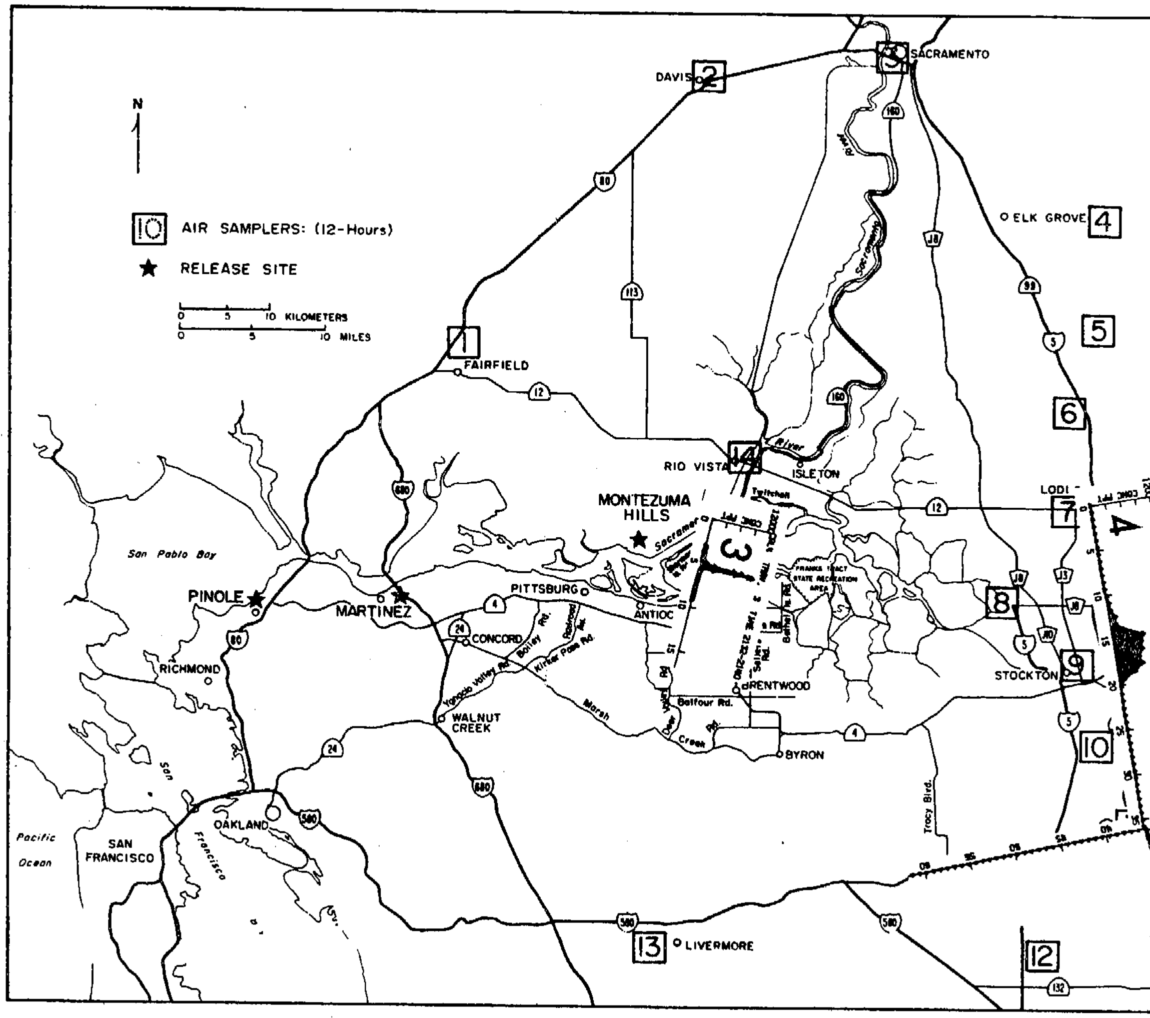

Figure 30. Overview of automobile traverse tracer data.

TEST 4

9/6/76

Auto Traverses:

3 2132 - 2140 PDT, SF_6(max) = 10,570 ppt

4 2200 - 2246 PDT, SF_6(max) = 628 ppt

SF_6 released from the Montezuma Hills from 1800-2300 PDT.

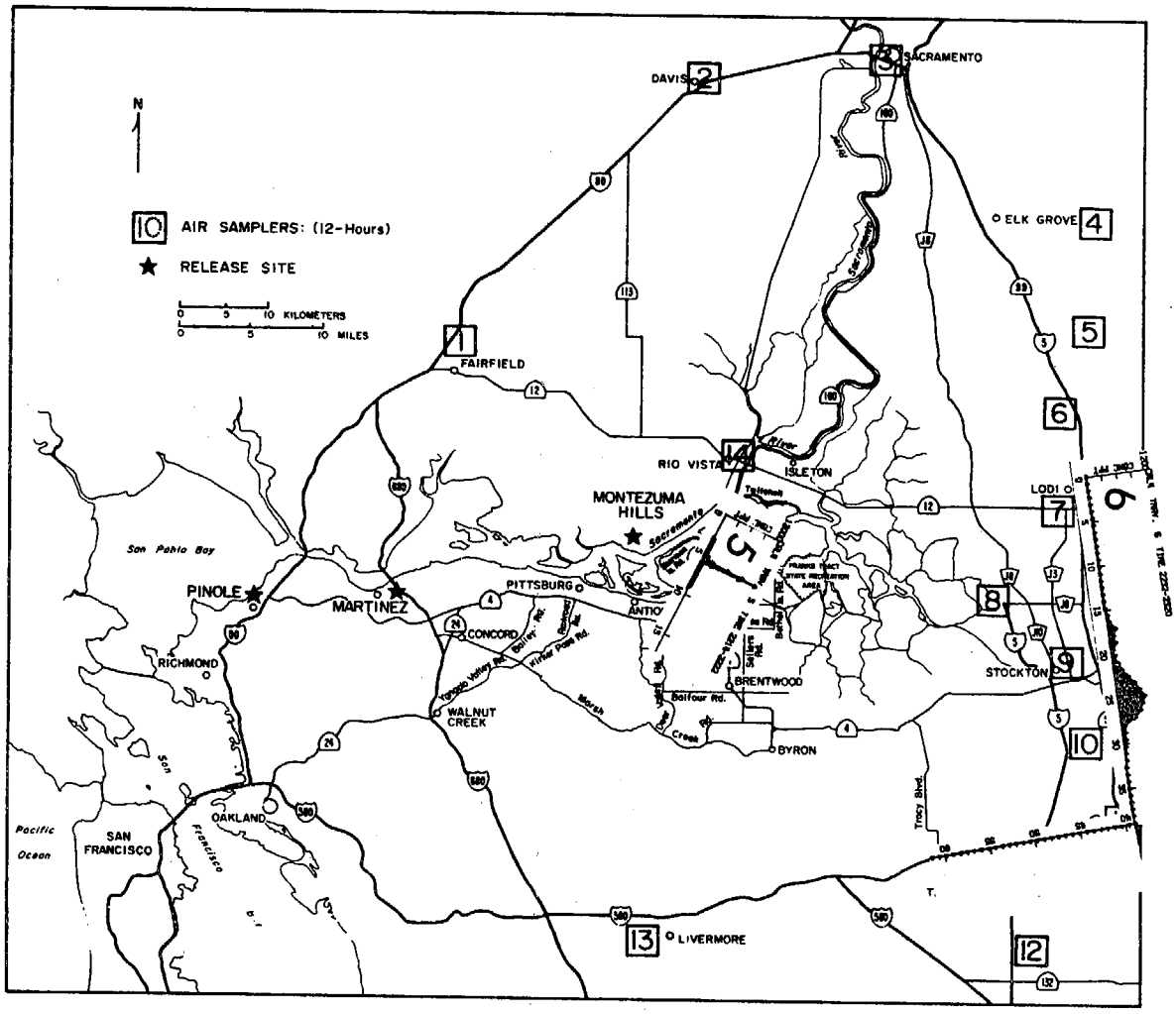

Figure 31. Overview of automobile traverse tracer data.

TEST 4

9/6/76

Auto Traverses:

5 2214 - 2222 PDT, SF_6(max) = 11,900 ppt

6 2232 - 2320 PDT, SF_6(max) = 553 ppt

SF_6 released from the Montezuma Hills from 1800-2300 PDT.

concentration observed along Highway 99 was 746 ppt. The profiles in Figure 31 suggest that the plume had shifted slightly to the south by 2300 PDT.

The hourly averaged concentration profiles in the overview map in Figure 32 also show that the plume moved south during the latter part of the test. The maximum concentration in the hourly averaged samples was 556 ppt, which was found between 2200 and 2300 PDT in downtown Stockton. The hourly crosswind profiles given in Figure 33 indicate that between 2000 and 2300 PDT, the tracer trajectory was very steady over Stockton. As shown in Figure 34, the winds shifted south to French Camp between 2300 and midnight PDT. The data in Figures 35 and 36 indicate that tracer concentrations on the order of 20 ppt were observed south of Manteca as late as 0700 PDT. The results indicate again that material emitted from the Montezuma Hills follow trajectories into the San Joaquin Valley.

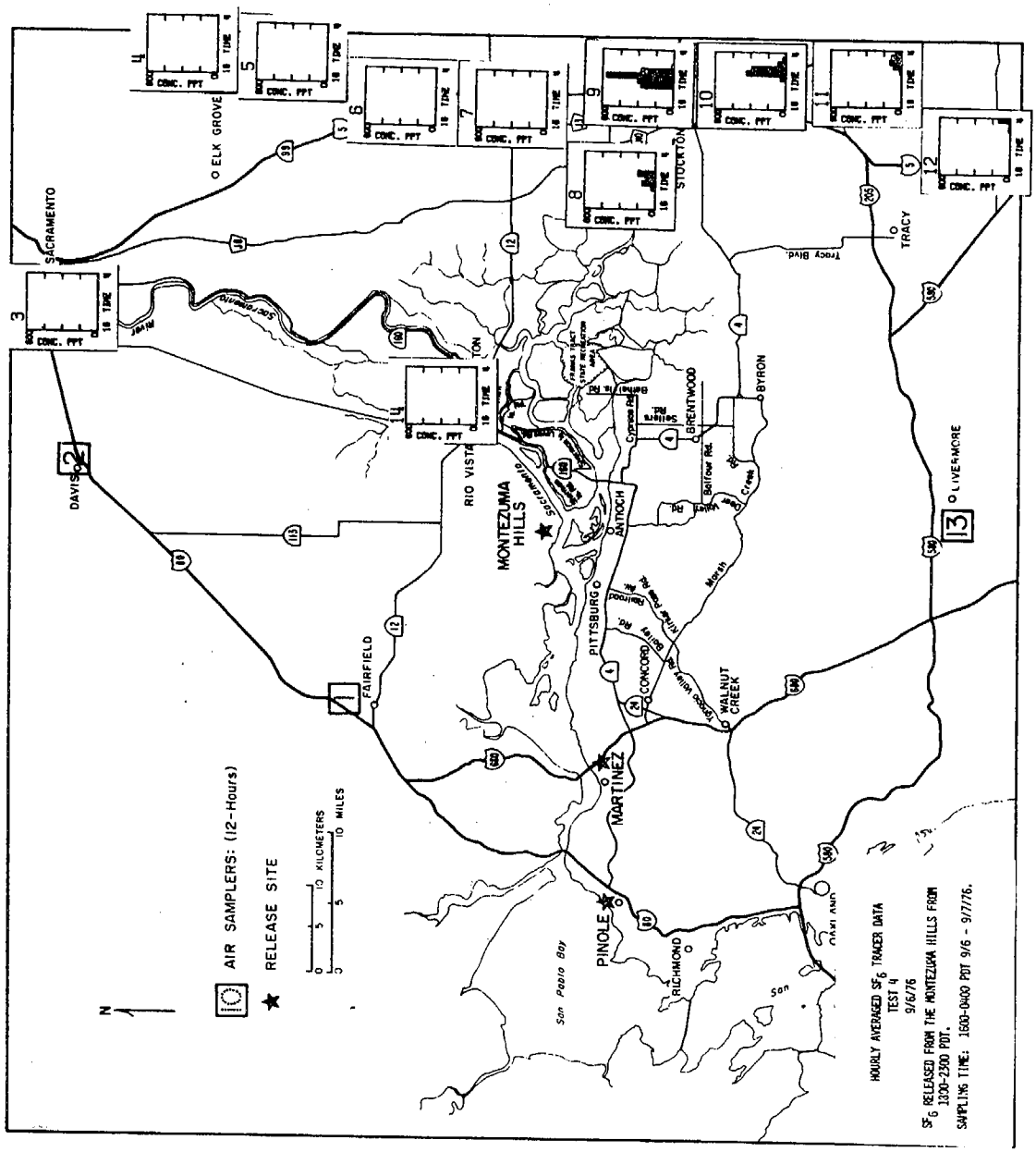

Figure 32. Overview of hourly averaged SF_6 data. Full scale SF_6 = 600 ppt.

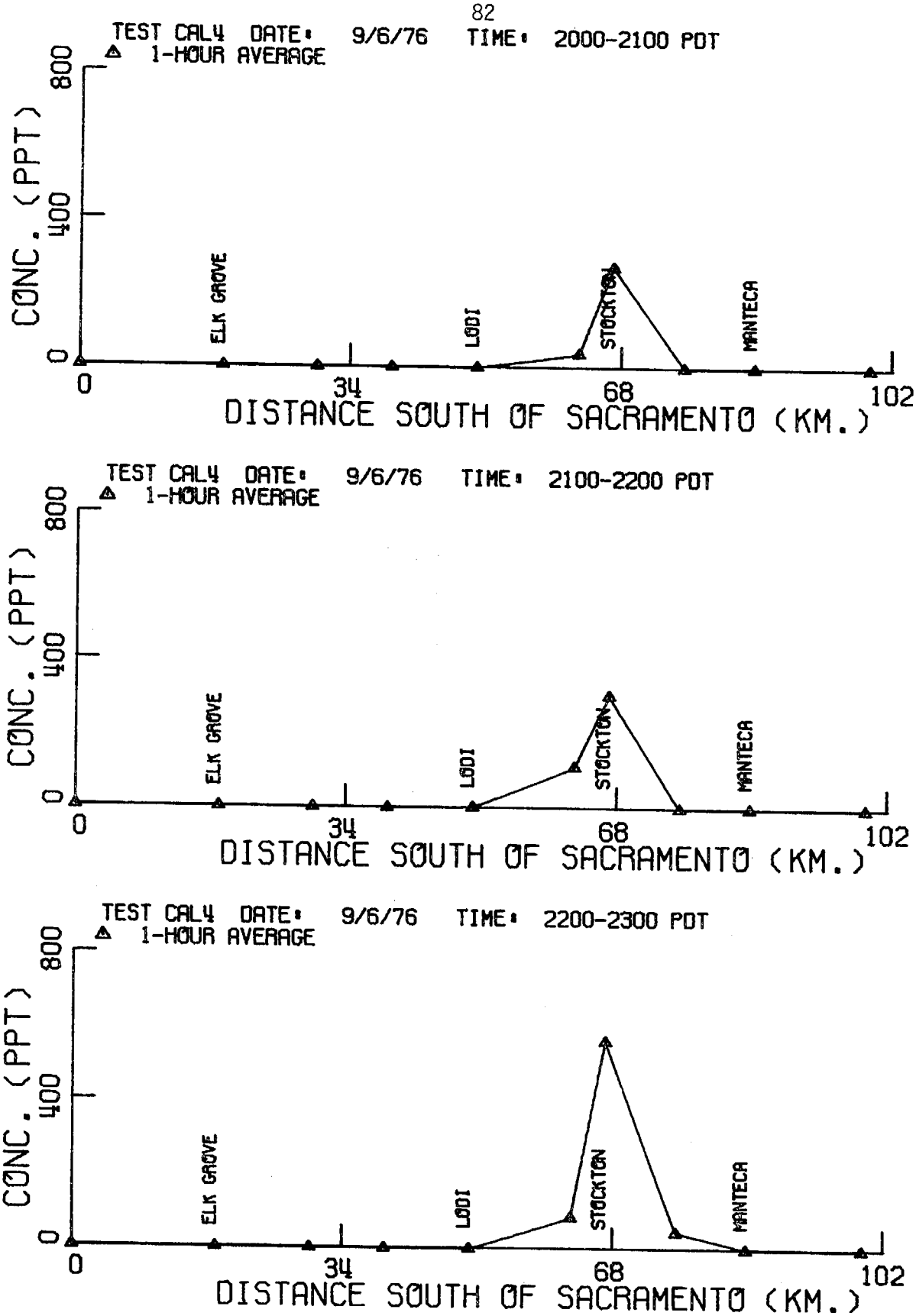

Figure 33. Hourly averaged crosswind SF_6 profiles measured along Highway 99.

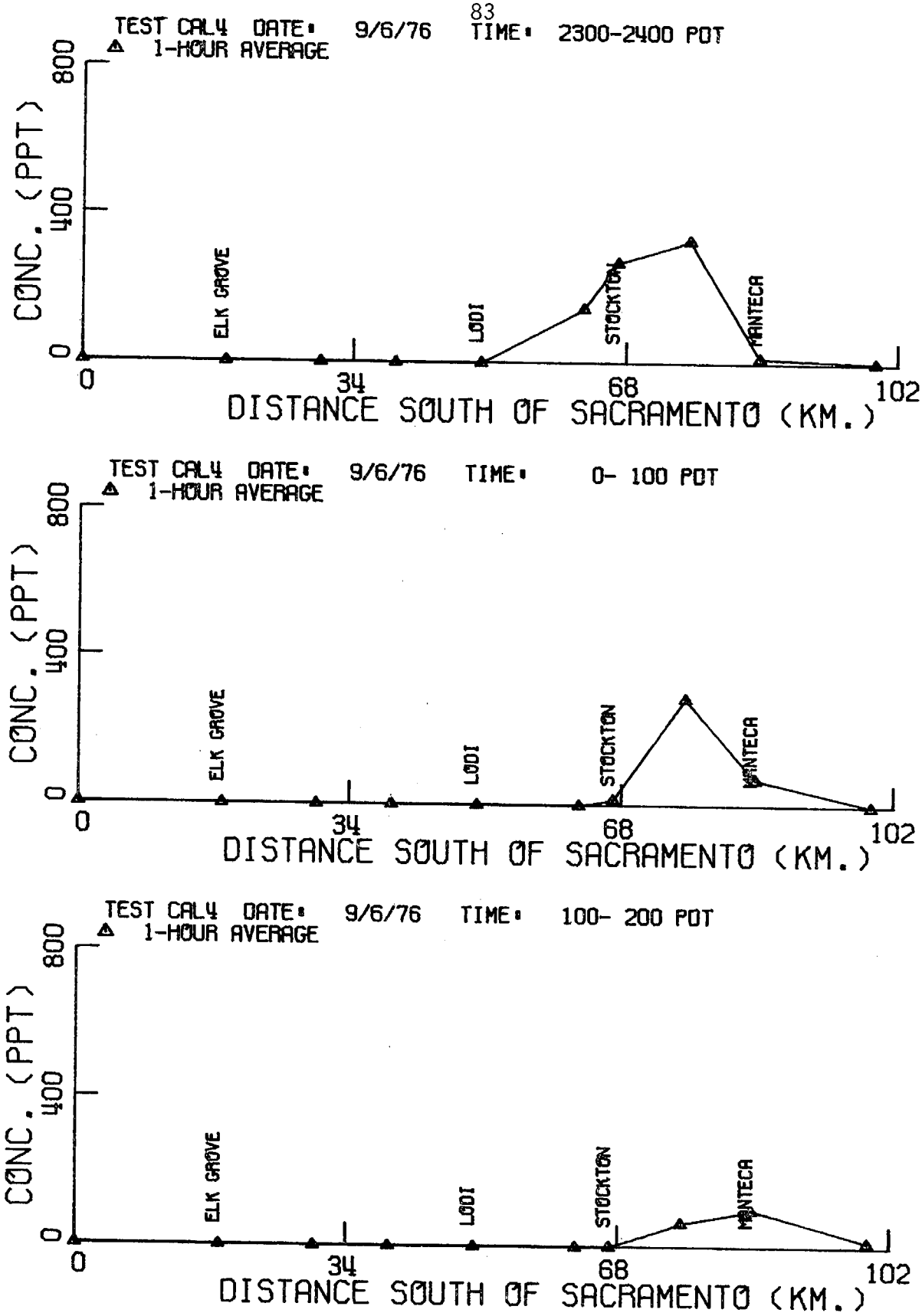

Figure 34. Hourly averaged crosswind SF_6 profiles measured along Highway 99.

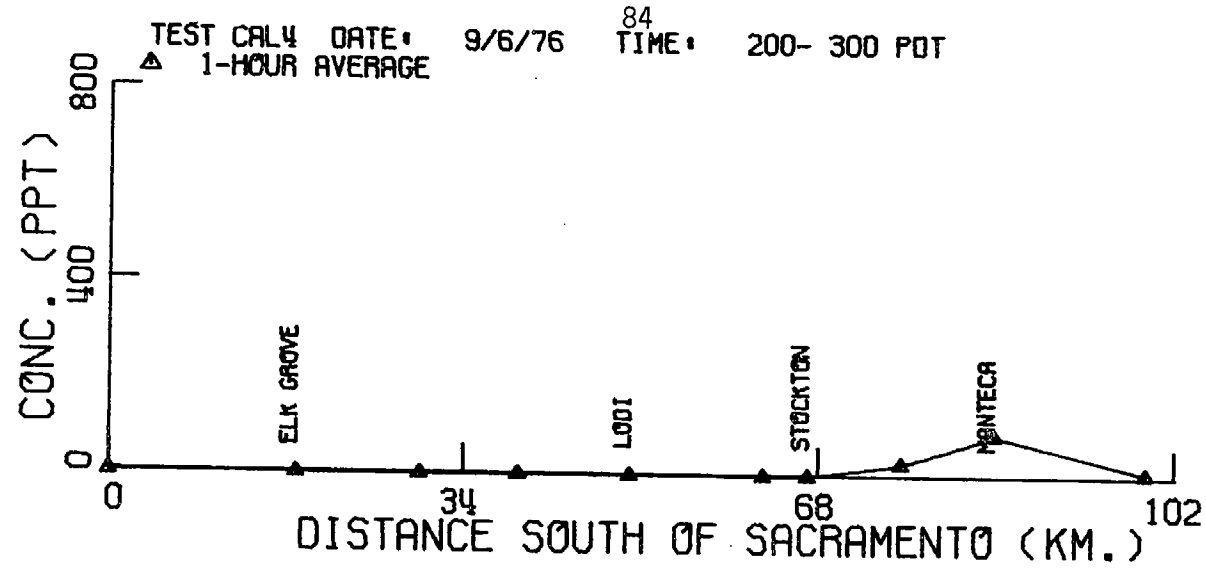

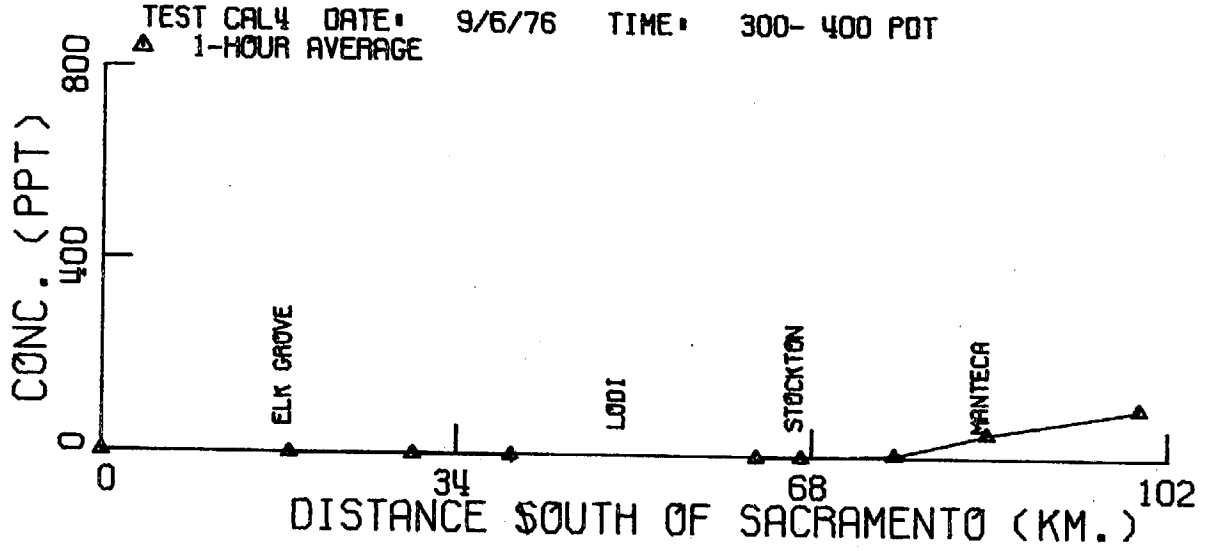

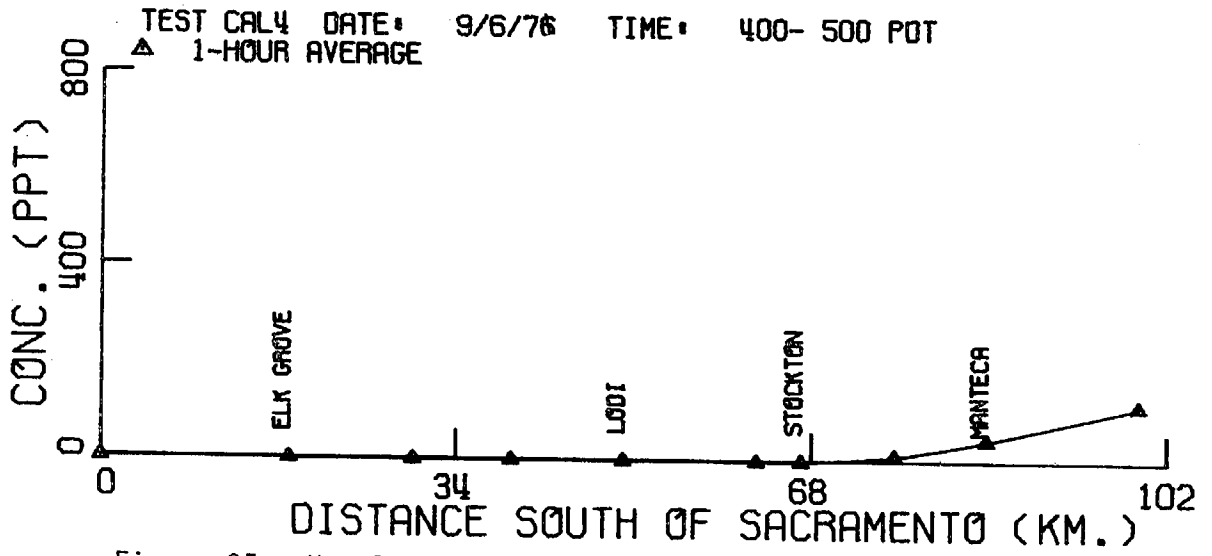

Figure 35. Hourly averaged crosswind SF_6 profiles measured along Highway 99.

4.25 Tracer Test 5 (9/9/76)

The purpose of this test was to study the transport and dispersion of pollutants emitted from the Montezuma Hills as the sea breeze developed. SF_6 was released at a constant rate of 10.7 g/sec (1.01 tons/day) from 1130 to 1330 PDT. The release was stopped after it became apparent that the afternoon sea breeze was not developing.

Because the winds were not steady through the test period, the calculated average wind is not significant. Winds at the Dow site during the test were between 270° and 40° at around 4 m/sec. The average standard deviation of the wind at the Dow site was 21°. There were only scattered clouds resulting in Pasquill class B-C conditions. The mixing height averaged 1910 meters with a maximum of 3000 meters during the afternoon. The wind pattern in Figure 37 for 1300 PDT shows the northerly flow sweeping through the area. This flow is similar to Smalley wind flow type NW-1, which occurred only 3.5% of the time on a yearly basis between 1952 and 1955; in September, this pattern occurred 0.6% of the time. In the Delta region, ozone levels reached 0.15 ppm; maximum levels of 0.25 ppm were observed in San Jose.

Eight automobile traverses were completed between 1255 and 1450 PDT. The tracer data are consistent with the wind streamlines; the plume moved south through Antioch towards Livermore. The maximum level observed along Highway 4, 9 km from the Dow site, was 801 ppt. Typical profiles of the tracer are shown in Figures 38 and 39. The traverses in the latter figure were taken along the same path at different times.

Although a maximum hourly averaged concentration of 47 ppt was observed near Stockton between 1700-1800 PDT, the lack of a plume pattern in the remaining stations suggests that the main plume trajectory crossed Highway 99 between Tracy and Livermore. Only 12 hours of data were collected during the test.

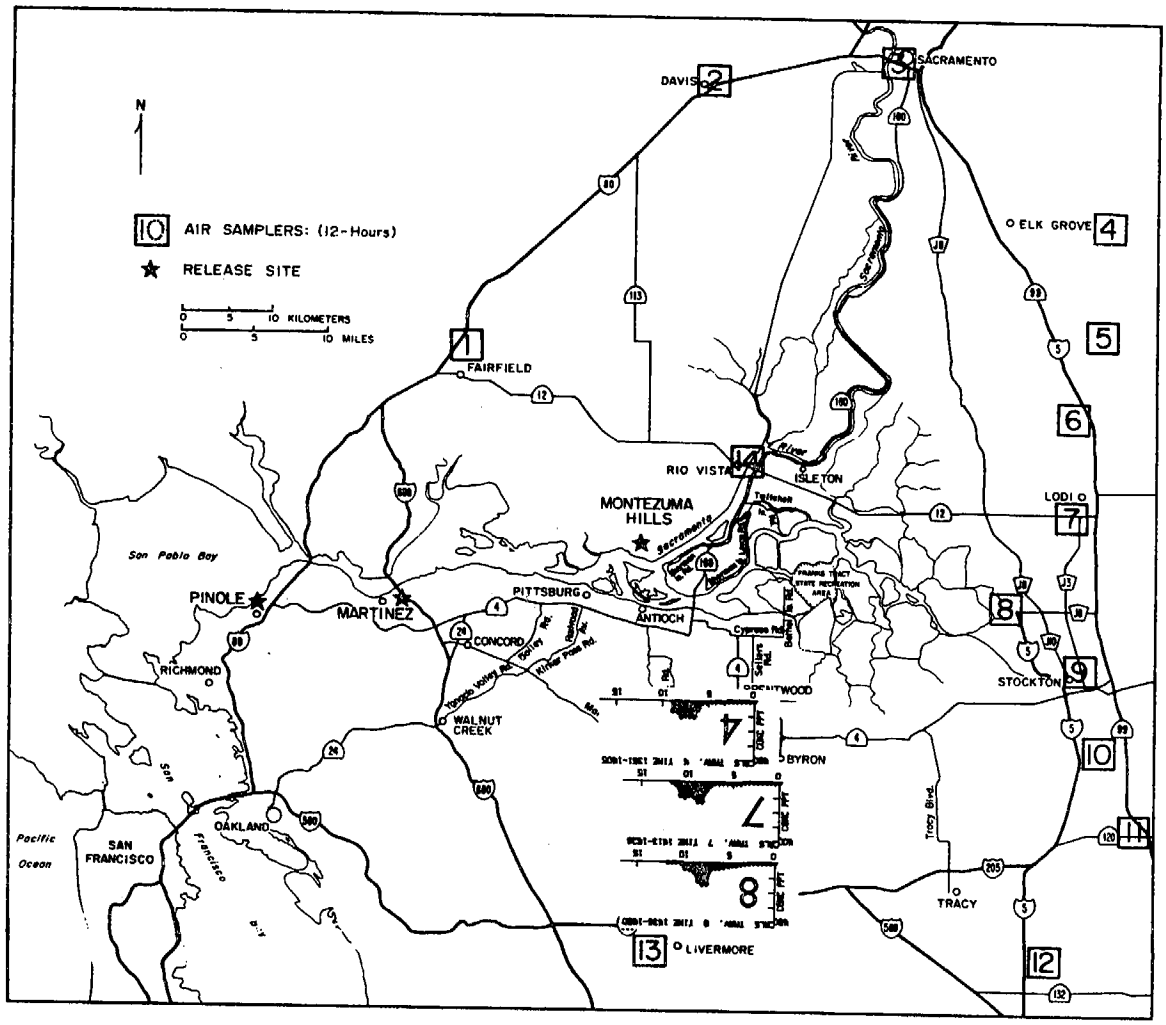

Figure 39. Overview of automobile traverse SF_6 data.

TEST 5

9/9/76

Auto Traverses: (along Balfour Road)

4 1351 - 1405 PDT, SF_6(max) = 138 ppt.

7 1413 - 1426 PDT, SF_6(max) = 141 ppt.

8 1436 - 1450 PDT, SF_6(max) = 183 ppt.

SF_6 released from the Montezuma Hills from 1130-1330 PDT.

4.26 Tracer Test 6 (9/10/76)

The purpose of the sixth tracer test was to examine the transport and dispersion of pollutants emitted from the Montezuma Hills under Pre-Sea Breeze conditions. SF_6 was released at a constant rate of 10.5 g/sec (0.99 tons/day) from 0600 to 1100 PDT.

The average wind vector at the Dow site at 1100 PDT was 280° at 6.3 m/sec, no data were available for earlier times. The average wind for the area was 270° at 1.2 m/sec. The average standard deviation of the wind was 8° at the Dow site at 1100 PDT. The sky was overcast, and Pasquill class D conditions existed. The mixing layer extended to 1250 meters on an average, with a maximum of 3000 meters occurring during the afternoon. The streamline map at 1000 PDT in Figure 40 suggests that westerly flow had almost reached Stockton by midmorning. Maximum ozone levels of 0.08 ppm were observed at the Dow site during the day.

Nine automobile traverses conducted from 0800 to 1230 PDT indicated the plume crossed Highway 160 7.2 km north of the Highway 160-Highway 4 junction and reached I 580 in the Tracy area. Although maximum levels observed along Highway 160 reached 9526 ppt, levels along Highway 99 and I 580 were no greater than 20 ppt. It is possible that the traverses far downwind did not cross the centerline of the plume. Typical traverses are shown in Figures 41 and 42.

Thirteen airborne traverses were completed from 0934 to 1339 PDT. Data obtained during Traverse 5 in Figure 43 indicated the plume moved directly east and mixed to at least 183 meters after traveling 18 km downwind. The maximum concentration at that height was 1387 ppt. As

Figure 40. Surface wind streamline, 1000 PDT, 9/10/76 (MRI).

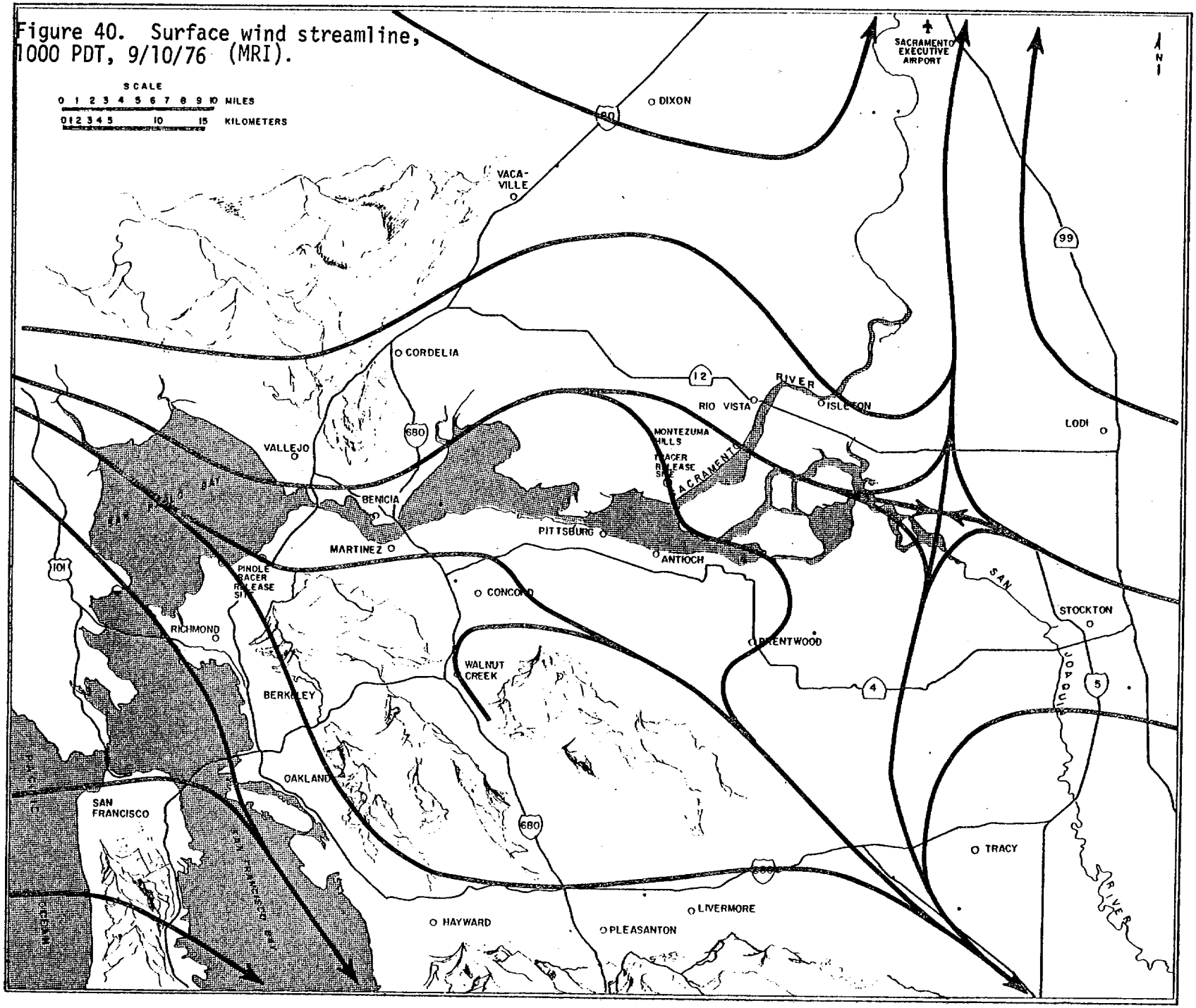

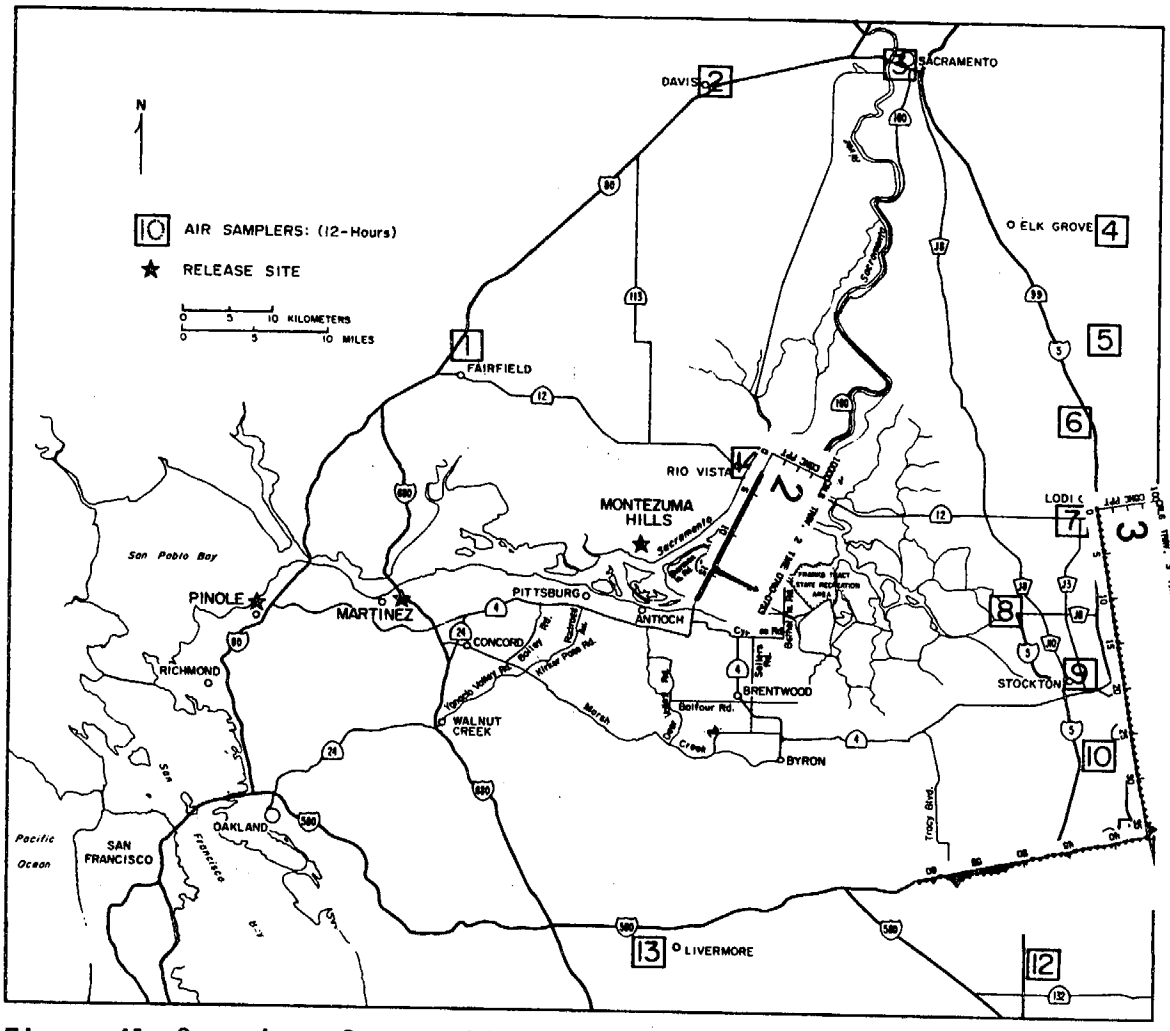

Figure 41. Overview of automobile traverse SF_6 data.

TEST 6

9/10/76

Auto Traverses:

2 0740 - 0753 PDT, SF_6(max) = 7981 ppt

3 1001 - 1051 PDT, SF_6(max) = 20 ppt

SF_6 released from the Montezuma Hills from 0600-1100 PDT.

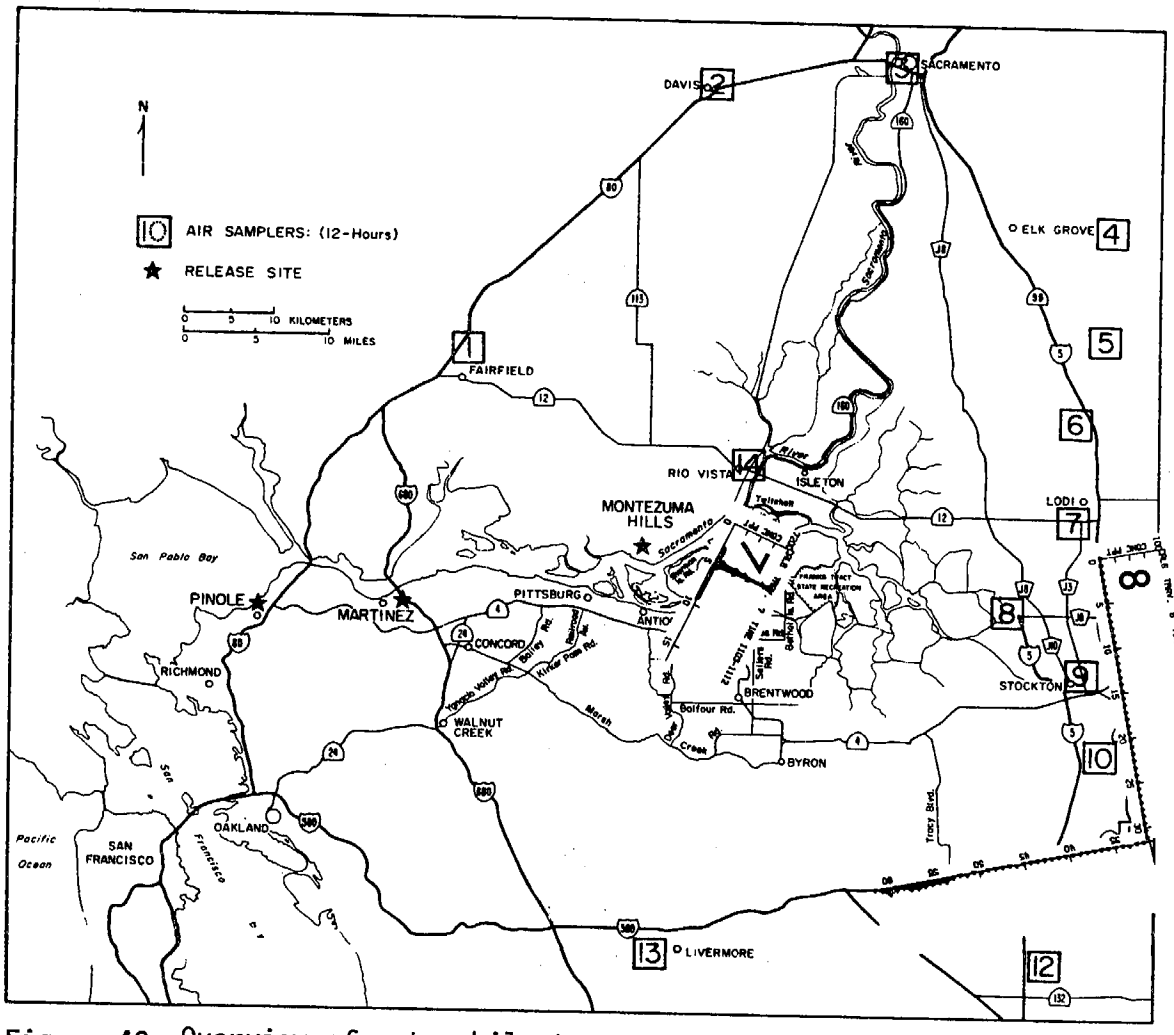

Figure 42. Overview of automobile traverse SF_6 data.

TEST 6

9/10/76

Auto Traverses:

7 1103 - 1112 PDT, SF_6(max) = 7155 ppt

8 1105 - 1203 PDT, SF_6(max) = 12 ppt

SF_6 released from the Montezuma Hills from 0600-1100 PDT.

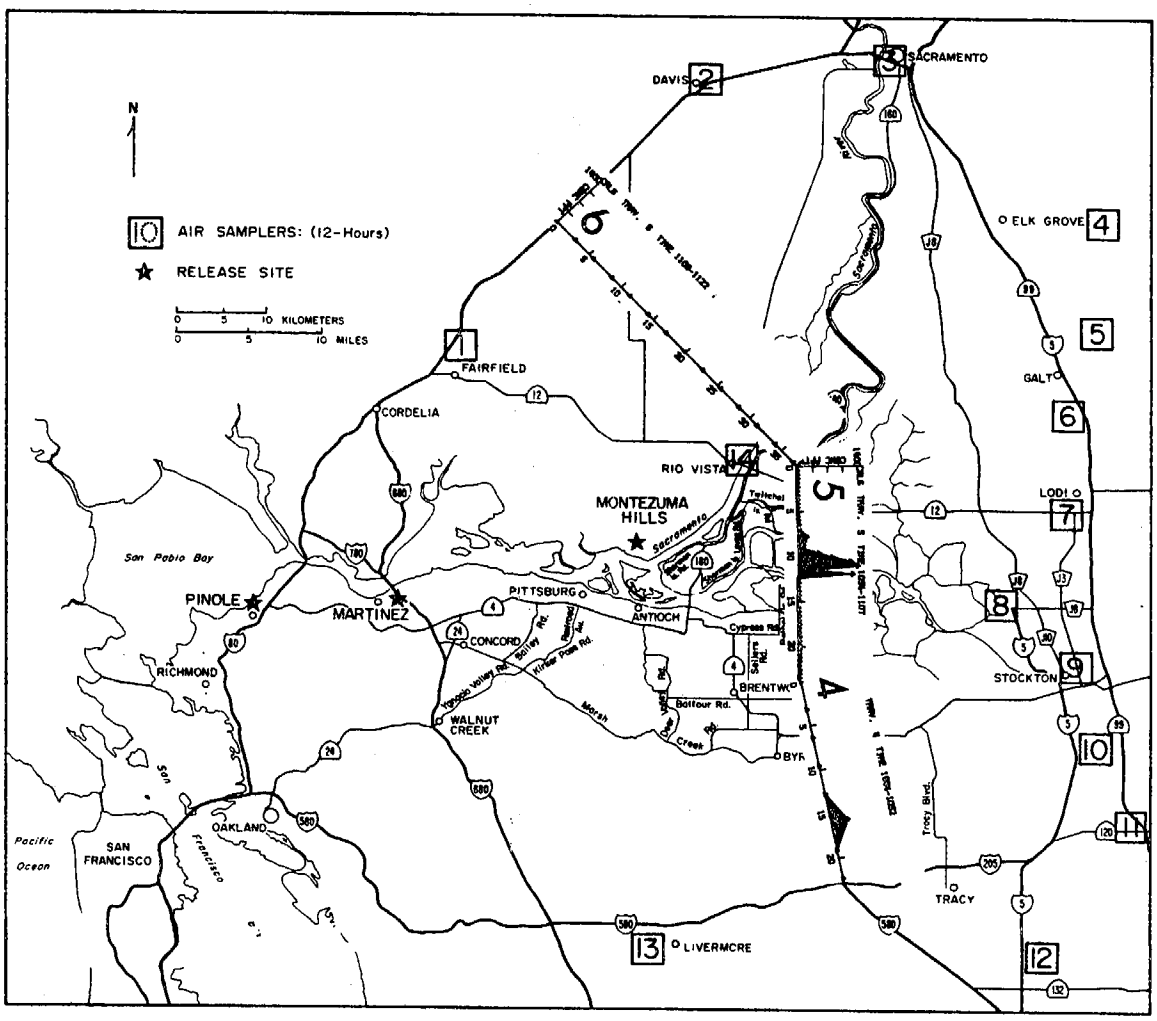

Figure 43. Overview of airborne traverse SF_6 data.

TEST 6

9/10/76

Airborne Traverses:

4 1044 - 1052 PDT, 183 m, SF_6(max) = 396 ppt

5 1054 - 1107 PDT, 183 m, SF_6(max) = 1387 ppt

6 1109 - 1122 PDT, 183 m, SF_6(max) = 0 ppt

SF_6 released from the Montezuma Hills from 0600-1100 PDT.

shown in Figure 44, an airborne spiral over Frank's Tract Recreation Area indicated the plume possibly moved aloft with a centerline at 122 meters. At higher elevations, data from only one traverse reached significant levels. In Traverse 7 in Figure 45 at 427 meters, a single grab sample indicated SF_6 was present at 33 ppt. Further downwind above Highway 99, a traverse taken by Caltrans at 183 meters had a maximum concentration of 21 ppt as shown in Figure 46.

The hourly averaged data covered 12 hours from 0400 to 1600 PDT. Maximum levels of 83 and 73 ppt were measured in the 1500-1600 PDT samples at stations 7 and 8 as indicated in Figures 47 and 48. These were the only stations where significant tracer levels were detected.

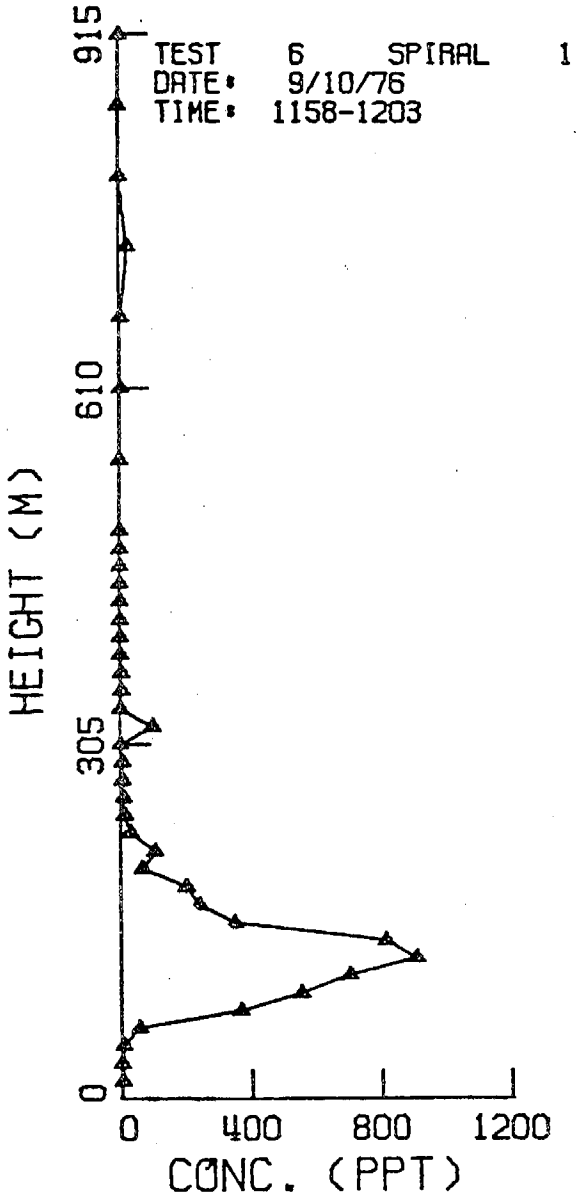

Figure 44. Airborne spiral over Frank's Tract Recreation Area.

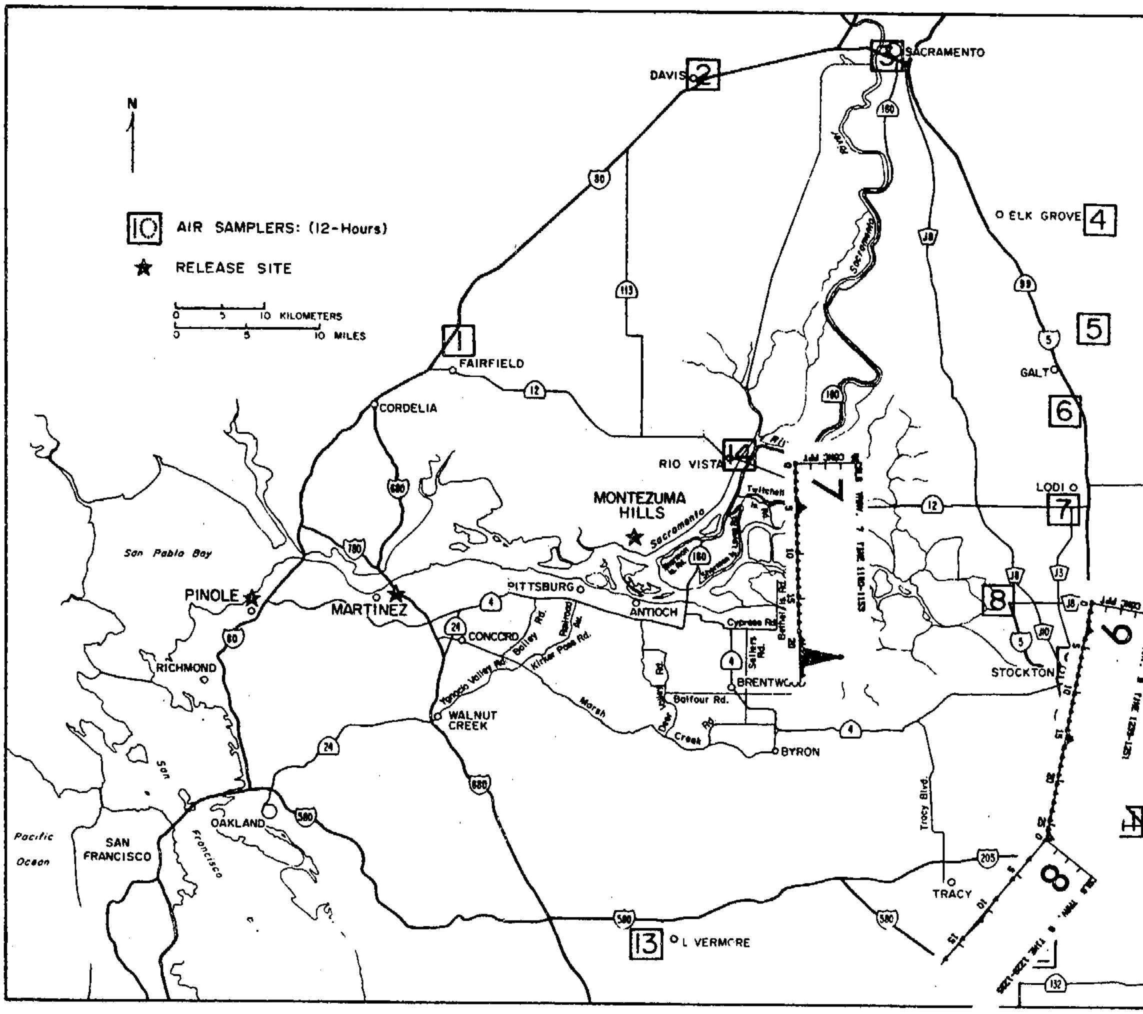

Figure 45. Overview of airborne traverse SF_6 data.

TEST 6

9/10/76

Airborne Traverses:

7 1140 - 1153 PDT, 427 m, SF_6(max) = 33 ppt

8 1229 - 1235 PDT, 305 m, SF_6(max) = 2 ppt

9 1238 - 1251 PDT, 305 m, SF_6(max) = 4 ppt

SF_6 released from the Montezuma Hills from 0600-1100 PDT.

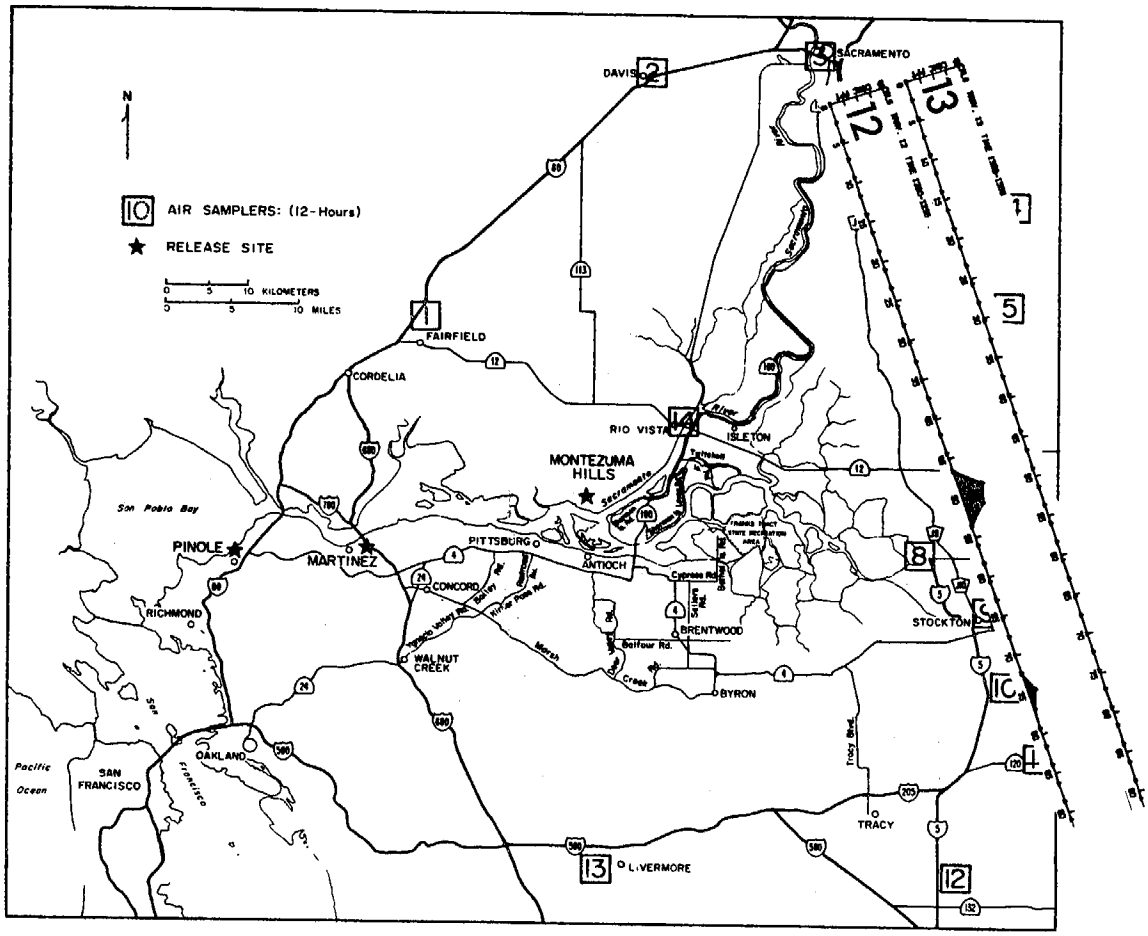

Figure 46. Overview of airborne traverse SF_6 data measured during two traverses between Manteca and Sacramento.

TEST 6

9/10/76

Airborne Traverses:

12 1200 - 1239 PDT, 183 m, SF_6(max) = 21 ppt

13 1300 - 1339 PDT, 183 m, SF_6(max) = 0 ppt

SF_6 released from the Montezuma Hills from 0600-1100 PDT.

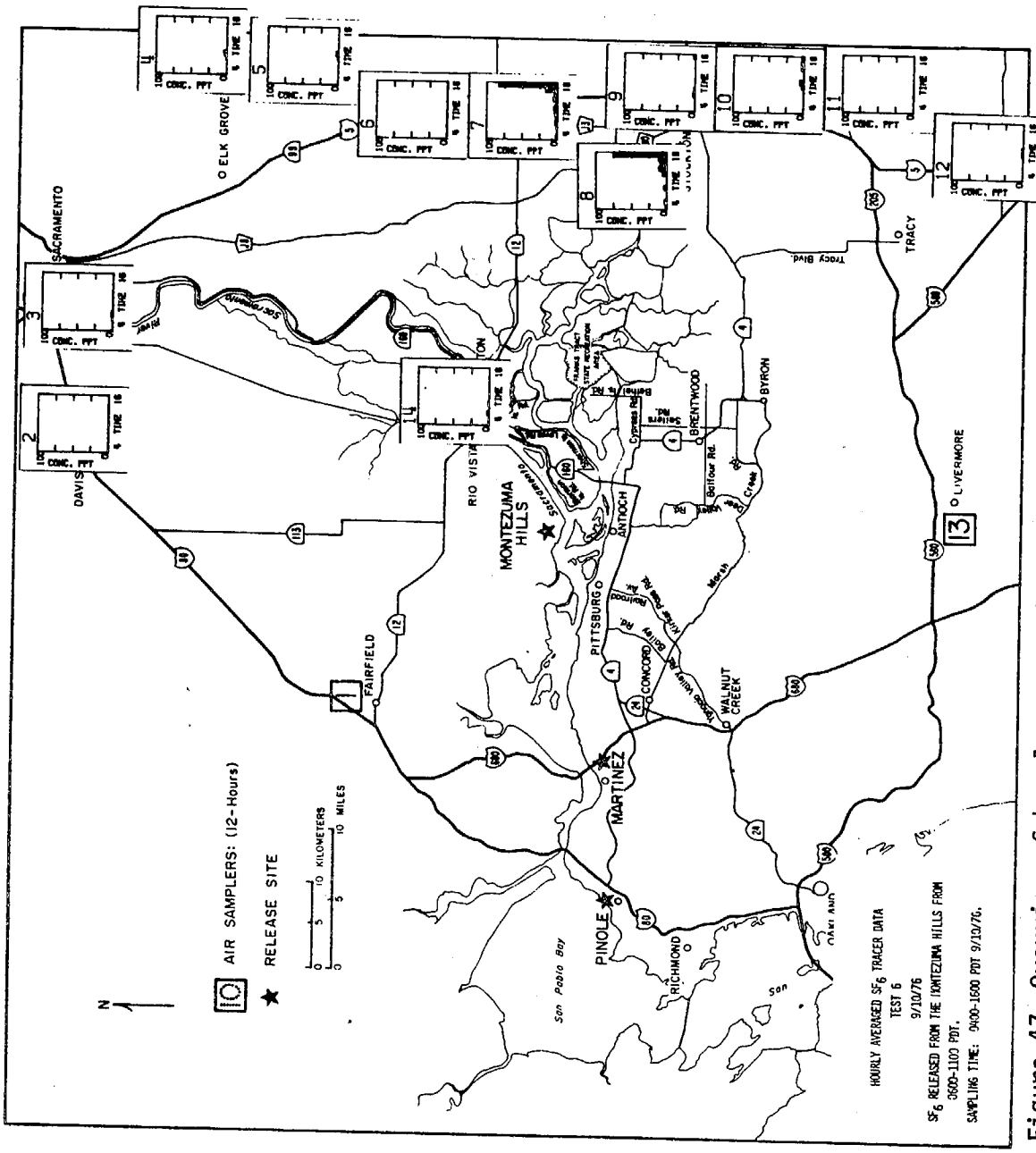

Figure 47. Overview of hourly averaged SF_6 data. Full scale SF_6 = 100 ppt.

4.27 Tracer Test 7 (9/13/76)

The purpose of this test was to tag the air upstream of the Montezuma Hills during the development and onset of the afternoon sea breeze. SF_6 was released at a constant rate of 11.6 g/sec (1.09 tons/day) from Pinole between 0600 and 1500 PDT. $CBrF_3$ was released from the Dow site at a constant rate of 16.0 g/sec (1.52 tons/day) from 0900-1100 PDT and from 1300-1400 PDT.

The average winds at Pinole as measured at Rodeo were 240° at 2.6 m/sec; at the Dow site winds were 270° at 4.6 m/sec. The average standard deviation of the winds at Dow was 8°. Pasquill conditions B-C were assumed to exist under scattered clouds. The average mixing height was 830 meters with a maximum of 1500 meters after 1200 PDT. The wind pattern observed at 1000 PDT in Figure 49 gives a general indication of the wind conditions during the test. Maximum ozone levels of 0.12 ppm were measured at the Montezuma Hills during the day.

Between 0924 and 1901 PDT twelve automobile traverses were conducted. The data from the traverses indicate that the SF_6 plume from Pinole diverged from the Carquinez Strait east past the Montezuma Hills and south through the Walnut Creek area towards Livermore. Figures 50 and 51 show the presence of SF_6 and $CBrF_3$ along Highway 160 downwind of the Montezuma Hills. The maximum $CBrF_3$ concentration was 12,140 ppt. SF_6 levels along I 680 15 km downwind of Pinole reached 614 ppt. Along Highway 160, the levels dropped to 94 ppt. Later traverses shown in Figures 52, 53, and 54 indicate that the SF_6 plume impacted in Livermore passing through Walnut Creek and also reached Tracy, possibly coming from both Livermore and

Figure 49. Surface wind streamlines, 1000 PDT, 9/13/76 (MRI).

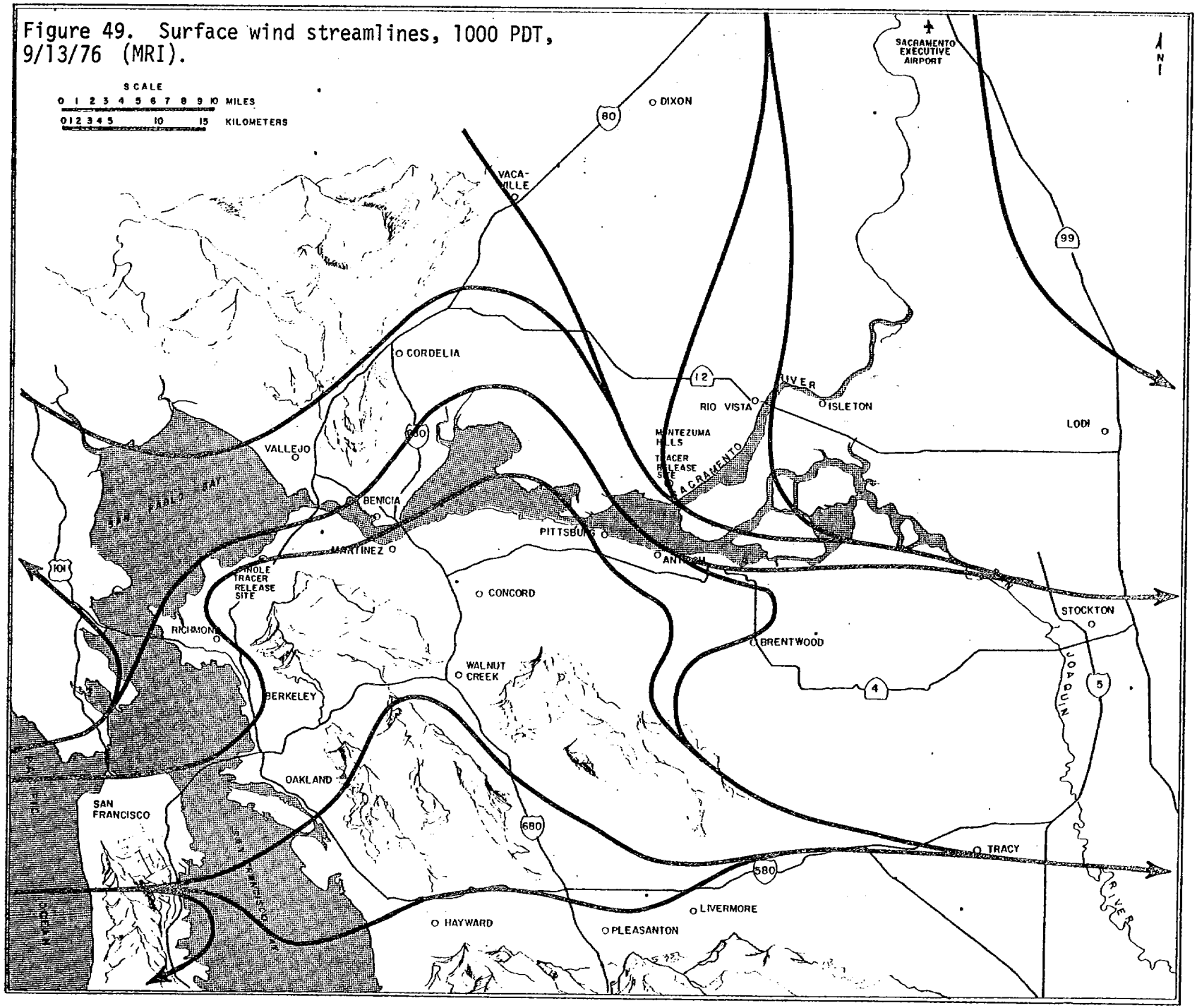

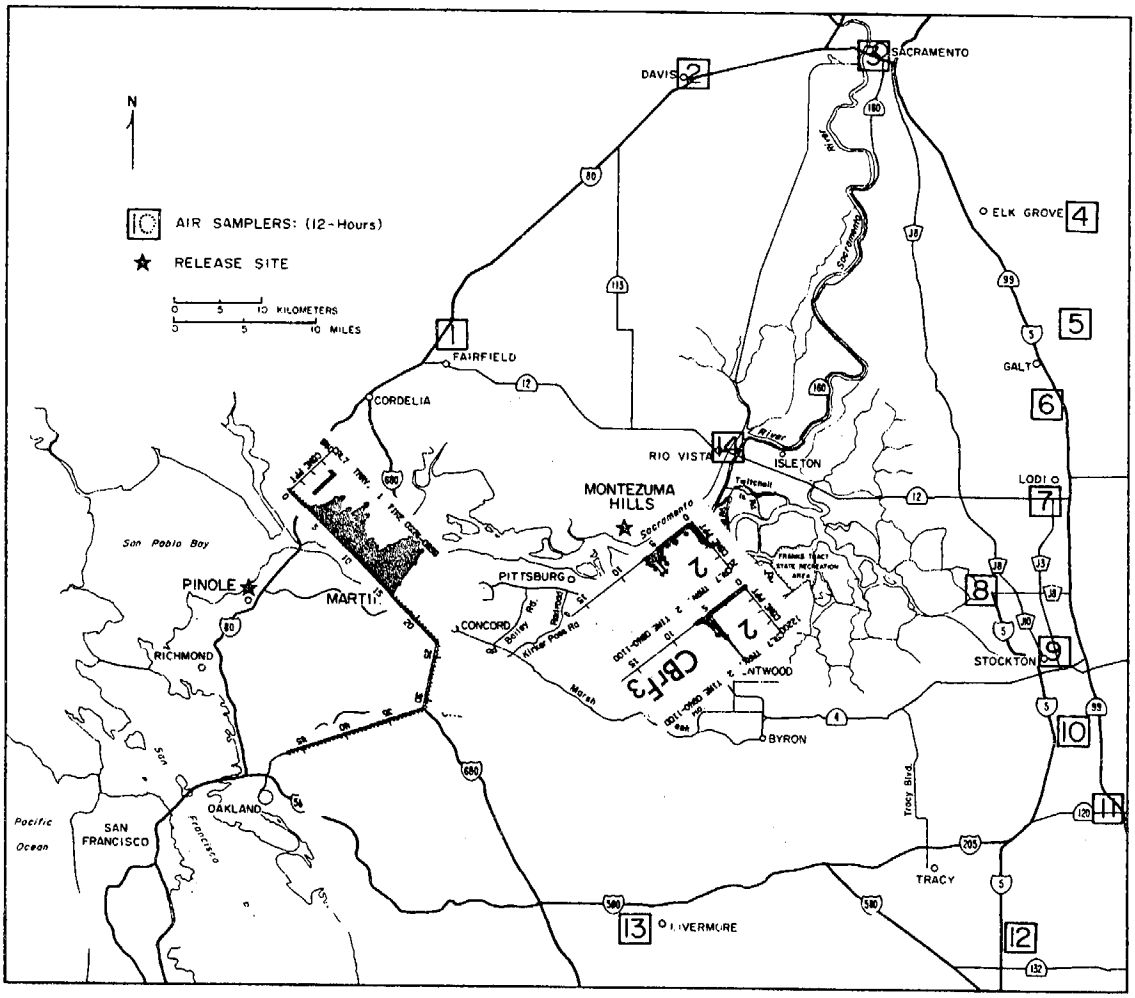

Figure 50. Overview of automobile traverse SF_6 and $CBrF_3$ data.

TEST 7

9/13/76

Auto Traverses:

1 0924-0925 PDT, SF_6(max) = 614 ppt.

2 0940-1100 PDT, SF_6(max) = 11 ppt.

0940-1100 PDT, $CBrF_3$(max) = 12,140 ppt.

SF_6 released from Pinole from 0600-1500 PDT.

$CBrF_3$ released from the Montezuma Hills from 0900-1100 PDT, and from 1300-1400 PDT.

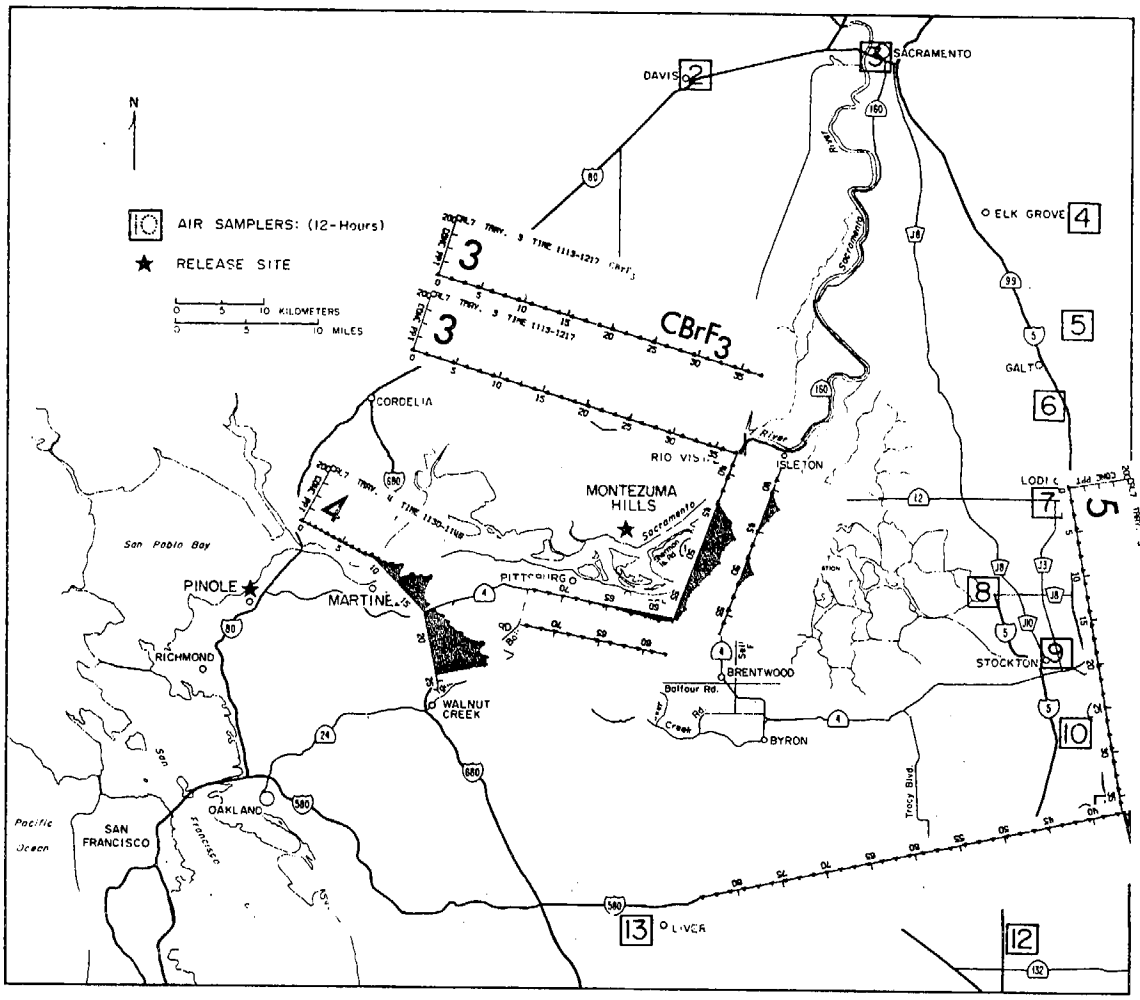

Figure 51. Overview of automobile traverse SF_6 and $CBrF_3$ data.

TEST 7

9/13/76

Auto Traverses:

3 1113-1217 PDT, SF_6(max) = 94 ppt.

1113-1217 PDT, $CBrF_3$(max) = 37 ppt.

4 1130-1146 PDT, SF_6(max) = 180 ppt.

5 1335-1458 PDT, SF_6(max) = 3 ppt.

SF_6 released from Pinole from 0600-1500 PDT.

$CBrF_3$ released from the Montezuma Hills from 0900-1100 PDT and from 1300-1400 PDT.

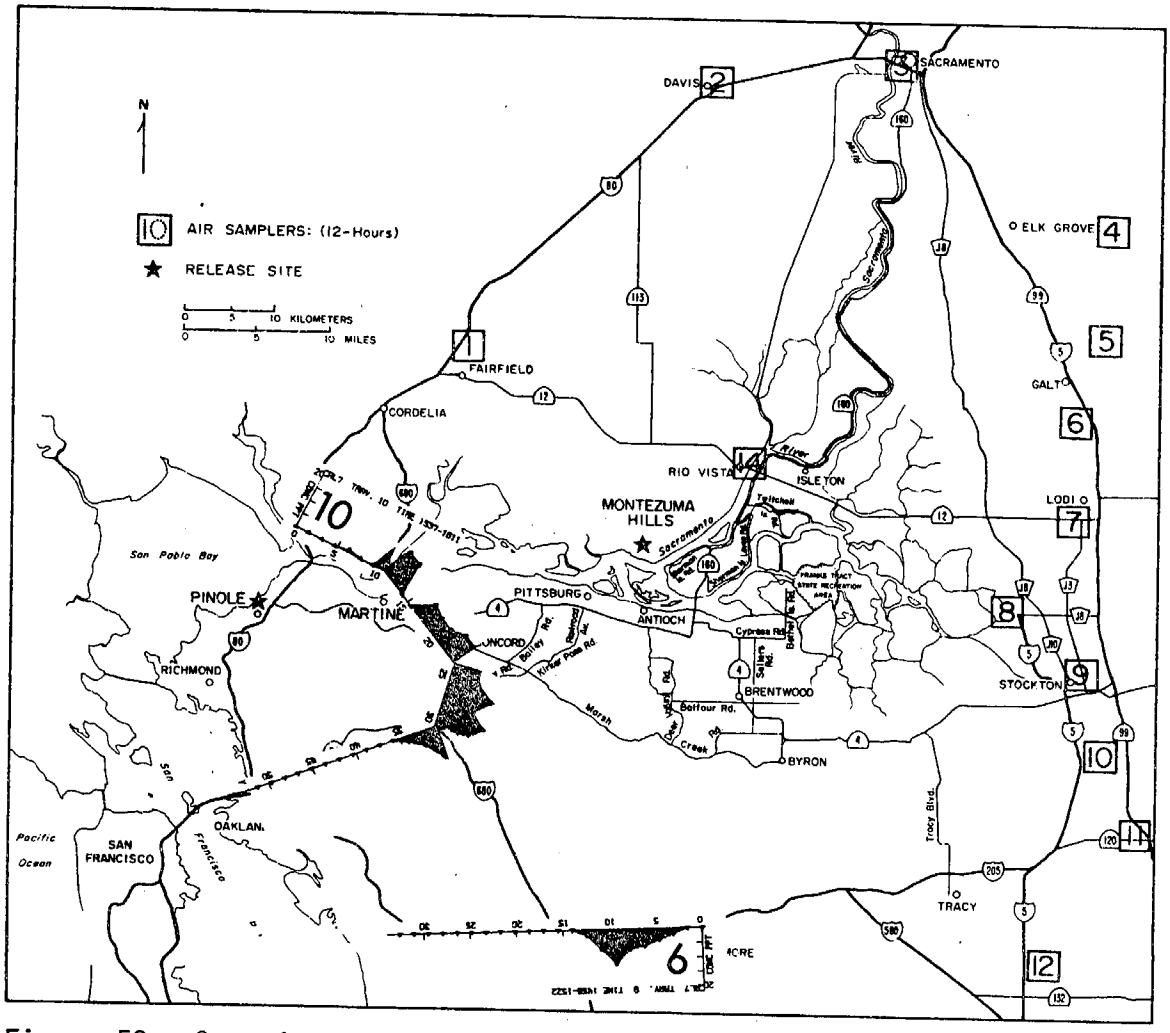

Figure 52. Overview of automobile traverse SF_6 data.

TEST 7

9/13/76

Auto Traverses:

9 1458 - 1522 PDT, SF_6(max) = 12 ppt.

10 1537 - 1611 PDT, SF_6(max) = 16 ppt.

SF_6 released from Pinole from 0600-1500 PDT.

$CBrF_3$ released from the Montezuma Hills from 0900-1100 PDT and from 1300-1400 PDT.

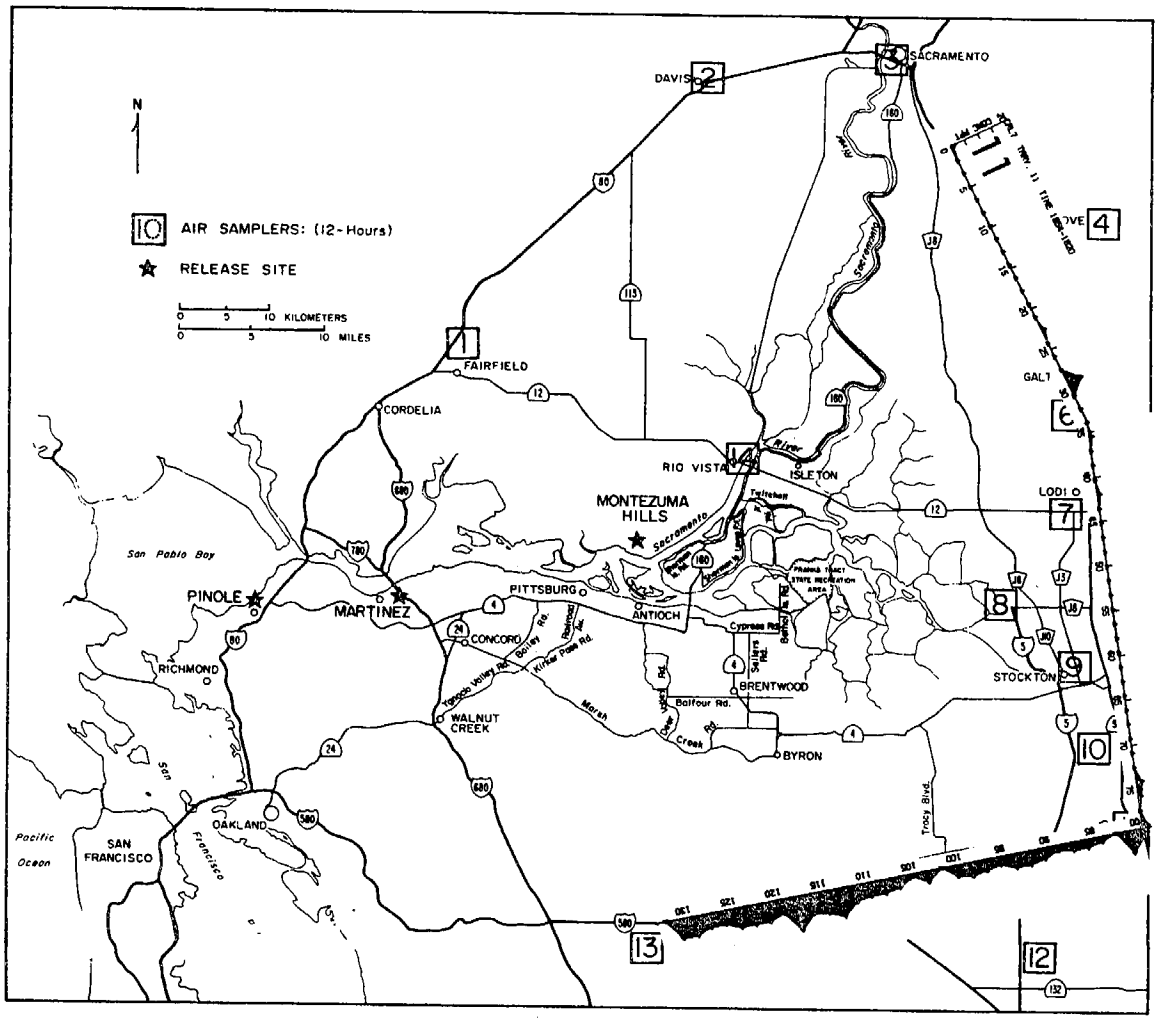

Figure 53. Overview of automobile traverse SF_6 data.

TEST 7

9/13/76

Auto Traverse:

11 1654 - 1820 PDT, SF_6(max) = 12 ppt.

SF_6 released from Pinole from 0600-1500 PDT.

$CBrF_3$ released from the Montezuma Hills from 0900-1100 PDT and from 1300-1400 PDT.

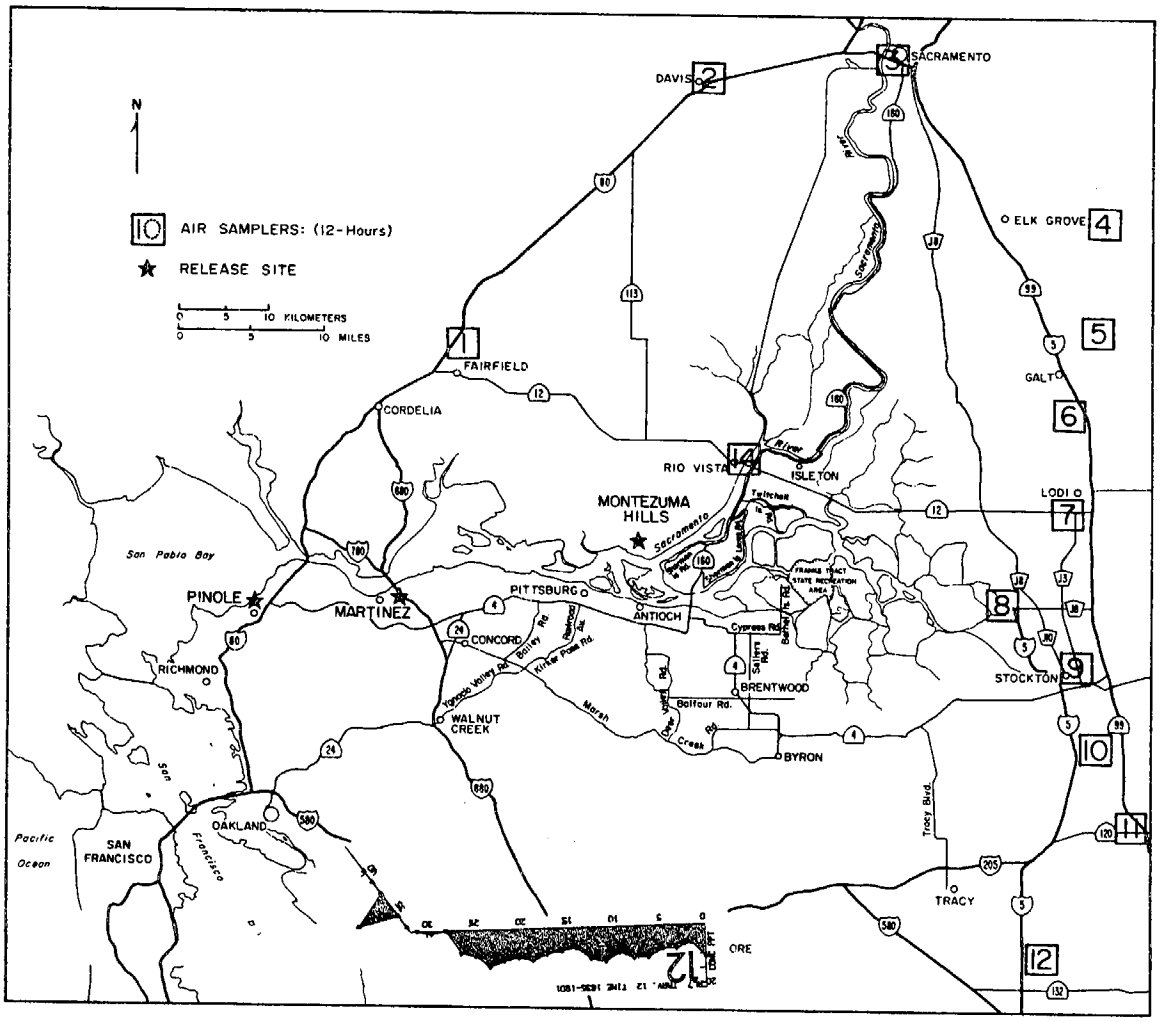

Figure 54. Overview of automobile traverse SF_6 data.

TEST 7

9/13/76

Auto Traverse:

12 1835 - 1901 PDT, SF_6(max) = 13 ppt

SF_6 released from Pinole from 0600-1500 PDT.

$CBrF_3$ released from the Montezuma Hills from 0900-1100 PDT, and from 1300-1400 PDT.

the Pittsburg-Antioch area. Concentration levels along I 580 reached 16 ppt.

Fourteen airborne traverses were conducted from Cordelia to Walnut Creek, from Vacaville to Tracy, and from Livermore to Stockton to Sacramento. Data from three traverses at three altitudes above I 680 are shown in Figure 55. Apparently, the plume had mixed no higher than 305 meters after traveling 17 km downwind. The maximum concentration at 183 meters was 199 ppt. The vertical profile of the plume is shown in Figure 56 where data from spirals 22 km downwind of Pinole are plotted. By 1000 PDT, the plume appeared to be vertically well-mixed to a height of about 300 meters. The crosswind data indicate that the spirals were taken very near the centerline of the plume. Further downwind between Isleton and Tracy, elevated concentration profiles also indicate that the plume was vertically well-mixed. As shown in Figure 57, maximum concentrations at 183, 305, and 427 meters were 19, 25, and 15 ppt, respectively. The data indicate that the plume was wider at the higher elevations, suggesting either increased wind shear or reflectance from an inversion layer. The last set of airborne traverses above I 580 and Highway 99 in Figure 58 show that the SF_6 plume was present at 457 meters between Livermore and Tracy. The maximum concentration was 29 ppt.

A spiral over Stockton at 1832 PDT suggested that a portion of the plume was transported between 900 m and 1200 m. Concentration levels were on the order of 30 ppt; however, the concentration in one sample at 1036 m was analyzed as 952 ppt. Since none of the data collected during the spiral or during the other traverses in the area

were over 50 ppt, it is assumed that the sample was contaminated and the data point should be disregarded.

As indicated in Figure 59, SF_6 was detected in hourly samples at very low levels (less than 10 ppt) from Elk Grove to Livermore along Highway 99. The major impact did not appear until after 1800 PDT. In general, the hourly averaged data also show that SF_6 reached Livermore and Tracy. Again, it appears that material emitted from the northern portions of the Bay Area can follow trajectories south through Stockton and Tracy into the San Joaquin Valley.

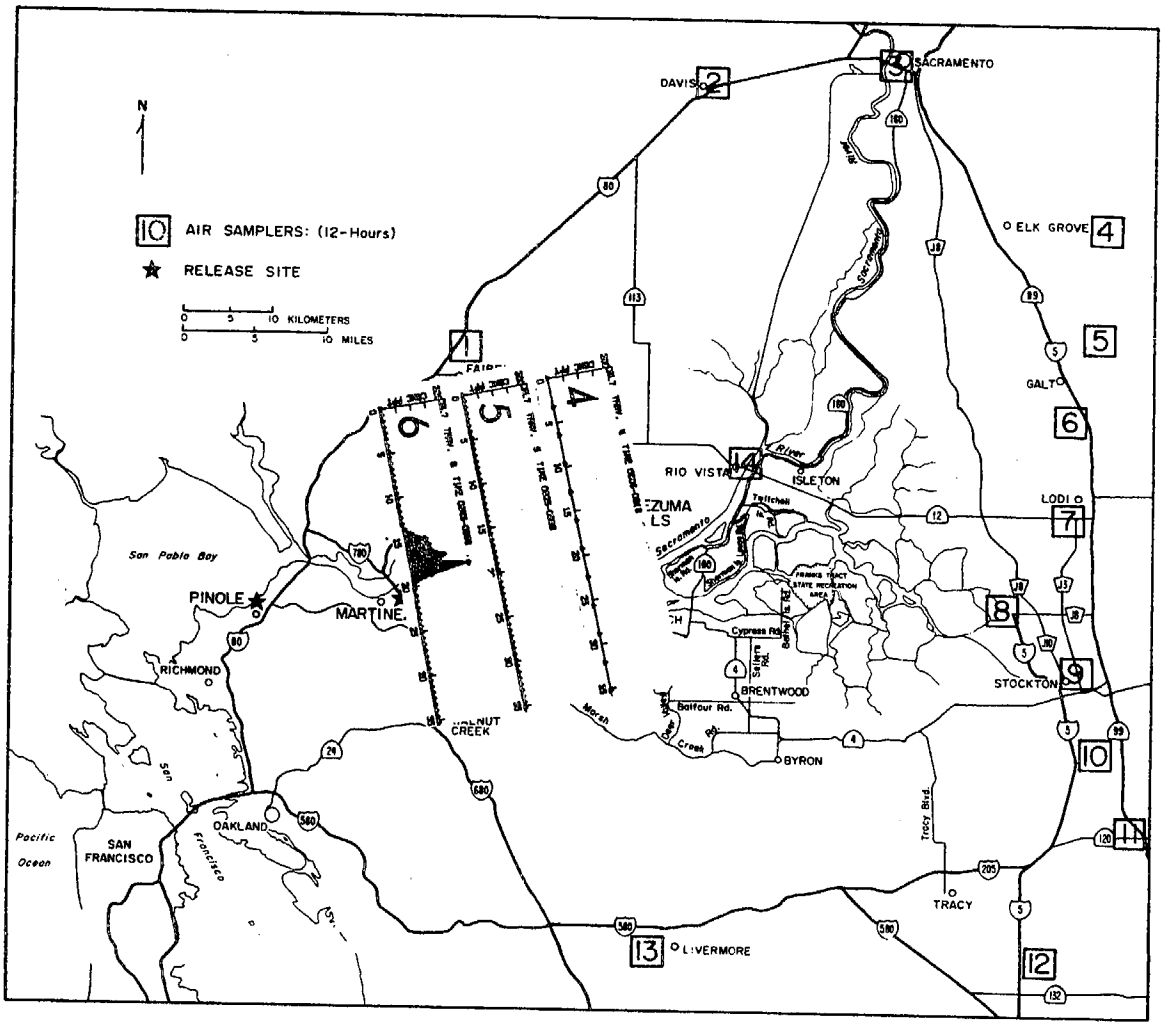

Figure 55. Overview of airborne traverse SF_6 data measured at three altitudes between Cordelia and Walnut Creek.

TEST 7

9/13/76

Airborne Traverses:

4 0906 - 0918 PDT, 427 m, SF_6(max) = 0 ppt
5 0925 - 0938 PDT, 305 m, SF_6(max) = 1 ppt
6 0945 - 0958 PDT, 183 m, SF_6(max) = 199 ppt

SF_6 released from Pinole from 0600-1500 PDT.

$CBrF_3$ released from the Montezuma Hills from 0900-1100 PDT and from 1300-1400 PDT.

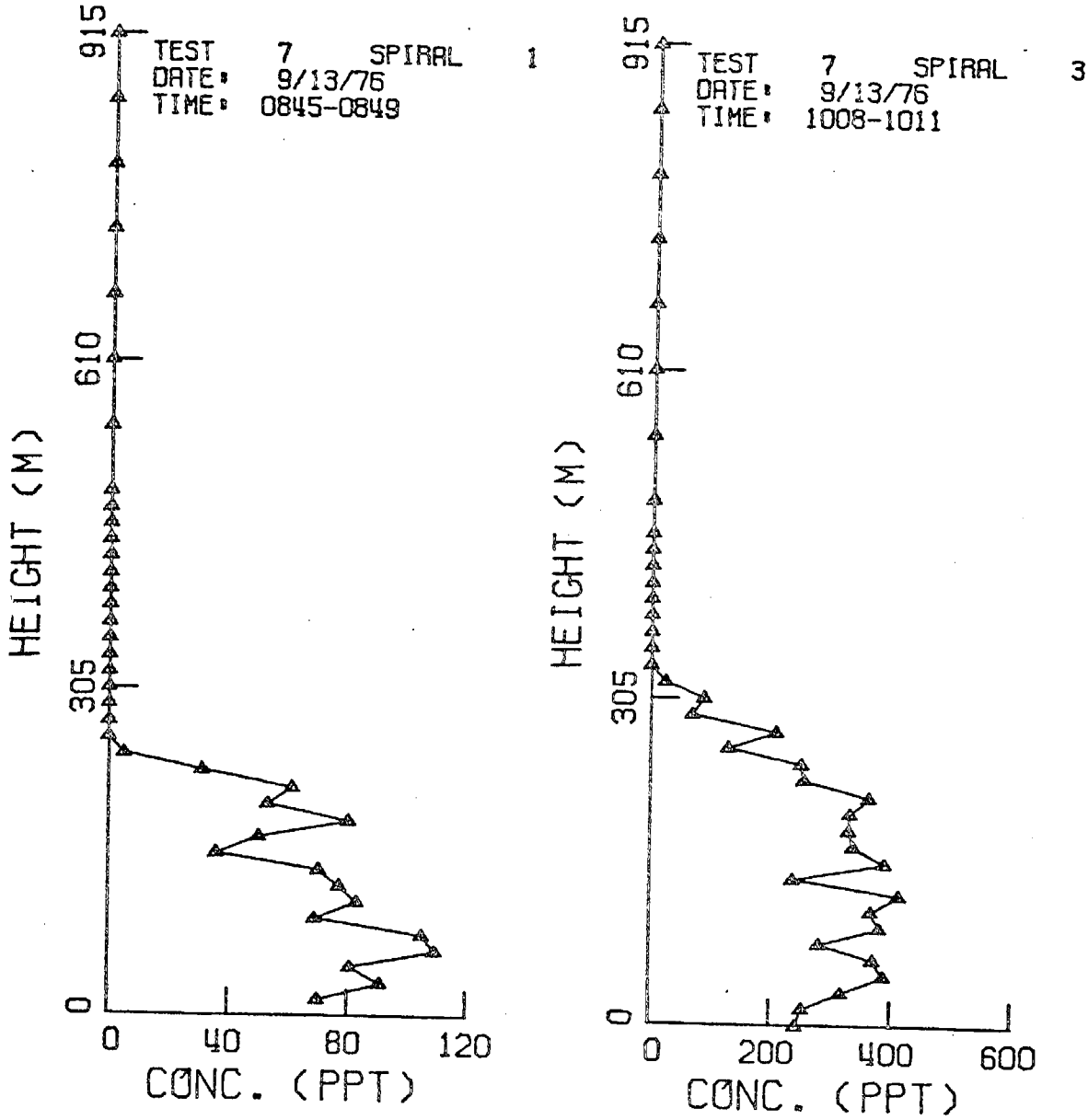

Figure 56. Vertical SF_6 profiles observed 0.8 Km north of the Port Chicago Naval Depot.

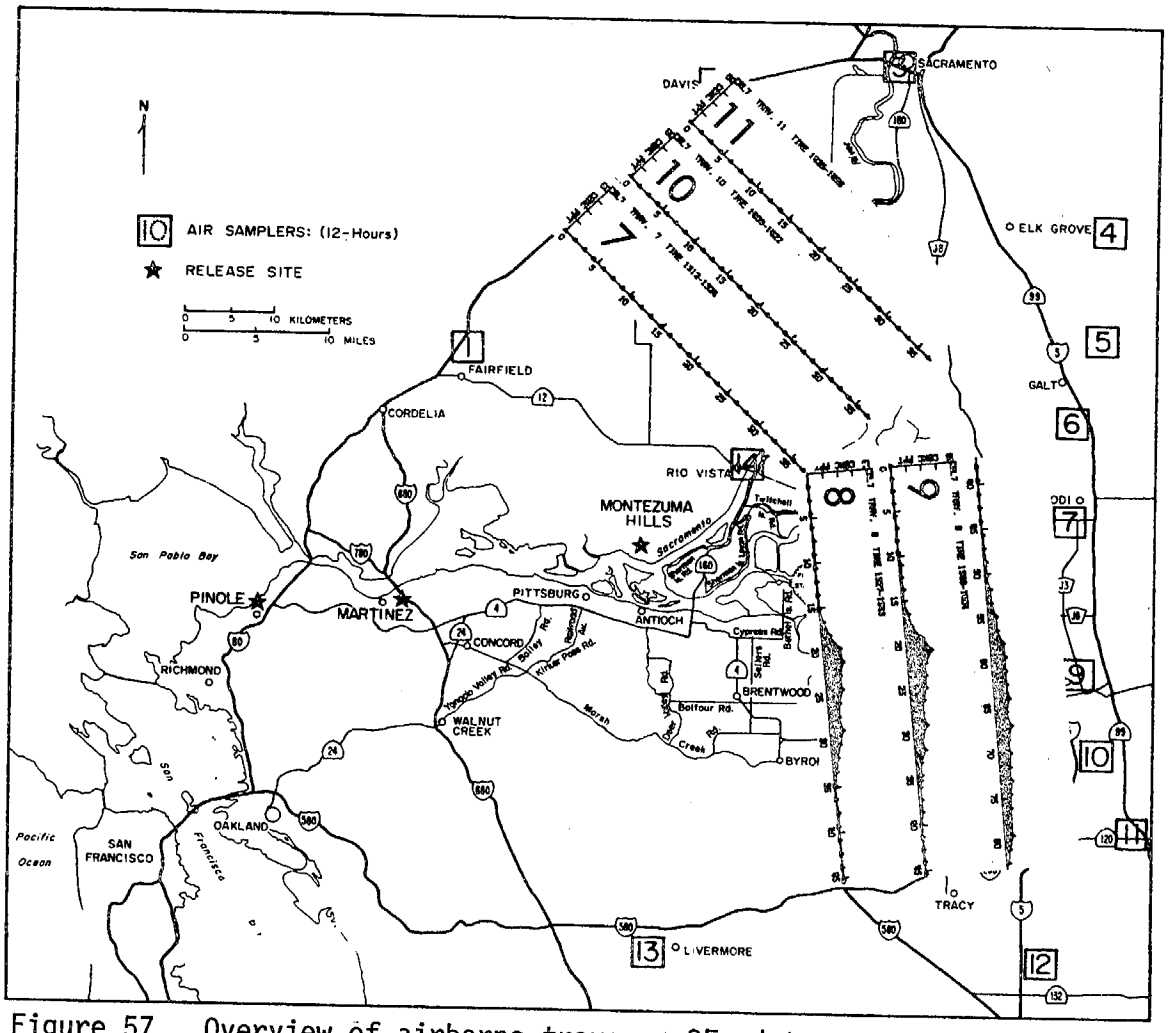

Figure 57. Overview of airborne traverse SF_6 data measured at three altitudes between Vacaville, Isleton, and the I580-I205 junction.

TEST 7

9/13/76

Airborne Traverses:

7	1312-1324 PDT, 183 m,	SF_6(max) =	0 ppt.
8	1327-1343 PDT, 183 m,	SF_6(max) =	19 ppt.
9	1348-1408 PDT, 305 m,	SF_6(max) =	25 ppt.
10	1409-1422 PDT, 305 m,	SF_6(max) =	1 ppt.
11	1428-1456 PDT, 427 m,	SF_6(max) =	15 ppt.

SF_6 released from Pinole from 0600-1500 PDT.

$CBrF_3$ released from the Montezuma Hills from 0900-1100 PDT and from 1300-1400 PDT.

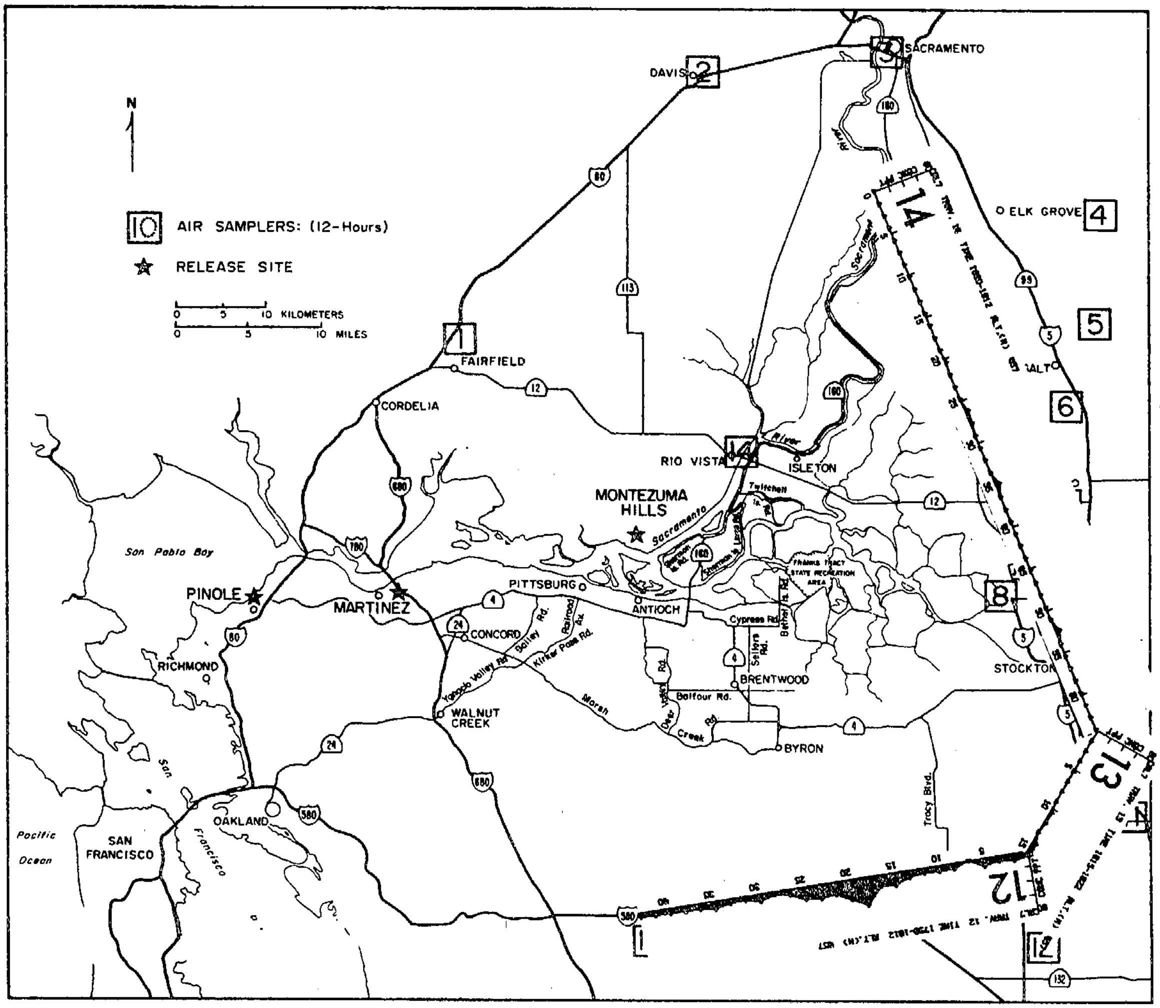

Figure 58. Overview of airborne traverse SF_6 data.

TEST 7

9/13/76

Airborne Traverses:

12 1759 - 1812 PDT, 457 m, SF_6(max) ≅ 29 ppt
13 1815 - 1822 PDT, 457 m, SF_6(max) ≅ 5 ppt
14 1850 - 1912 PDT, 457 m, SF_6(max) ≅ 4 ppt

SF_6 released from Pinole from 0600-1500 PDT.

$CBrF_3$ released from the Montezuma Hills from 0900-1100 PDT and from 1300-1400 PDT.

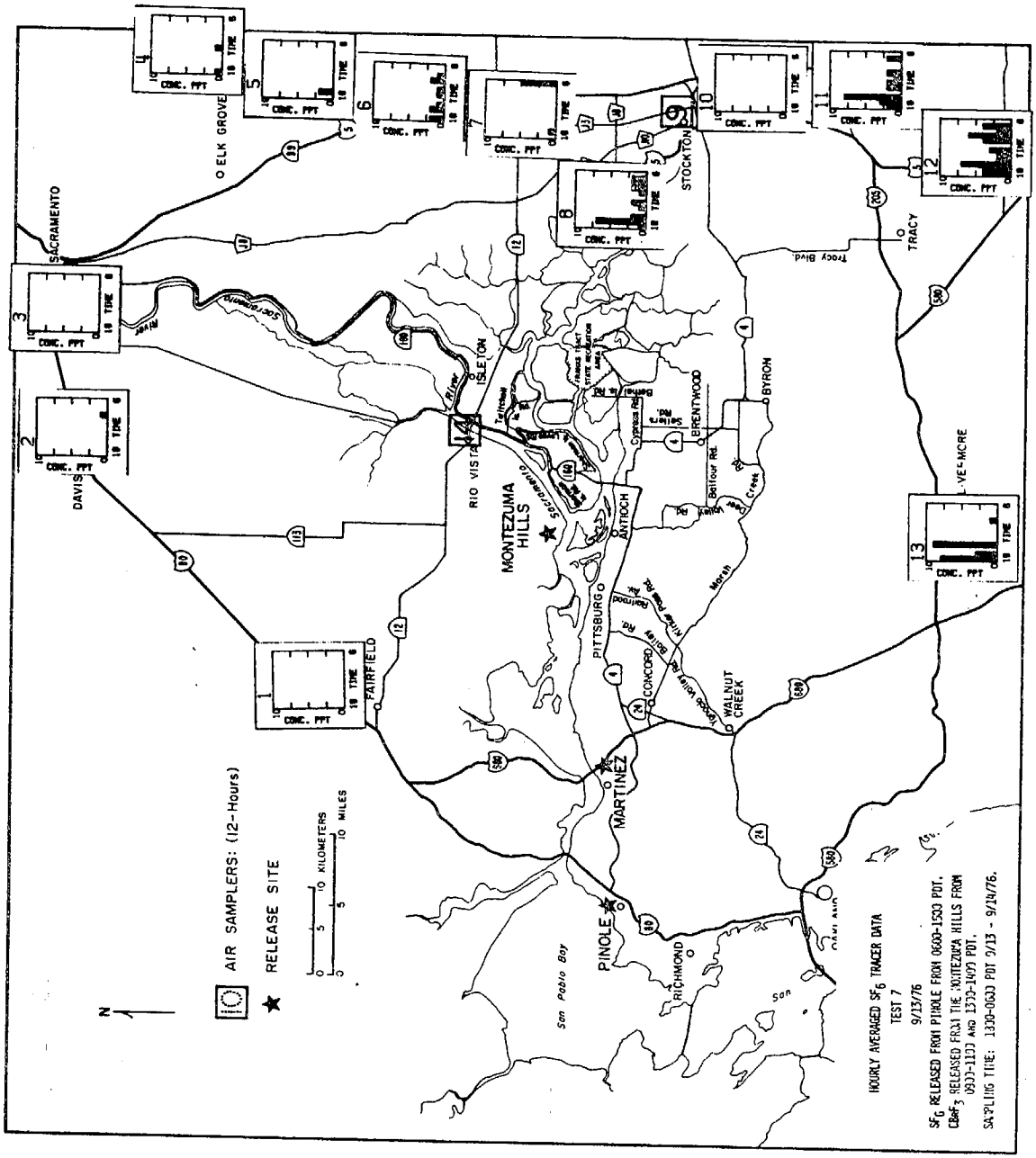

Figure 59. Overview of hourly averaged SF_6 data. Full scale SF_6 = 10 ppt.

4.28 Tracer Test 8 (9/14/76)

The purpose of the final tracer test was to study the transport and dispersion of pollutants flowing through the Carquinez Strait during the development of the afternoon sea breeze. SF_6 was released at a constant rate of 10.9 g/sec (1.04 tons/day) from Pinole between 0730 and 1300 PDT.

The average winds at Rodeo near Pinole were 220° at 3.7 m/sec. The area averaged winds were from 250° at 3.6 m/sec. There were scattered clouds. Stability conditions were assumed to be Pasquill classes B-C. The average mixing height was 1200 meters, and the maximum height observed was 3000 meters around 1200 PDT. The winds during the test followed the streamlines shown in Figure 60 for 1000 PDT. Ozone levels reached no greater than 0.08 ppm in the area during the day.

Four automobile traverses were conducted between 0906 and 1218 PDT along I 680 and Highway 160. As indicated in Figures 61 and 62, the plume passed through the Carquinez Strait at levels as high as 1598 ppt. A wide SF_6 plume was detected along Highway 160 with a maximum level of 78 ppt. No data were collected along Highway 99.

Six airborne traverses were completed above I 680 17 km downwind of Pinole. The data shown in Figure 63 indicate that the plume mixed vertically to 427 meters by the time it passed over I 680. The vertical profile in Spiral 1, Figure 64 , agrees with the crosswind data. As will be discussed in Section 4.4, the elevated crosswind data provide a very accurate means of performing a mass balance on the tracer. In this case, 102% of the material emitted was accounted for by the traverse data. During the final test, no hourly data were collected.

Figure 60. Surface wind streamlines, 1000 PDT, 9/14/76 (MRI).

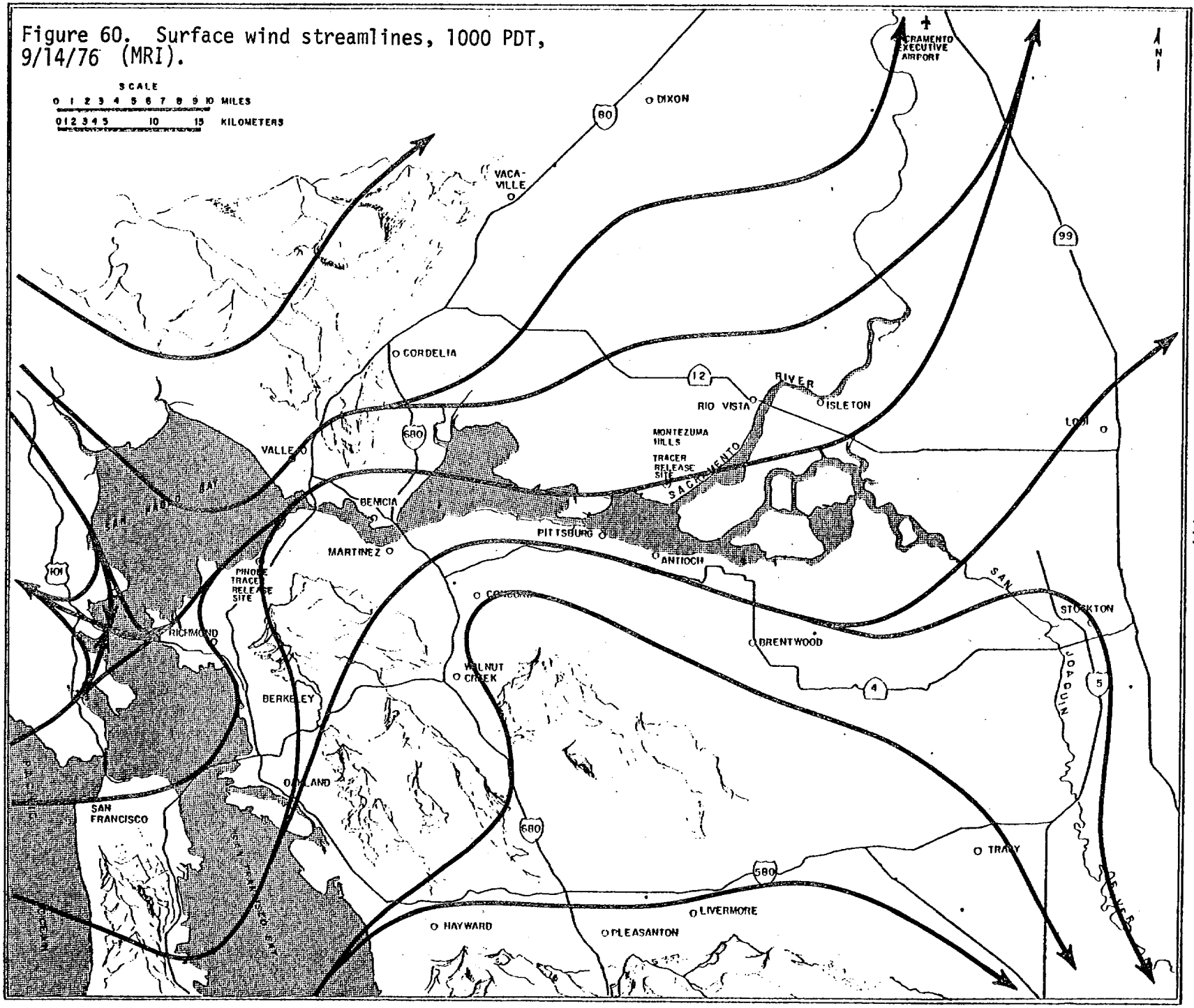

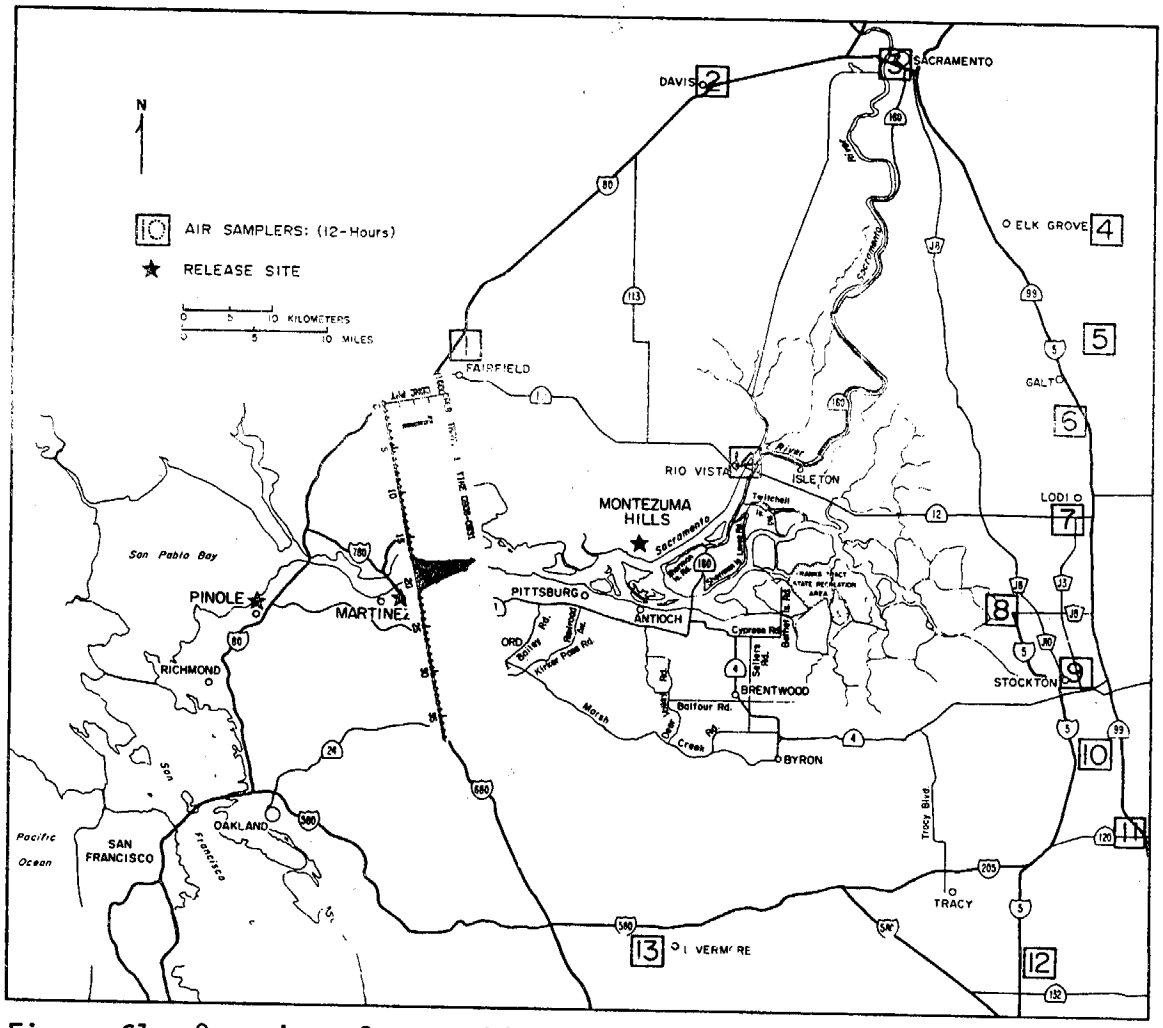

Figure 61. Overview of automobile traverse SF_6 data.

TEST 8

9/14/76

Auto Traverse:

1 0906 - 0931 PDT, SF_6(max) = 1598 ppt

SF_6 released from Pinole from 0730-1300 PDT.

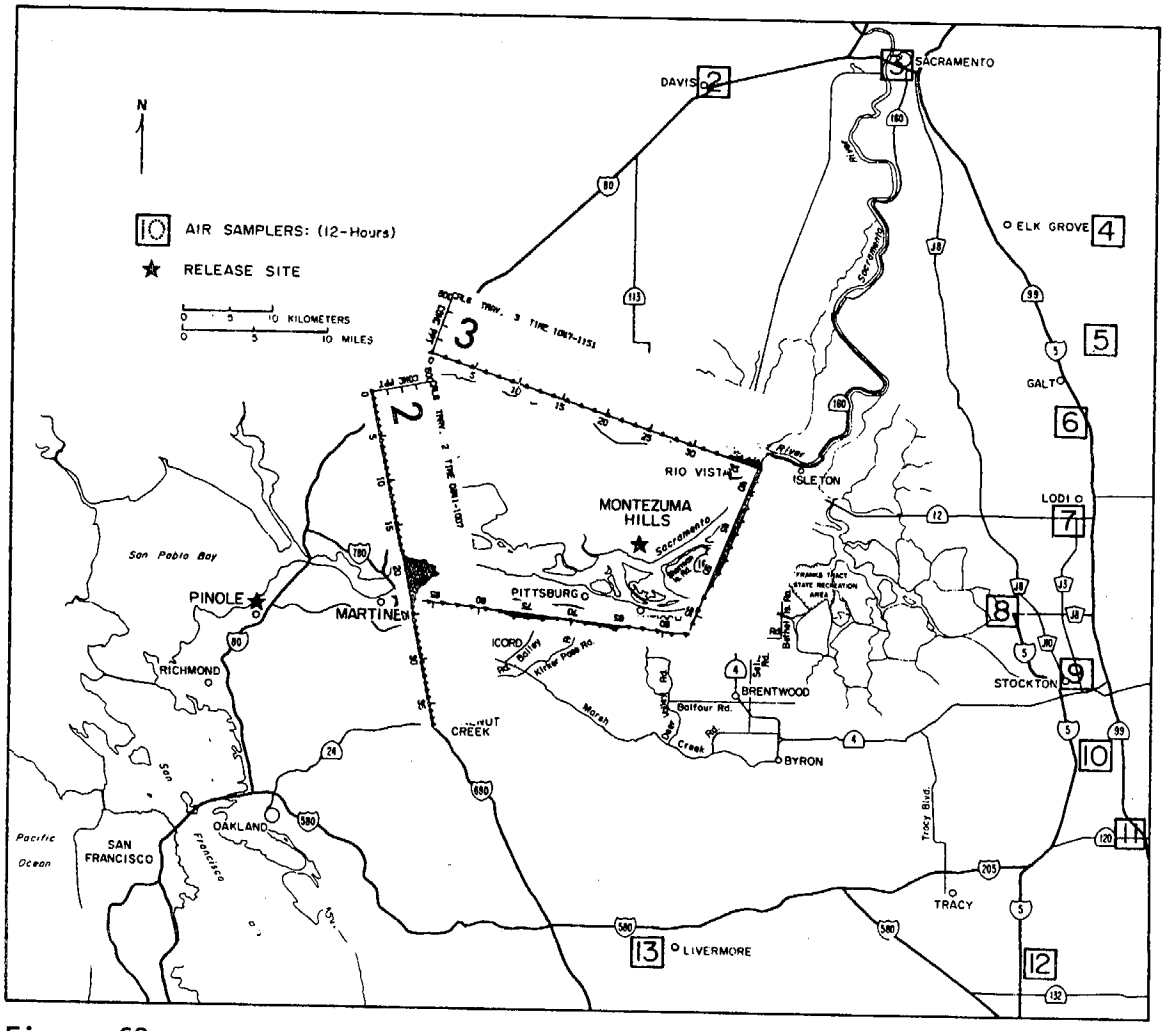

Figure 62. Overview of automobile traverse SF_6 data.

TEST 8

9/14/76

Auto Traverses:

2 0941 - 1007 PDT, SF_6(max) = 412 ppt

3 1047 - 1151 PDT, SF_6(max) = 78 ppt

SF_6 released from Pinole from 0730-1300 PDT.

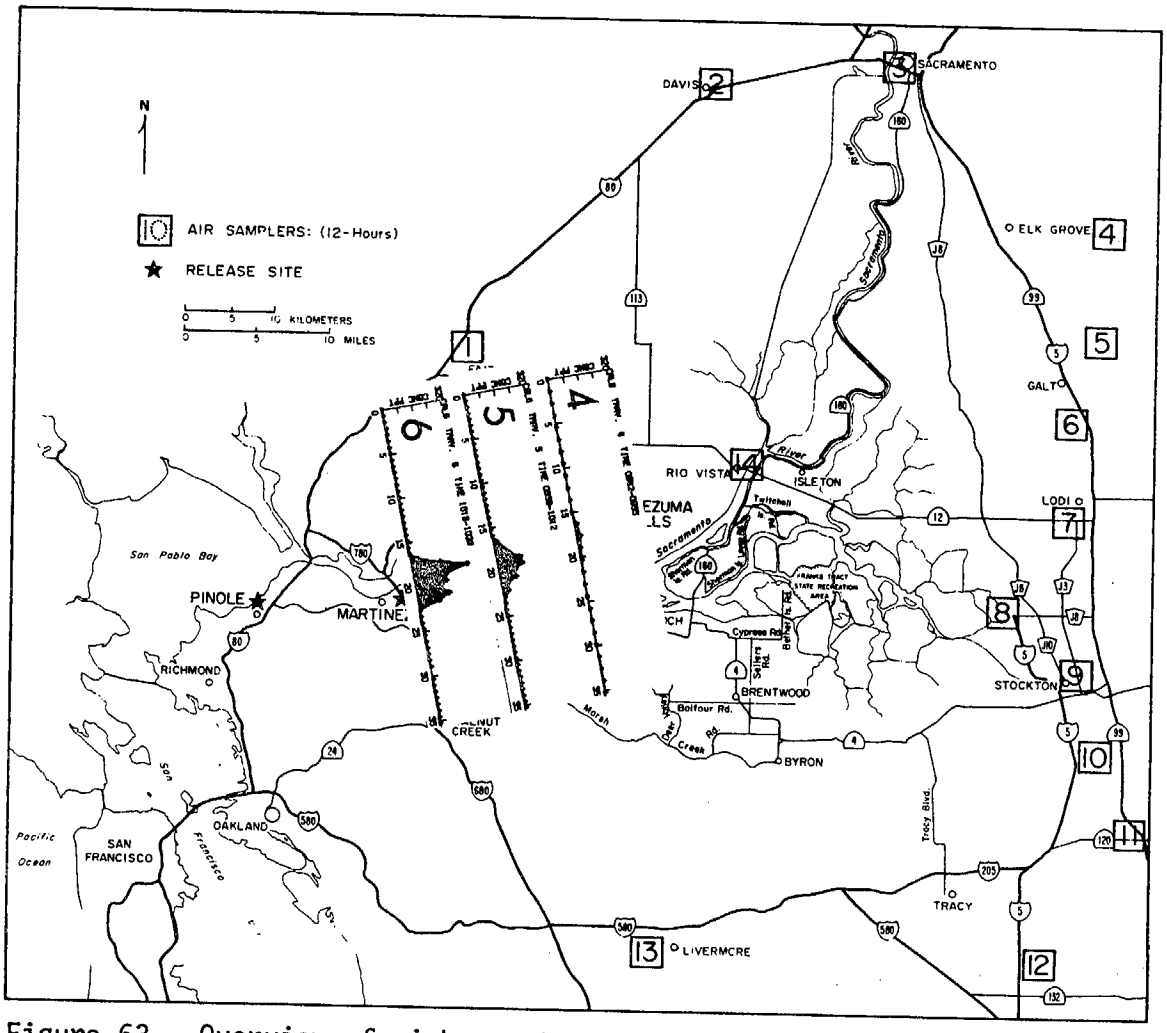

Figure 63. Overview of airborne traverse SF_6 data measured at three altitudes between Cordelia and Walnut Creek.

TEST 8

9/14/76

Airborne Traverses:

4 0942-0955 PDT, 427 m, SF_6(max) = 22 ppt.

5 0959-1012 PDT, 305 m, SF_6(max) = 134 ppt.

6 1016-1028 PDT, 183 m, SF_6(max) = 304 ppt.

SF_6 released from Pinole from 0730-1300 PDT.

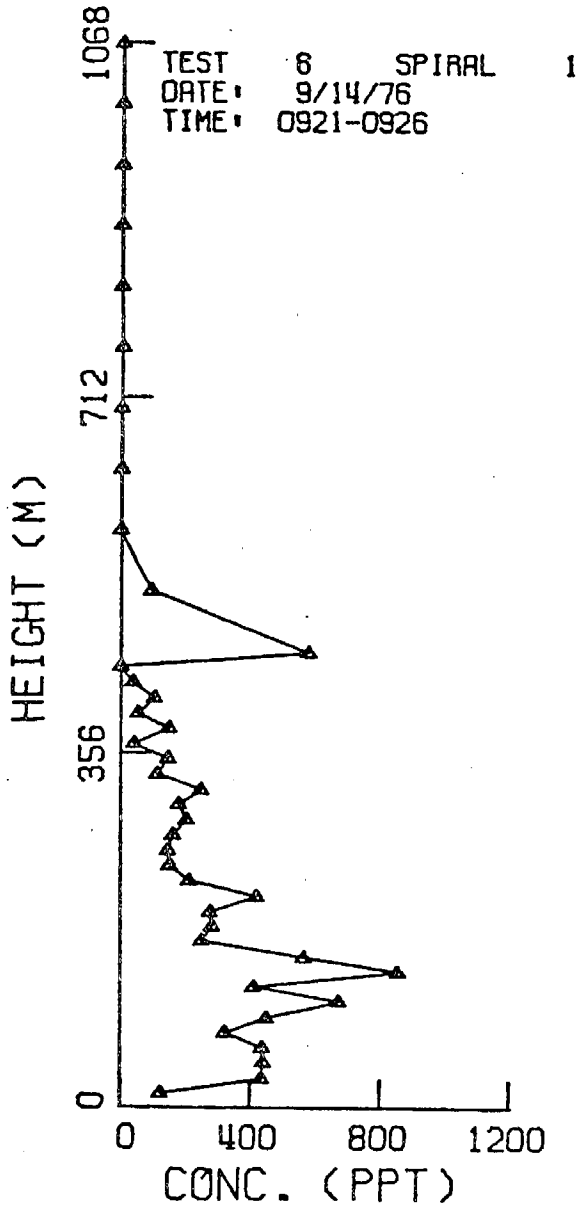

Figure 64. Vertical SF_6 profile observed 0.8 Km north of the Port Chicago Naval Depot.

4.3 Determination of Dispersion Parameters from Automobile Traverse and Airborne Spiral Tracer Data

In order to quantify the dispersion of tracer and pollutants along transport paths through the Delta Region, the Gaussian horizontal crosswind standard deviation for each automobile traverse was determined. By definition

$$Y_0 = \frac{\int_{-\infty}^{\infty} yC(y)dy}{\int_{-\infty}^{\infty} C(y)dy} \tag{2}$$

and

$$\sigma_y = \left[\frac{\int_{-\infty}^{\infty} y^2C(y)dy}{\int_{-\infty}^{\infty} C(y)dy} - Y_0^2\right]^{\frac{1}{2}} \tag{3}$$

where Y_0 is the distance along the traverse to the center line, $C(y)$ is the concentration as a function of distance along the traverse, and σ_y is the horizontal crosswind standard deviation. The centerline concentration, C_0, is given by:

$$C_0 = \frac{\int_{-\infty}^{\infty} C(y)dy}{\sqrt{2\pi}\,\sigma_y} \tag{4}$$

These parameters were determined by numerical integration of the data; see Appendix B for details. When integrated in an iterative procedure, the parameters yield a best-fit Gaussian curve to the traverse data:

$$C(y) = C_0 \exp\left[-\frac{1}{2}\left(\frac{y-Y_0}{\sigma_y}\right)^2\right] \tag{5}$$

The best-fit curves resulting from this analysis are given in Section 3.6 of Volume II, Part A. Typical curves are shown in Figures 65 and 66 of this report; the experimental and best-fit parameters are listed in Table 9. As indicated in the figures, generally most of the traverses conform fairly well to a Gaussian profile.

A similar procedure can be applied to the airborne spiral data to give a best-fit Gaussian vertical profile. The results are shown in Figures 67 and 68. In this case, the curves do not fit the data as well as for the crosswind data. This is a result of the spiral pattern involved in obtaining the data. While we assume that the data represent a vertical profile at a constant crosswind distance from the plume centerline, in reality, the plane was spiraling around a radius of several hundred meters. Also, because the ground is a reflecting plane to the tracer, the tracer material connot be distributed in a perfect Gaussian form. However, determining σ_z from the data does give a measure of the extent of vertical spread. The best-fit results are given in Table 9. We have not presented best-fit crosswind curves to the airborne traverses because the release height was approximately $z = 0$. Correct determination of σ_y for use in the Gaussian model should occur at the plume centerline.

Although airborne data were collected only during the latter three tests, it is possible to estimate values of the vertical crosswind standard deviation, σ_z, for all the tests from the automobile traverse data. If one assumes that the Gaussian plume model can be used to describe the tracer results and, furthermore, that the tracer is conserved between the surface and the height of the mixing layer,

then the crosswind integral of the experimental horizontal tracer data can be written

$$\int_{-\infty}^{\infty} C(y)\,dy \equiv C_{CWI} = \frac{Q}{\sqrt{2\pi}\,\sigma_z\,u}\left\{\exp\left[-\tfrac{1}{2}\left(\frac{Z+H}{\sigma_z}\right)^2\right] + \exp\left[-\tfrac{1}{2}\left(\frac{Z-H}{\sigma_z}\right)^2\right] + \sum_{n=1}^{4}\left(\exp\left[-\tfrac{1}{2}\left(\frac{z+H-2nL}{\sigma}\right)^2\right] + \exp\left[-\tfrac{1}{2}\left(\frac{z-H-2nL}{\sigma_z}\right)^2\right] + \exp\left[-\tfrac{1}{2}\left(\frac{z-H+2nL}{\sigma_z}\right)^2\right] + \exp\left[-\tfrac{1}{2}\left(\frac{z+H+2nL}{\sigma_z}\right)^2\right]\right)\right\} \quad (6)$$

when C_{CWI} has been defined as the crosswind-integrated concentration, Q is the average tracer release rate, u is the average wind velocity, H is the release height and L is the mixing layer height. The summation terms represent reflection of tracer from the top of the mixing layer. Equation (6) can be solved for σ_z using a numerical iterative procedure. The accuracy of such a solution is a function of the accuracy with which measured values of u and L represent the actual average meteorological conditions. In this analysis values of u were obtained by vector-averaging wind data available downwind of the release point. Values of L were obtained by averaging the data from the available measurements. The results of the analysis are presented in Table 9 for traverses where it appeared that the assumptions and necessary conditions were reasonable.

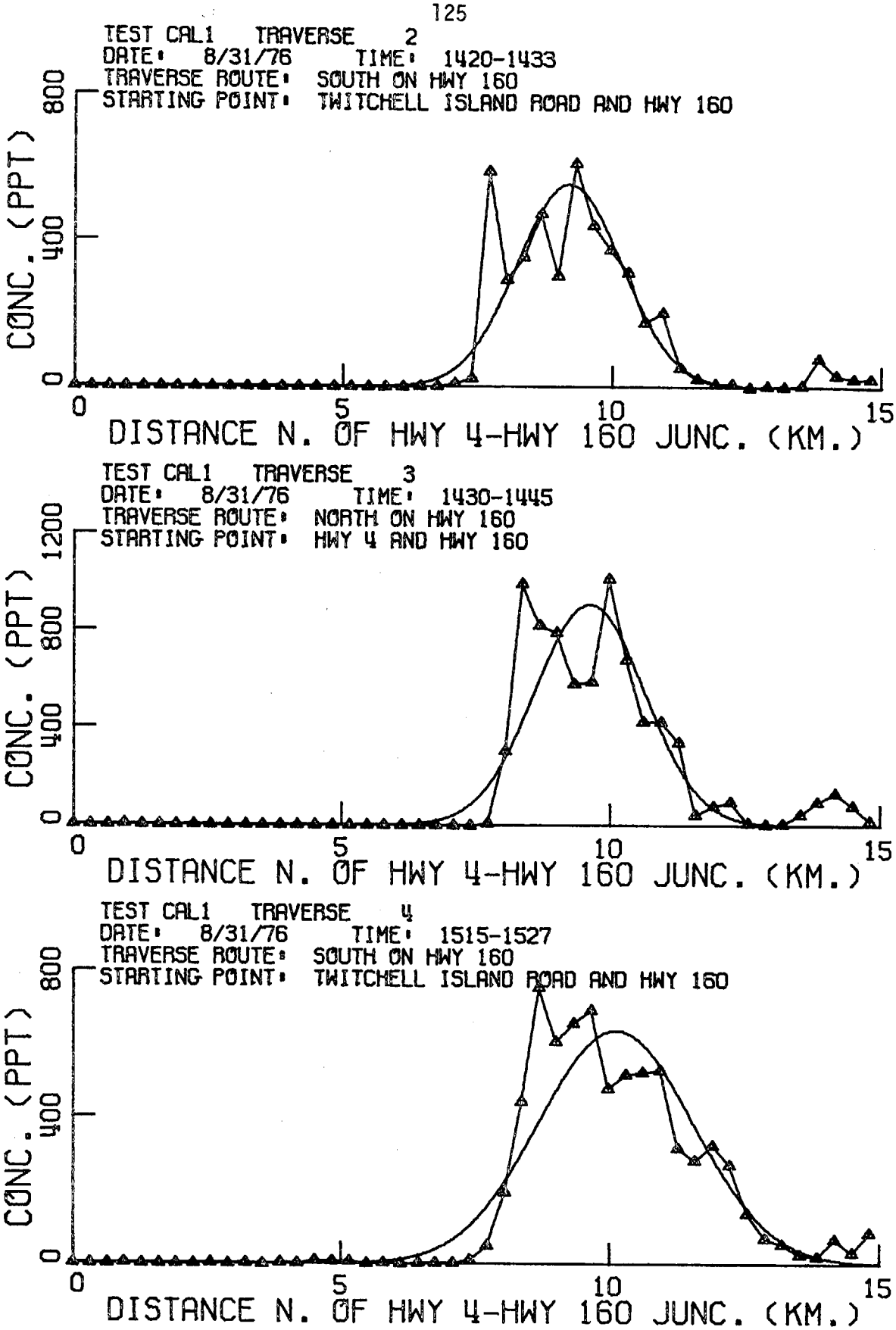

Figure 65. Gaussian best-fit curves through the automobile traverse tracer data.

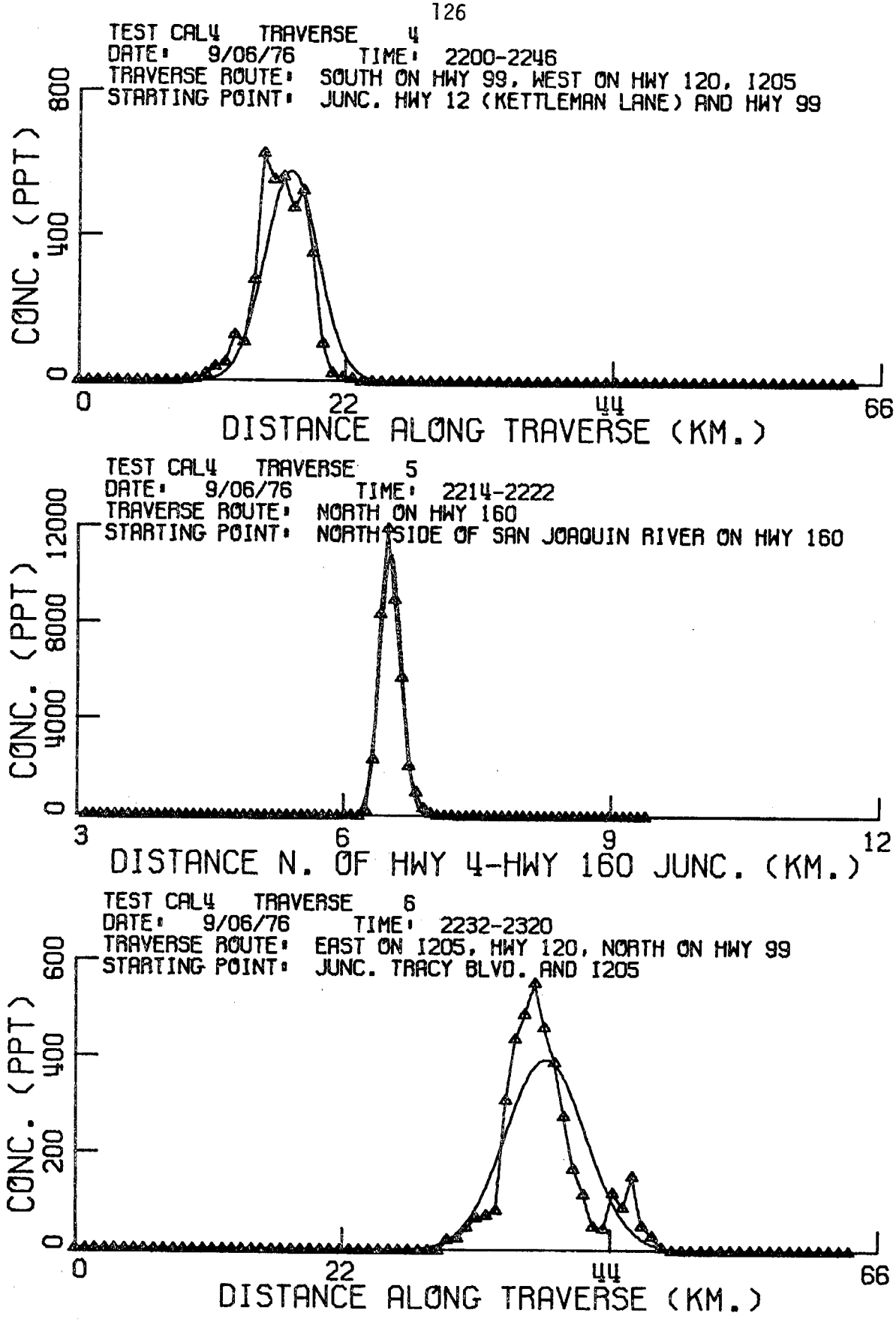

Figure 66. Gaussian best-fit curves through the automobile traverse tracer data.

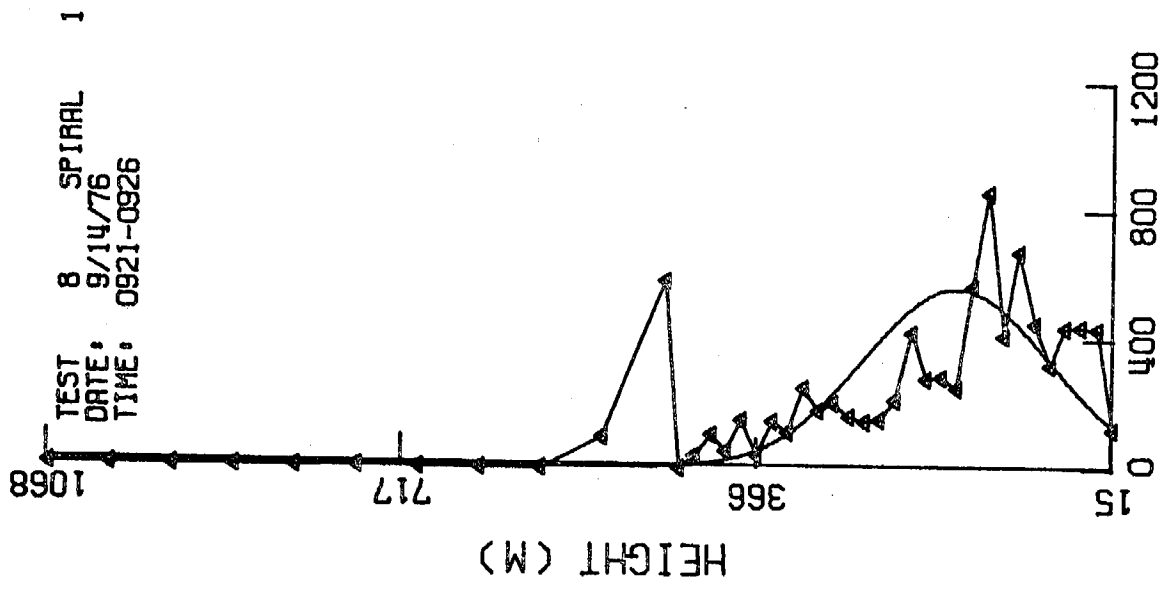

Figure 68. Gaussian best-fit curve through the airborne spiral tracer data.

TABLE 9

BEST-FIT GAUSSIAN CURVE RESULTS

Automobile Traverse Data

Trav	Time PDT	C_o exp	C_o fitted (PPT)	Y_o exp	Y_o fitted (Km)	X (km)	σ_y (meters)	σ_z* (meters)
Test 1 (8/31/76) SF_6 Release Rate = 10.6 grams/sec								
2	1420-1433	611	554	9.3	9.2	7.3	879	200
3	1430-1445	1013	908	10.0	9.6	8.1	909	118
4	1515-1527	756	638	8.7	10.1	6.6	1299	126
6	1630-1641	1223	560	8.0	8.9	6.5	946	198
7	1701-1753	64	41	65.2	65.8	51.9	9446	626
Test 2 (9/02/76) SF_6 Release Rate = 11.4 g/sec $CBrF_3$ Release Rate = 16.6 g/sec								
1	1130-1143	30000	21830	5.5	5.9	1.3	312	22
2	1215-1228	30000	30210	13.8	14.2	0.8	296	17
4	1400-1415	33	26	11.6	11.6	35.2	2235	
($CBrF_3$) 4	1400-1415	2168	1228	7.7	7.7	10.7	138	657
5	1445-1503	19	10	10.6	11.4	34.1	2673	
($CBrF_3$) 5	1445-1503	840	510	8.7	9.1	10.0	487	405
6	1515-1530	28	4	8.7	10.2	32.8	4289	
7	1545-1635	304	251	6.8	5.0	25.3	115	394
9	1630-1715	29	12	57.9	60.2	70.9	24950	1169
10	1630-1737	91	16	48.3	61.2	67.4	10692	1014
($CBrF_3$) 10	1630-1737	300	111	82.1	80.6	57.0	6227	317
11	1731-1815	32	17	49.1	35.2	73.5	18340	479

*Values of σ_z were determined from a mass-balance procedure using the horizontal crosswind traverse data.

TABLE 9 (cont.)

BEST-FIT GAUSSIAN CURVE RESULTS

Automobile Traverse Data

Trav	Time PDT	C_o exp (PPT)	C_o fitted (PPT)	Y_o exp (Km)	Y_o fitted (Km)	X (km)	σ_y (meters)	σ_z* (meters)
Test 3 (9/5/76) SF_6 Release Rate = 9.5 g/sec								
1	0100-0112	8146	9476	6.1	6.1	7.3	142	35
3	0213-0259	537	458	32.2	34.4	51.7	2480	72
4	0240-0300	1856	1944	7.4	7.4	7.3	141	166
6	0259-0306	8660	4298	6.8	6.8	7.3	136	97
8	0414-0545	370	283	54.7	55.8	47.4	4503	85
9	0430-0445	6178	6775	7.2	7.3	7.3	116	80
10	0432-0517	608	506	29.5	31.3	39.5	1936	100
11	0441-0450	2852	2288	7.1	7.2	7.3	151	183
12	0502-0511	2261	1502	6.6	6.6	7.3	195	229
14	0637-0647	173	121	1.6	0.5	37.2	4685	517
Test 4 (9/6/76) SF_6 Release Rate = 10.8 g/sec								
1	1928-1946	873	710	7.1	7.2	7.3	210	
2	2130-2217	746	680	15.3	15.8	50.9	2072	93
3	2132-2140	10570	8825	7.1	7.2	7.3	191	45
4	2200-2246	628	580	15.3	17.5	50.9	1987	109
5	2214-2222	11900	10820	6.5	6.5	7.3	118	59
6	2232-2320	553	396	37.8	38.7	54.5	2787	114
7	2315-2400	553	281	35.4	39.9	58.8	3819	142

*Values of σ_z were determined from a mass-balance procedure using the horizontal crosswind traverse data.

TABLE 9 (cont.)

BEST-FIT GAUSSIAN CURVE RESULTS

Automobile Traverse Data

Trav	Time PDT	C_o exp (PPT)	C_o fitted (PPT)	Y_o exp (Km)	Y_o fitted (Km)	X (km)	σ_y (meters)	σ_z* (meters)
Test 5 (9/9/76) SF_6 Release Rate = 10.7 g/sec								
1	1255-1315	801	363	11.9	12.6	9.1	721	
2	1314-1330	528	288	8.4	8.9	9.4	877	
4	1351-1405	138	136	1.0	1.4	17.7	1192	
5	1356-1428	108	87	2.9	1.1	24.3	2416	
6	1359-1416	445	285	18.3	15.8	10.6	1636	1228
7	1413-1426	141	111	8.7	9.5	18.5	1525	
8	1436-1450	183	131	3.9	4.2	18.6	1382	
Test 6 (9/10/76) SF_6 Release Rate								
1	0800-0815	9526	21500	1.8	1.8	4.8	27	196
2	0740-0753	7981	9257	6.6	6.5	7.3	110	110
3	1001-1051	20	10	59.5	56.8	47.6	4164	
4	1023-1033	3739	2393	6.0	6.1	11.7	275	135
5	1030-1115	11	11	59.5	60.3	47.6	3062	
6	1022-1033	5954	4179	7.6	7.6	7.3	129	165
7	1103-1112	7155	6346	7.5	7.5	7.3	185	76
8	1105-1203	12	10	1.6	4.7	45.8	2975	
Airborne Spirals								
				(m)	(m)		σ_z**	
1	1158-1203	908	692	122	112	19.5	38	

* Values of σ_z were determined from a mass-balance procedure using the horizontal crosswind traverse data.

** Values of σ_z were obtained from a Gaussian best-fit of the spiral tracer data.

TABLE 9 (cont.)

BEST-FIT GAUSSIAN CURVE RESULTS

Automobile Traverse Data

	Trav	Time PDT	C_o exp	C_o fitted	Y_o exp	Y_o fitted	X (km)	σ_y (meters)	σ_z* (meters)
			(PPT)		(Km)				
Test 7 (9/13/76) SF_6 Release Rate = 11.5 g/sec									
$CBrF_3$ Release Rate = 16.0 g/sec									
	1	0924-0956	614	459	33.8	37.2	15.3	3714	1388
($CBrF_3$)	2	0940	12140	5896	1.7	1.5	4.6	310	106
	3	1113-1217	94	60	48.3	52.3	50.7	4697	736
	4	1130-1146	180	151	24.1	25.1	22.0	6165	3481
	6	1340-1414	131	87	30.6	23.0	22.4	6944	792
	7	1429-1451	14	15	14.5	19.6	47.4	3881	
	8	1450-1706	200	95	29.0	27.8	5.6	375	492
	8	1450-1706	30	21	141.6	140.9	54.7	13203	
	9	1458-1532	12	10	9.7	8.5	52.7	1654	
	10	1537-1611	16	12	22.5	29.0	22.9	6746	
	11	1654-1820	12	7	117.5	118	65.9	14520	
	12	1654-1820	13	11	24.1	13.6	42.8	9881	
			Spirals						
					(m)	(m)		σ_z**	
	1	0854-0849	109	109	61	113	21.5	59	
	3	1008-1011	413	485	122	141	21.5	77	

*Values of σ_z were determined from a mass-balance procedure using the horizontal crosswind traverse data.

**Values of σ_z were obtained from a Gaussian best-fit of the spiral tracer data.

4.4 Mass Balance of Tracer Data

The integration of the automobile and airborne traverse data over the crosswind traverse distance can be used to determine the average flux of tracer gas passing through the traverse vertical plane. This flux can then be compared to the amount of tracer released at the source to provide a mass balance on the experimental data:

$$\% \text{ tracer observed} = \left(\frac{\int_{-\infty}^{\infty} \int_{0}^{L} u(z) C(y,z) \, dz \, dy}{Q} \right) \cdot 100 \qquad (7)$$

where Q is the release rate, L is the height of the mixing layer, u(z) is the wind velocity, and C(y,z) is the tracer concentration. The accuracy of this mass balance is obviously subject to the uncertainties involved in determining the vertical profiles of the wind speed and tracer concentration. This expression may be simplified by considering a constant average wind velocity, $u(z) = \bar{u}$, and a uniform vertical tracer distribution, $C(z,y) = \bar{C}(y)$, over a height ℓ. For convenience in treating the data, the double integral is approximated by a series of single integrals:

$$\% \text{ tracer observed} = \bar{u} \sum_{i=1}^{n} \ell_i \left(\int_{-\infty}^{\infty} \bar{C}(y) \, dy \right)_i \cdot \frac{100}{Q} \qquad (8)$$

where $\sum_{i}^{n} \ell_i$ equals the height of the mixing layer. In the following calculations, $\bar{u}$ was obtained by vector averaging the available hourly wind data from points downwind of the source and the average mixing height was also obtained from the available data. For cases where only surface tracer data were available, we took n=1 and assumed that the tracer was

vertically well-mixed from the surface to the height of the mixing layer, ℓ=L. Where traverse data were available at more than one height, n was taken to be the number of traverses and ℓ_i was taken to be a height arbitrarily assigned to each crosswind traverse. In this case, the tracer was assumed to be vertically well-mixed over a discrete portion of the mixing layer.

During Test 7 and 8, two sets of airborne traverses provided data for using the expression $n > 1$. In both cases, the mass balance results were remarkably accurate; the estimates of 113% and 102% of the tracer observed for Traverses 8, 9, 11 (Test 7) and for Traverses 4, 5, 6 (Test 8) give an indication of the usefulness of deriving the mass balance in this manner.

In many cases, particularly for automobile traverses close to the source, assuming a uniform vertical concentration distribution widely overestimates the flux of tracer. For this reason, we have performed the mass balance only where airborne data were available or transport distances were large. The results are given in Table 10.

In view of the assumptions necessary for the analysis, the mass balance results are very good. During the daytime tests when the extent of vertical mixing was the greatest, the results generally are no more than a factor of 2 over 100% of the tracer observed. In cases where the results are too low, closer examination of the traverses indicates that, in most cases, the traverses did not cover the entire plume. For example, in Test 2, Traverses 4, 5, and 6 were taken along Highway 160 where it appears that the SF_6 tracer plume was wider than the traverse paths.

The mass balance analysis can be reversed by assuming 100% of the tracer was observed and by predicting either the mixing height or wind velocity necessary to achieve this condition. These results are also given in Table 10. In traverses where the mass balance was overestimated, the predicted mixing height gives an indication of the extent of vertical mixing which did occur. During Tests 3 and 4 under nighttime stable conditions, the predicted heights are approximately between 100 and 200 meters while the estimated mixing height was between 500 and 800 meters. Although no airborne data were available, one can assume from the mass balance results that the plume remained within the lowest 100-200 meters of the atmosphere. Even though the estimated mixing heights were relatively low, the extent of vertical mixing of the tracer plume was not great enough to be influenced by the depth of the mixing layer. During nighttime conditions, the tracer was not well-mixed in the vertical direction even at downwind distances of 50 km.

Another means of determining the extent of vertical mixing is to solve the transient diffusion equation and estimate the distance in the vertical direction to which tracer diffuses. This leads to the approximation:

$$\frac{K_{zz}t}{L_z^2} \sim 1 \tag{9}$$

or

$$L_z = \sqrt{K_{zz}t} \tag{10}$$

where K_{zz} is the vertical eddy diffusivity, t is the transport time and L_z is the vertical distance to which tracer diffuses. Values of L_z can be

calculated if one assumes that

$$\sigma_z = \sqrt{2K_{zz}t} \tag{11}$$

which is obtained from comparing the solution of the diffusion equation with the Gaussian plume model expression (Seinfeld, 1975).

Substituting for $K_{zz}t$ gives

$$L_z = \frac{\sigma_z}{\sqrt{2}} \tag{12}$$

where σ_z can be determined from the automobile traverse data. For example, using Test 3, Traverse 3 data, we take σ_z to equal 72 meters and calculate that L_z equals 51 meters. Thus, the tracer only diffuses to 51 meters over a transport distance of 52 km. The estimated depth of the mixing layer during this time was 700 meters.

The overall average % of tracer observed as given in Table 10 indicates that essentially all of the tracer released was accounted for in the traverse tracer data. During the daytime hours, the plumes appear to be relatively well-mixed in the vertical direction at downwind distances of 30 km or more. Results from the evening and nighttime tests indicate that the plumes were not vertically well-mixed even at downwind distances of 50 km. We have already seen in the individual test summaries that tracer concentrations measured during the evening and nighttime tests were much higher than concentrations observed during the daytime. The mass balance results confirm the description of evening and nighttime plumes as being narrow and having extremely low rates of dispersion with travel distance.

TABLE 10

TRACER MASS BALANCE RESULTS

Trav	Time	X (km)	L (m)	u (m/sec)	% tracer observed	L_{pred} (m)	u_{pred} (m/sec)
Test 1 (8/31/76)							
7*	1701-1753	51.9	1600	295/3.5	204	784	1.7
Test 2 (9/2/76)							
4*	1400-1415	35.2	780	290/6.2	36	2167	17.2
4	1400-1415	10.7	780	290/6.2	74($CBrF_3$)	1053	8.4
5*	1445-1503	34.1	980	290/6.2	20	4900	31.0
5	1400-1415	10.0	980	290/6.2	134($CBrF_3$)	731	4.6
6*	1515-1530	32.8	980	290/6.8	14	7000	49
7	1545-1635	25.3	1180	290/5.4	239	494	2.3
9*	1630-1715	70.9	1500	290/4.6	110	1364	4.2
10*	1630-1737	67.4	1500	300/4.2	121	1240	3.5
10	1630-1737	57.0	1500	300/4.2	331($CBrF_3$)	416	1.2
11*	1731-1815	73.5	1500	290/4.8	250	600	1.9
				AVE.	136		
Test 3 (9/5/76)							
3	0213-0259	51.7	700	280/6.2	774	90	0.8
8	0414-0545	47.4	690	280/4.7	649	106	0.7
10	0432-0517	39.5	700	270/5.2	558	125	0.9
14*	0637-0647	37.2	740	306/3.3	118	627	2.8
				AVE.	525		

* Traverse data indicate that only a portion of the plume was traversed.

TABLE 10 (cont.)

TRACER MASS BALANCE RESULTS

Trav	Time	X (km)	L (m)	u (m/sec)	% tracer observed	L pred (m)	u pred (m/sec)
Test 4 (9/6/76)							
2	2130-2217	50.9	600	280/4.4	515	117	0.9
4	2200-2248	50.9	600	270/4.6	440	136	1.0
6	2232-2320	54.5	570	270/4.6	400	143	1.2
7	2315-2400	58.8	545	300/3.8	307	178	1.2
					AVE. 416		
Test 5 (9/9/76)							
1	1255-1315	9.4	3000	31/1.8	198	1515	0.9
2	1314-1330	9.4	3000	31/1.8	189	1587	1.0
4*	1351-1405	17.7	3000	9/1.1	66	4545	1.7
5*	1356-1428	24.3	3000	338/0.8	47	6383	1.7
6	1359-1416	10.6	3000	252/1.0	195	1538	0.5
7	1413-1426	18.5	3000	338/0.8	53	5660	1.5
8	1436-1450	18.6	3000	338/0.8	61	4918	1.3
					AVE. 116		
Test 6 (9/10/76)							
3*	1001-1051	47.6	540	115/1.1	3	18000	37
5*	1030-1115	47.6	810	272/1.1	4	20000	28
8*	1106-1203	45.8	930	270/2.1	7	13000	30
Airborne							
4	1044-1052	37.2	810	260/5.5	89	909	6.2
10	1000-1039	43.3	540	260/5.5	15	3666	37
12	1200-1239	43.8	1200	270/3.0	21	5669	14
					AVE. 23		

TABLE 10(cont.)

TRACER MASS BALANCE RESULTS

Trav	Time	X (km)	L (m)	u (m/sec)	% tracer observed		L_{pred} (m)	u_{pred} (m/sec)
Test 7 (9/13/76)								
1	0924-0956	15.3	300	230/1.5	95		316	1.6
3	1113-1217	50.7	1475	290/3.0	160		922	1.9
4*	1130-1146	22.0	400	290/2.8	70		571	4.0
6	1340-1414	22.4	1500	230/1.3	151		993	0.9
7	1429-1451	47.4	1100	310/4.1	33		3333	12.4
8	1450-1706	54.7	1500	270/4.5	243		617	1.9
9	1458-1522	52.7	960	280/3.6	7		14000	51
10	1537-1611	22.9	1500	280/3.5	56		2679	6.3
11*	1654-1820	65.9	545	260/4.5	24		2271	18.7
12*	1835-1901	42.8	500	260/4.8	30		1667	16.0
				AVE.	87			
Airborne								
6	0945-0958	17.1	300	310/0.9	8		3807	11.4
8	1327-1343	61.6	244=ℓ_1	280/1.7	4	} 113 total		
9	1348-1404	61.4	122=ℓ_2	280/1.7	3			
11	1428-1456	61.7	2134=ℓ_3 L=2500	290/1.3	106		2212	1.5
12	1759-1812	72.7	2500	280/4.2	120		2079	3.5
				AVE.	80			

TABLE 10 (cont.)

TRACER MASS BALANCE RESULTS

Trav	Time	X (km)	L (m)	u (m/sec)	% tracer observed	L_{pred} (m)	u_{pred} (m/sec)
Test 8 (9/14/76)							
1	0906-0931	14.4	350	270/2.2	110	318	2.0
2	0941-1007	15.7	480	270/2.2	61	787	3.6
3	1047-1151	48.9	800	240/4.2	168	476	2.5
4	1154-1218	18.4	300	270/3.1	13	2308	23.8
				AVE.	88		
Airborne							
3	0858-0911	17.4	350	270/3.6	18	1951	20.1
4	0942-0955	17.4	114=ℓ_1	220/3.6	2		
5	0959-1012	17.2	122=ℓ_2	190/6.3	20	102 total	
6	1016-1028	17.2	244=ℓ_3	190/6.3	80	471	6.2
			L=480	AVE.	60		

Overall Average: 154% of tracer observed in 51 crosswind traverses

With Tests 3 and 4 omitted,

Overall Average: 95% of tracer observed in 43 crosswind traverses

4.5 Analysis of Dispersion

The results of the Gaussian best-fit procedure for the automobile traverse data can be used to determine the relationship of the dispersion parameters, σ_y and σ_z, to the transport distance, x. In terms of the usual dispersion coefficients, these relationships are given by

$$\sigma_y = ax^b \tag{13}$$

and

$$\sigma_z = cx^d \tag{14}$$

where x is taken to be in meters. The values of the coefficients a, b and c, d can be found by plotting each dispersion parameter as a function of x and determining a linear least-squares fit to the data. Typical results of this calculation are shown in Figures 69 - 72; dispersion data for every tracer test are given in Volume II, Part A, Section 3.11. The dispersion coefficients associated with each tracer release are listed in Table 11.

We have considered only the automobile traverse data in this analysis. The results for Tests 2 and 7 were determined separately for each of the release points. Generally, the scatter in the σ_y data is reasonably small, and the best-fit lines provide good representations of the dispersion data. The best-fit of Test 2 data does not include two points at 0.8 km; effects of the local terrain appear to dominate the dispersion at close downwind distances. In the Test 7 results, the scatter is larger and the line serves only as a rough approximation to the data. During Test 7, no single well-defined plume was observed; tracer released from Pinole diverged widely across the Delta Region and into the Livermore-Stockton area. Automobile traverses in several cases did

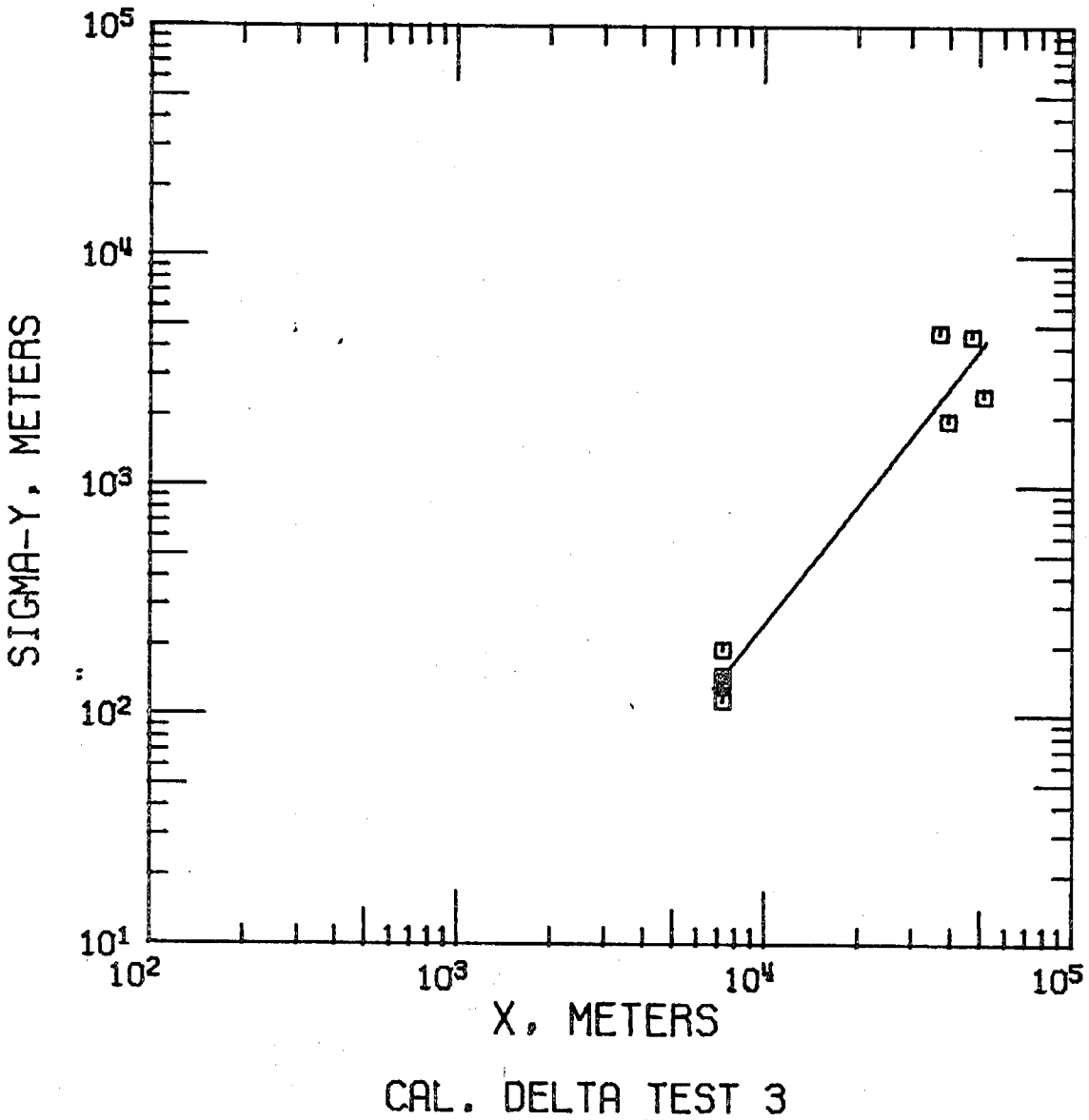

Figure 69. Horizontal crosswind dispersion parameter, σ_y, as a function of distance downwind of the Dow site.

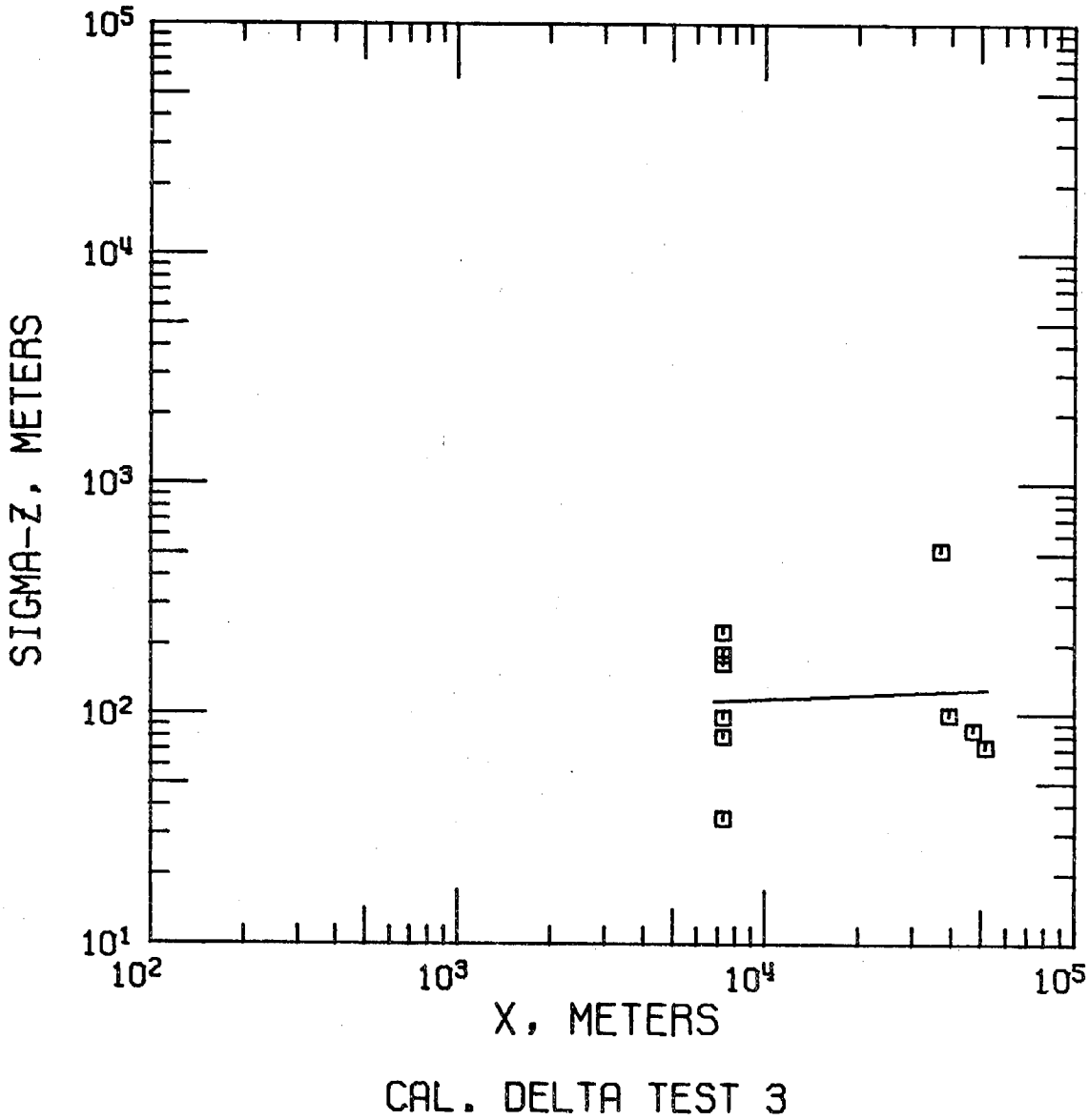

Figure 70. Vertical crosswind dispersion parameter, σ_z, as a function of distance downwind of the Dow site.

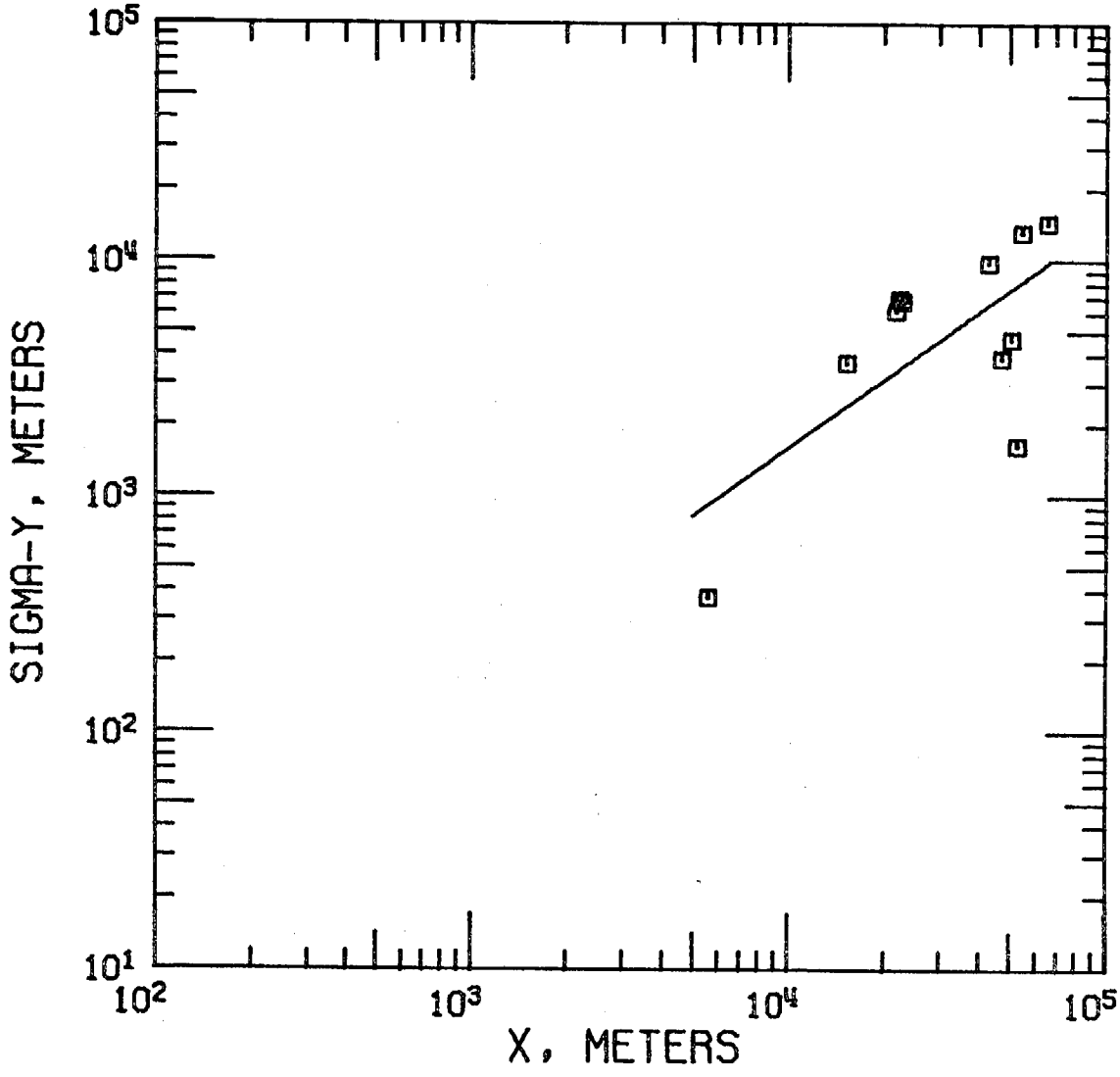

Figure 71. Horizontal crosswind dispersion parameter, σ_y, as a function of distance downwind of Pinole.

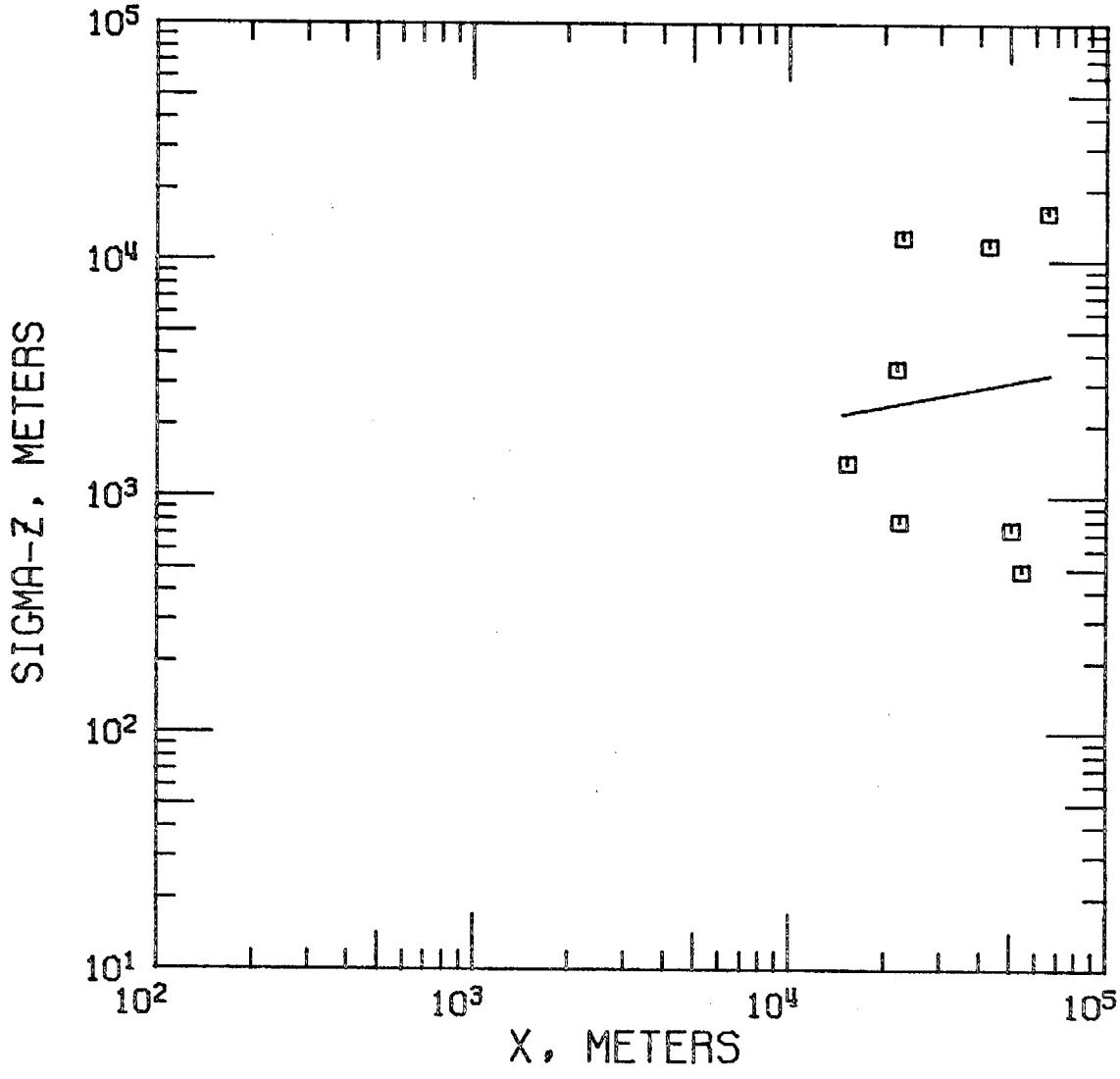

Figure 72. Vertical crosswind dispersion parameter, σ_z, as a function of distance downwind of Pinole.

TABLE 11

HORIZONTAL CROSSWIND DISPERSION COEFFICIENTS

$$\sigma_y = a X^b$$

Test, Release Point	a (m^{1-b})	b	σ (std. dev. about best-fit line)* (m)
Test 1, Dow	$5.31 \cdot 10^{-2}$	1.11	284
Test 2, Dow	$1.12 \cdot 10^{-5}$	1.84	230
Test 2, Martinez	$1.31 \cdot 10^{-8}$	2.50	3710
Test 3, Dow	$3.71 \cdot 10^{-5}$	1.71	1030
Test 4, Dow	$8.17 \cdot 10^{-4}$	1.37	428
Test 5, Dow	$7.09 \cdot 10^{-1}$	0.784	362
Test 6, Dow	$6.52 \cdot 10^{-6}$	1.87	331
Test 7, Dow	-	-	
Test 7, Pinole	$2.40 \cdot 10^{-1}$	0.958	3850
Test 8, Pinole	$5.33 \cdot 10^{-4}$	1.48	75

$$* \sigma = \left[\frac{\sum_{i=1}^{n} (\sigma_{y_i} - \sigma_y)^2}{n - 1} \right]^{1/2}$$ where σ_{y_i} are the data points and $\sigma_y = aX^b$

Meteorological Period, Release Point	a	b	σ (m) (std. dev. about best-fit line)
Pre-Sea Breeze, Dow	$8.34 \cdot 10^{-5}$	1.62	344
Pre-Sea Breeze, Pinole	$4.54 \cdot 10^{-2}$	1.08	1960
Sea Breeze, Dow	$4.74 \cdot 10^{-2}$	1.07	1230
Sea Breeze, Martinez	$1.31 \cdot 10^{-8}$	2.50	3710
Sea Breeze, Pinole	$4.06 \cdot 10^{-2}$	1.12	4330
Sea Breeze, Pinole & Martinez	$3.57 \cdot 10^{-3}$	1.34	5050
Sea Breeze Tail, Dow	$8.17 \cdot 10^{-4}$	1.37	428
Nighttime, Dow	$3.71 \cdot 10^{-5}$	1.71	1030

TABLE T1 (cont.)

Pasquill Stability Class	a*	b*
A (very unstable)	0.40	0.85
B (unstable)	0.40	0.87
C (slightly unstable)	0.23	0.89
D (neutral)	0.14	0.89
E (slightly stable)	0.11	0.89
F (stable)	0.072	0.89

*Determined from dispersion curves given by Turner (1970); x is taken to be in meters.

TABLE 11 (cont.)

VERTICAL CROSSWIND DISPERSION COEFFICIENTS

$$\sigma_z = c\, X^d$$

Test, Release Point	c (m^{1-b})	d	σ (std. dev. about best-fit line)* (m)
Test 1, Dow	$3.37 \cdot 10^{-1}$	0.681	45
Test 2, Dow	-	-	-
Test 2, Martinez	$6.61 \cdot 10^{-2}$	0.847	246
Test 3, Dow	$6.83 \cdot 10^{1}$	0.0582	146
Test 4, Dow	1.46	0.400	14
Test 5, Dow	-	-	-
Test 6, Dow	-	-	-
Test 7, Dow	-	-	-
Test 7, Pinole	$1.90 \cdot 10^{2}$	0.257	5228
Test 8, Pinole	-	-	-

$$* \sigma = \left[\frac{\sum_{i=1}^{n} (\sigma_{z_i} - \sigma_z)^2}{n - 1} \right]^{\frac{1}{2}}$$ where σ_{z_i} are the data points and $\sigma_z = cX^d$

Meteorological Period, Release Point	c	d	σ (m) (std. dev. about best-fit line)
Pre-Sea Breeze, Dow	-	-	-
Pre-Sea Breeze, Pinole	-	-	-
Sea Breeze, Dow	4.93	0.424	194
Sea Breeze, Martinez	$6.61 \cdot 10^{-2}$	0.847	246
Sea Breeze, Pinole	$4.96 \cdot 10^{1}$	0.414	8529
Sea Breeze, Pinole & Martinez	$2.52 \cdot 10^{-2}$	1.04	6570
Sea Breeze Tail, Dow	1.46	0.400	14
Nighttime, Dow	$6.83 \cdot 10^{1}$	0.0582	146

TABLE 11 (cont.)

$$^{*}\sigma_z = \exp\left[a_0 + a_1 \ln X + a_2 (\ln X)^2 + a_3 (\ln X)^3\right]$$

Pasquill Stability Class	a_0	a_1	a_2	a_3
A (very unstable)	6.10	2.11	0	0
B (unstable)	4.70	1.09	$9.12 \cdot 10^{-3}$	$-2.14 \cdot 10^{-3}$
C (slightly unstable)	4.10	0.940	$-7.56 \cdot 10^{-3}$	$2.86 \cdot 10^{-4}$
D (neutral)	3.46	0.662	$-1.28 \cdot 10^{-2}$	$-1.12 \cdot 10^{-3}$
E (slightly stable)	3.12	0.592	$-9.61 \cdot 10^{-3}$	$-4.24 \cdot 10^{-3}$
F (stable)	2.63	0.651	$-6.08 \cdot 10^{-2}$	$2.03 \cdot 10^{-3}$

*Best-fit expression for Pasquill dispersion curves, determined from Turner (1970); x is taken to be in kilometers.

not appear to cross the entire width of the plume. The scatter in the vertical dispersion data is generally worse than that for the horizontal dispersion data. This can be attributed to the dependence of the accuracy of σ_z upon estimations of the mixing height and average wind speed.

The automobile traverse data can be grouped into the four meteorological periods based upon the time of the traverse. Data from Tests 1, 2 and the latter part of Test 7 (7-5 through 7-12) were obtained during the Sea Breeze period. Traverses during Tests 6, 7 (7-1 through 7-4) and 8 occurred during the Pre-Sea Breeze period. Tests 3 and 4 were conducted during the Nighttime and Sea Breeze Tail periods, respectively. Typical horizontal and vertical dispersion data for the meteorological periods are presented in Figures 73 - 78. The remainder of the data is shown in Volume II, Section 3.11, Part A. Data for the Martinez and Pinole tracer releases have been plotted together to represent a northeastern Bay Area source. The dispersion coefficients of the best-fit lines for the meteorological periods are given in Table 11. Grouping data from different test days together increases the scatter about the best-fit lines. Scatter in the horizontal data for the combined Pinole-Martinez plot does not appear excessive; the scatter in the vertical data is worse. The best-fit lines generally give a reasonable approximation of the dispersion data.

The horizontal and vertical dispersion characteristics of the atmosphere during the study period are compared to the empirical dispersion relationships associated with the standard Pasquill stability classes as given by Turner (1970) in Figures 79 - 92 for each tracer test.

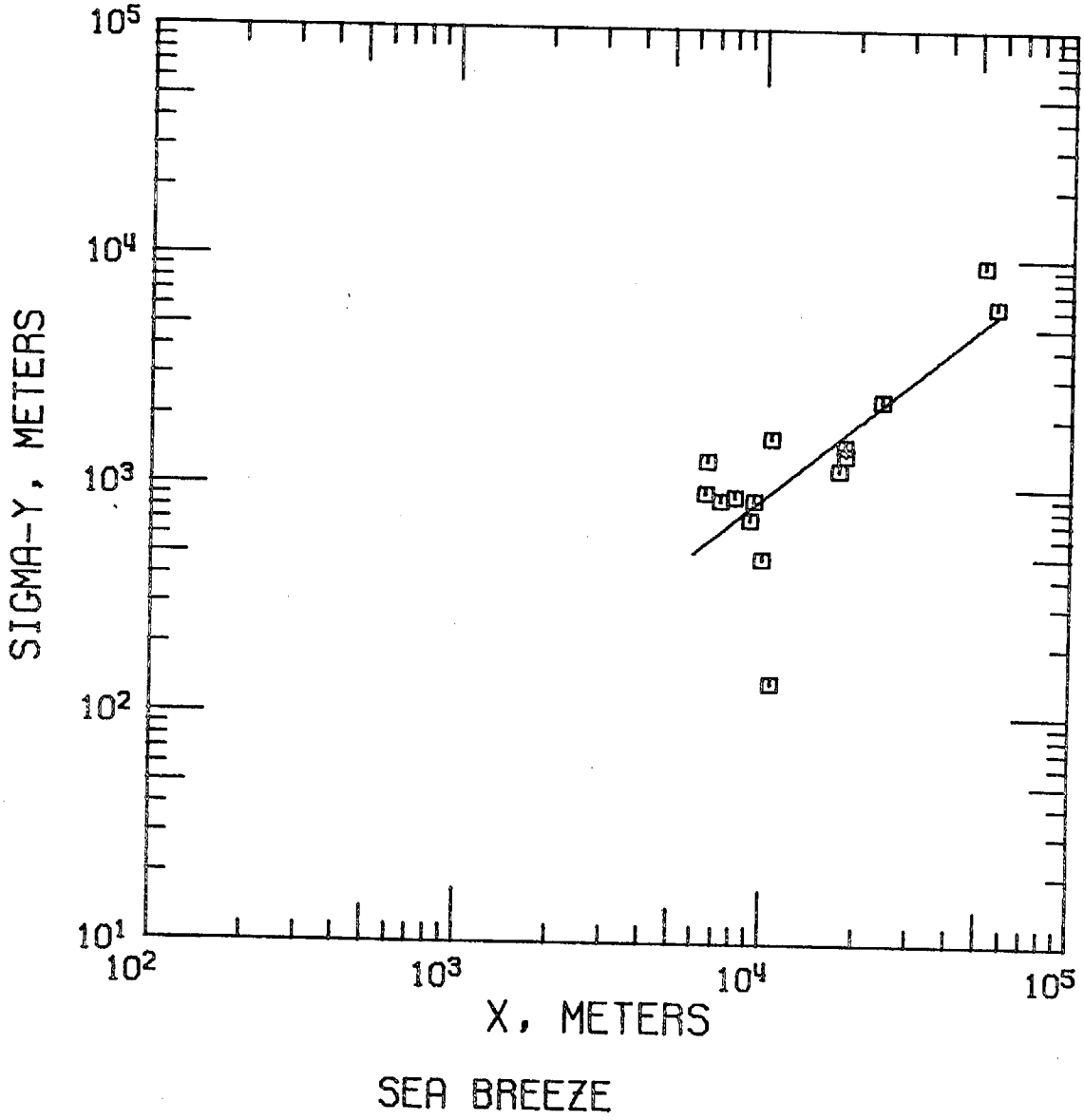

Dow Auto Traverse

Figure 73. Horizontal crosswind dispersion parameter, σ_y, as a function of distance downwind of the Dow site.

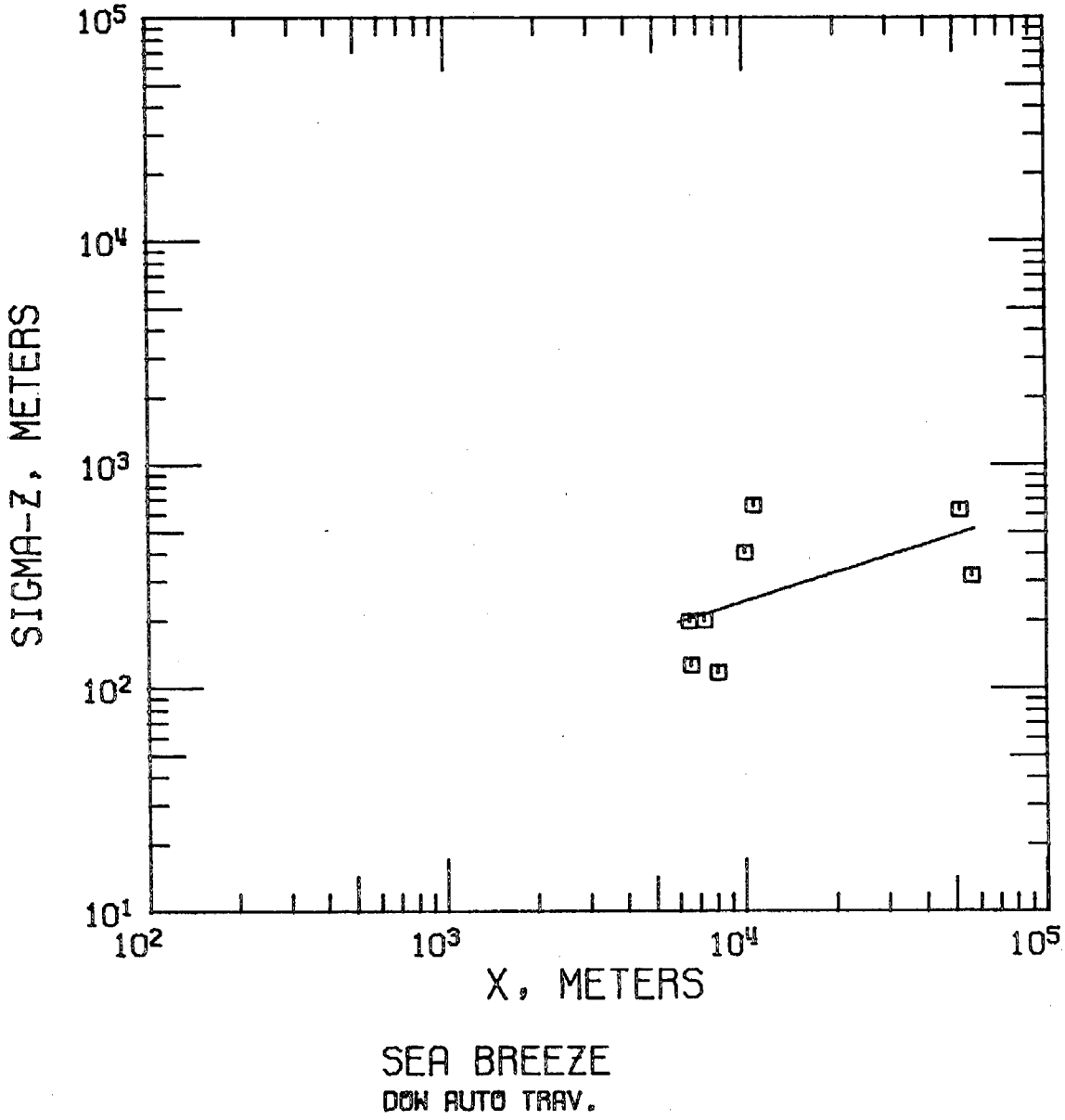

Figure 74. Vertical crosswind dispersion parameter, σ_z, as a function of distance downwind of the Dow site.

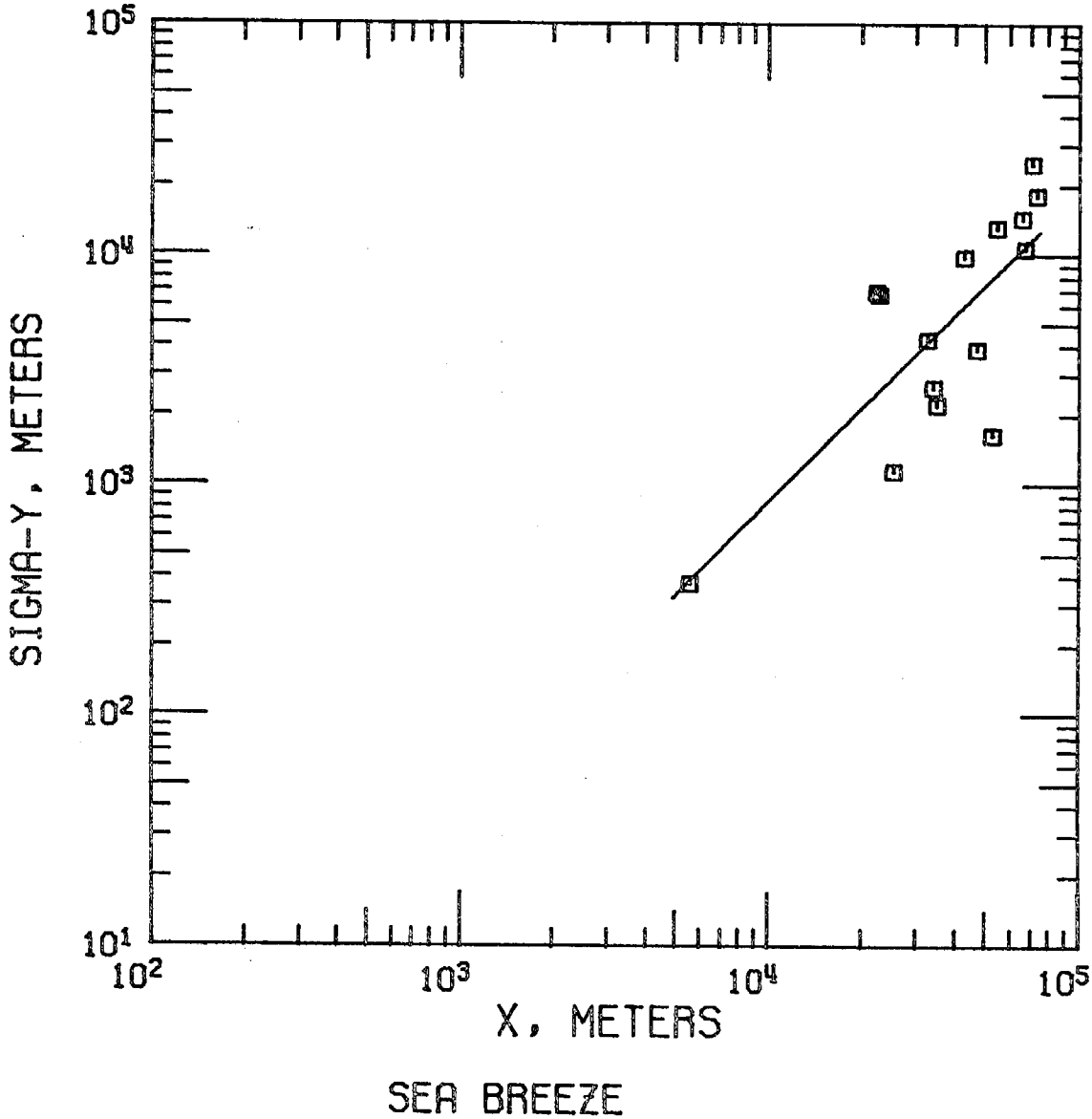

Pinole-Martinez Auto Traverse

Figure 75. Horizontal crosswind dispersion parameter, σ_y, as functions of distance downwind of Pinole and Martinez.

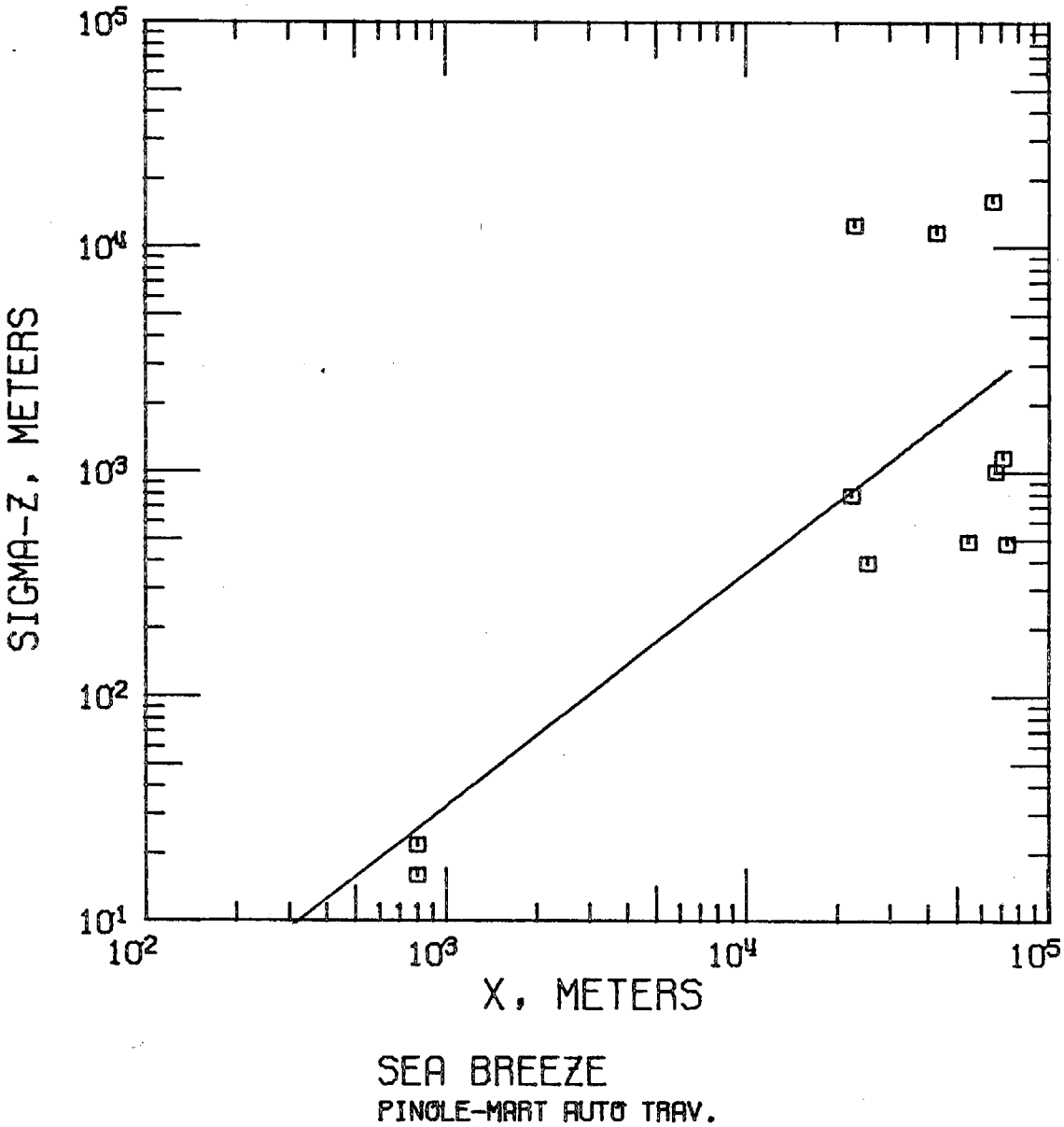

Figure 76. Vertical crosswind dispersion parameter, σ_z, as a function of distance downwind of Pinole and Martinez.

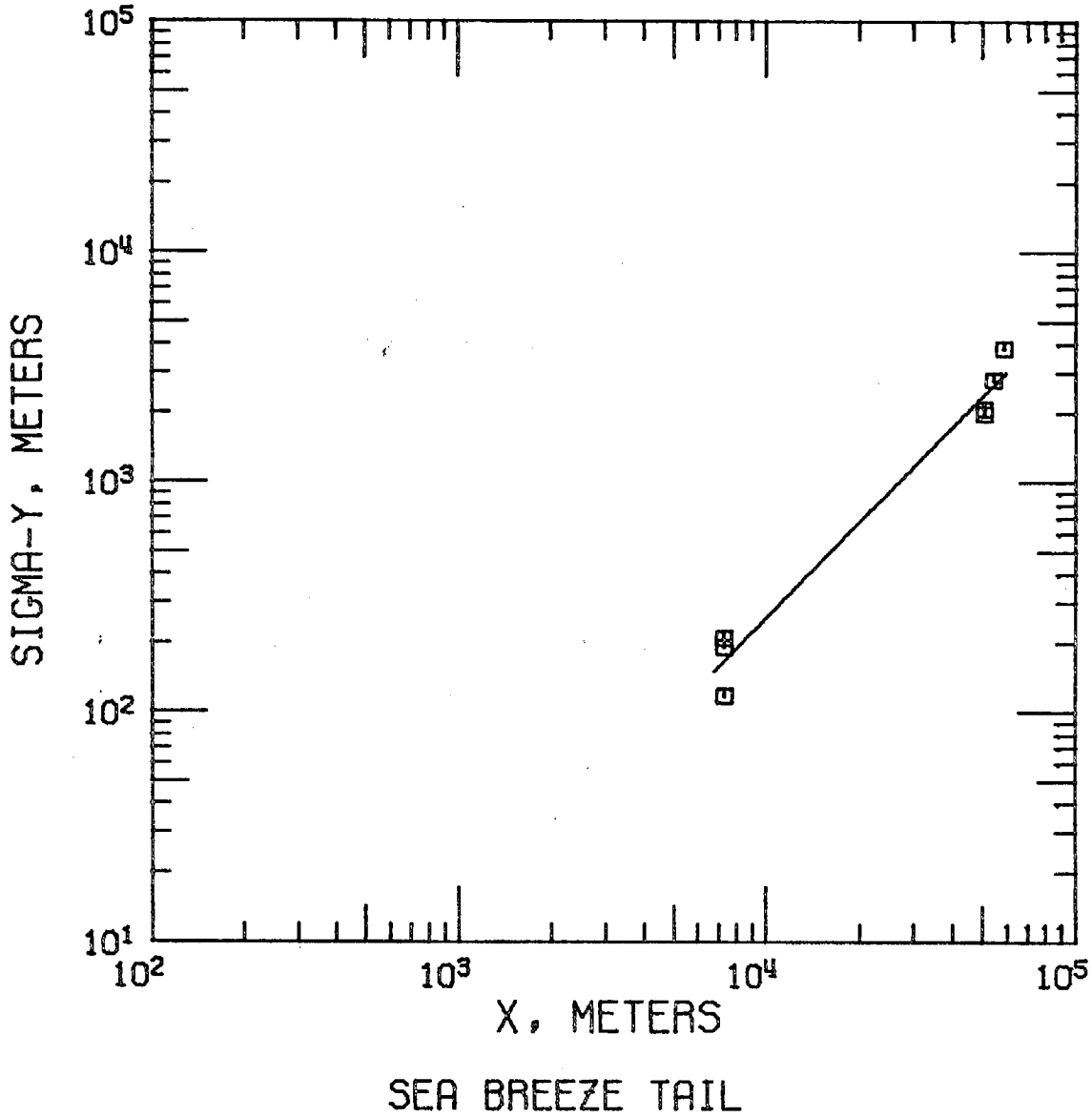

Figure 77. Horizontal crosswind dispersion parameter, σ_y, as a function of distance downwind of the Dow site.

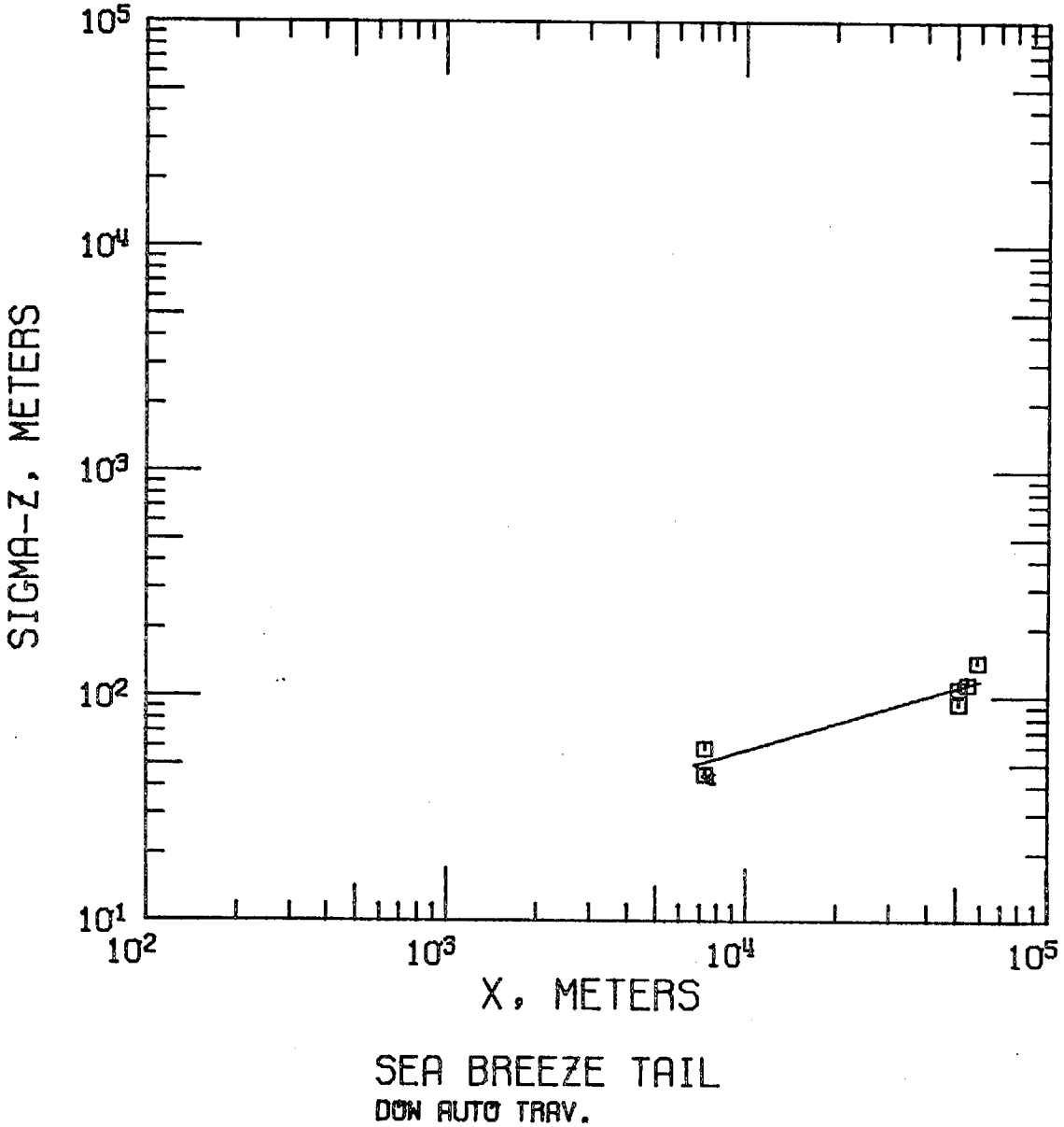

Figure 78. Vertical crosswind dispersion parameter, σ_z, as a function of distance downwind of the Dow site.

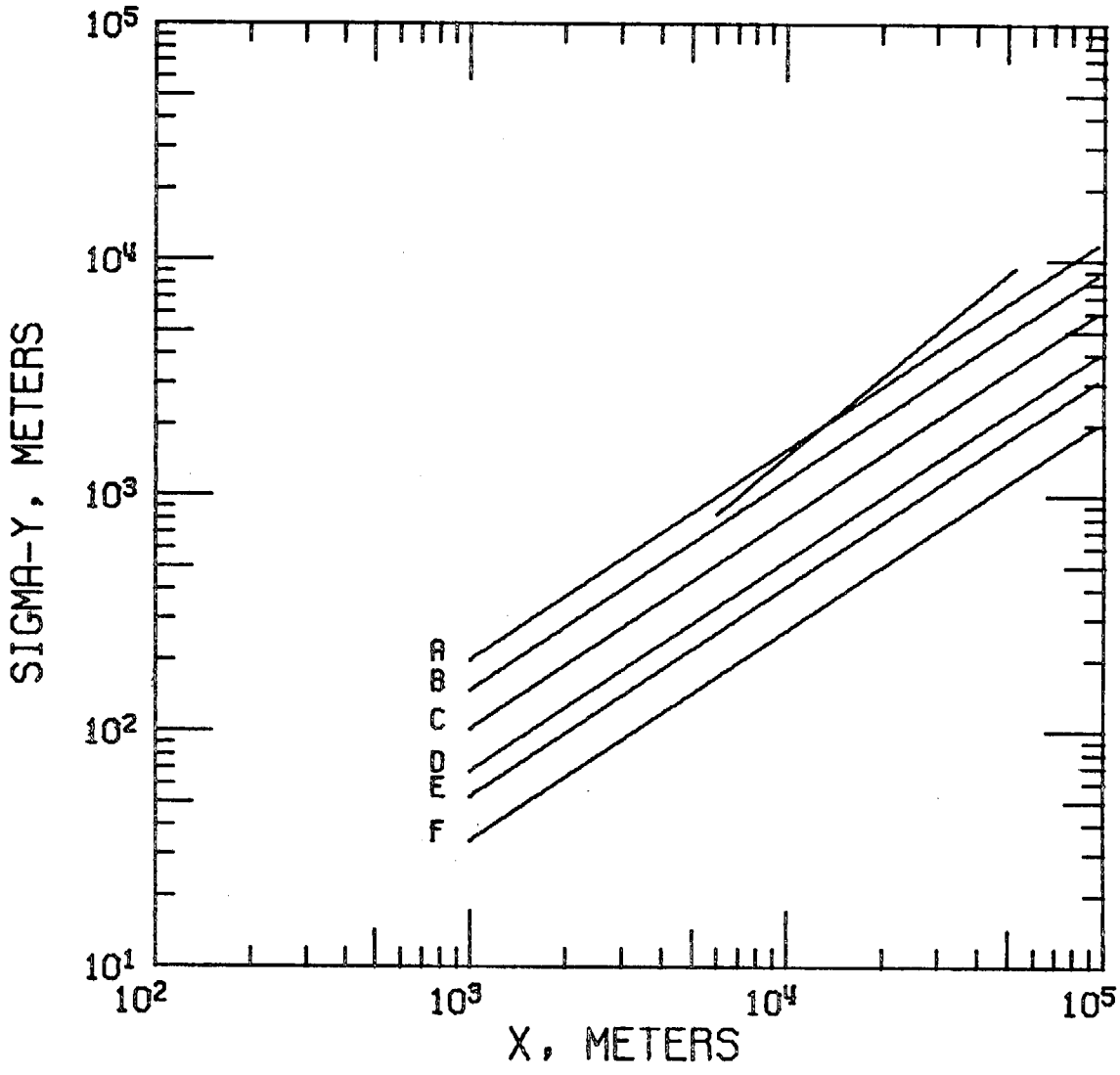

Figure 79. Comparison of horizontal dispersion of plumes emitted from the Dow site with the horizontal dispersion of plumes associated with Pasquill atmospheric stability classes.

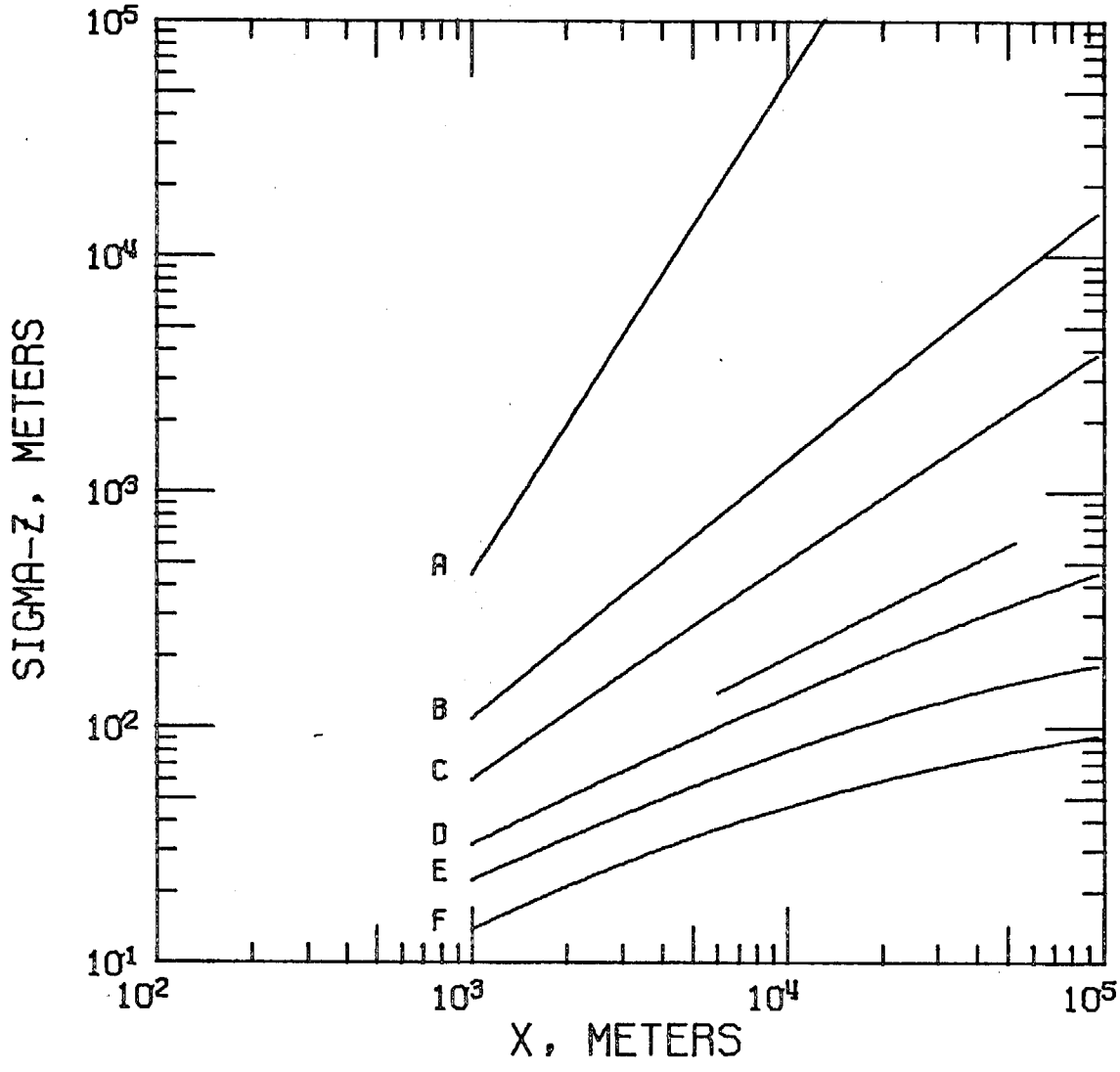

Figure 80. Comparison of vertical dispersion of plumes emitted from the Dow site with the vertical dispersion of plumes associated with Pasquill atmospheric stability classes.

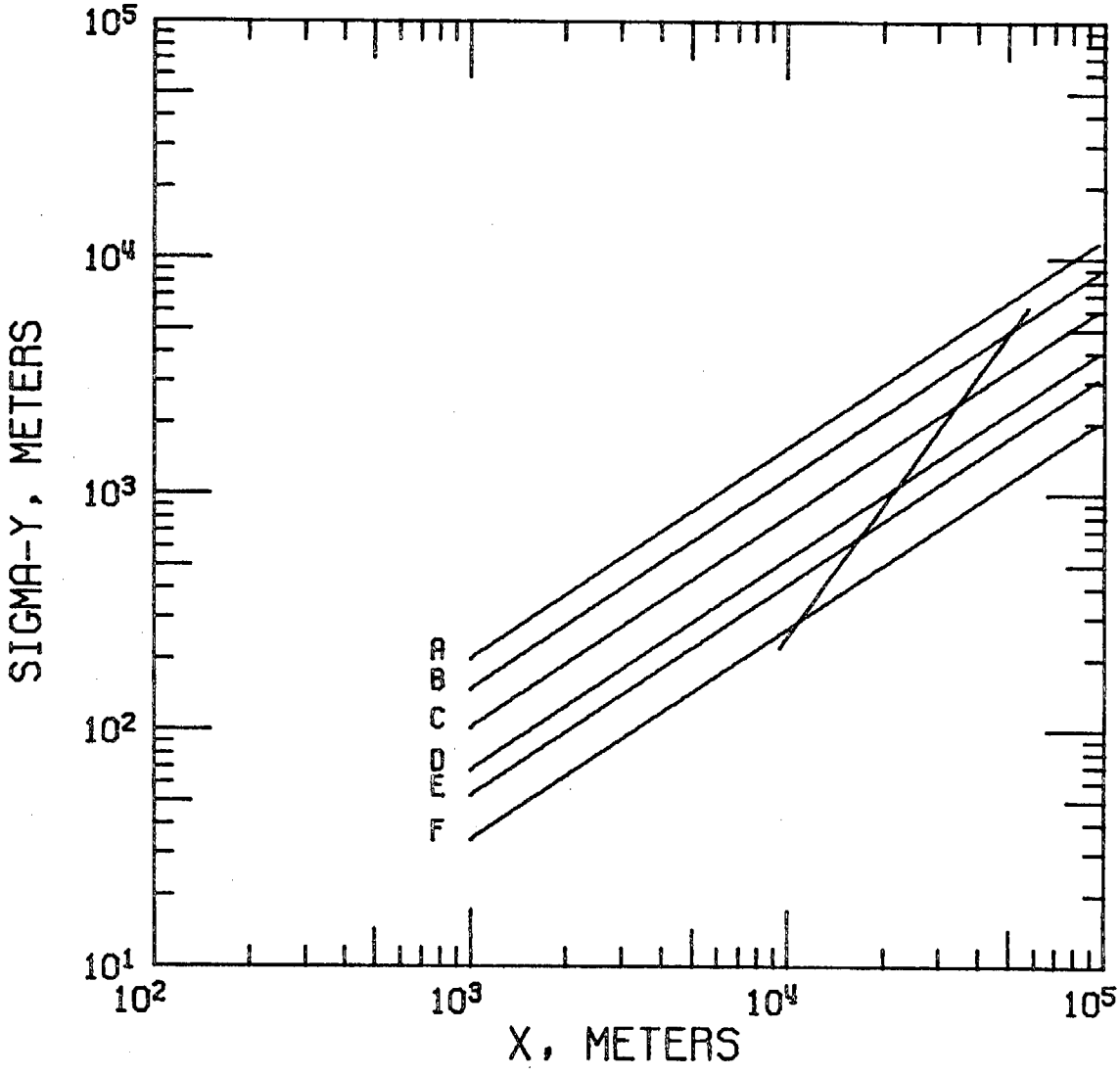

Figure 81. Comparison of horizontal dispersion of plumes emitted from the Dow site with the horizontal dispersion of plumes associated with Pasquill atmospheric stability classes.

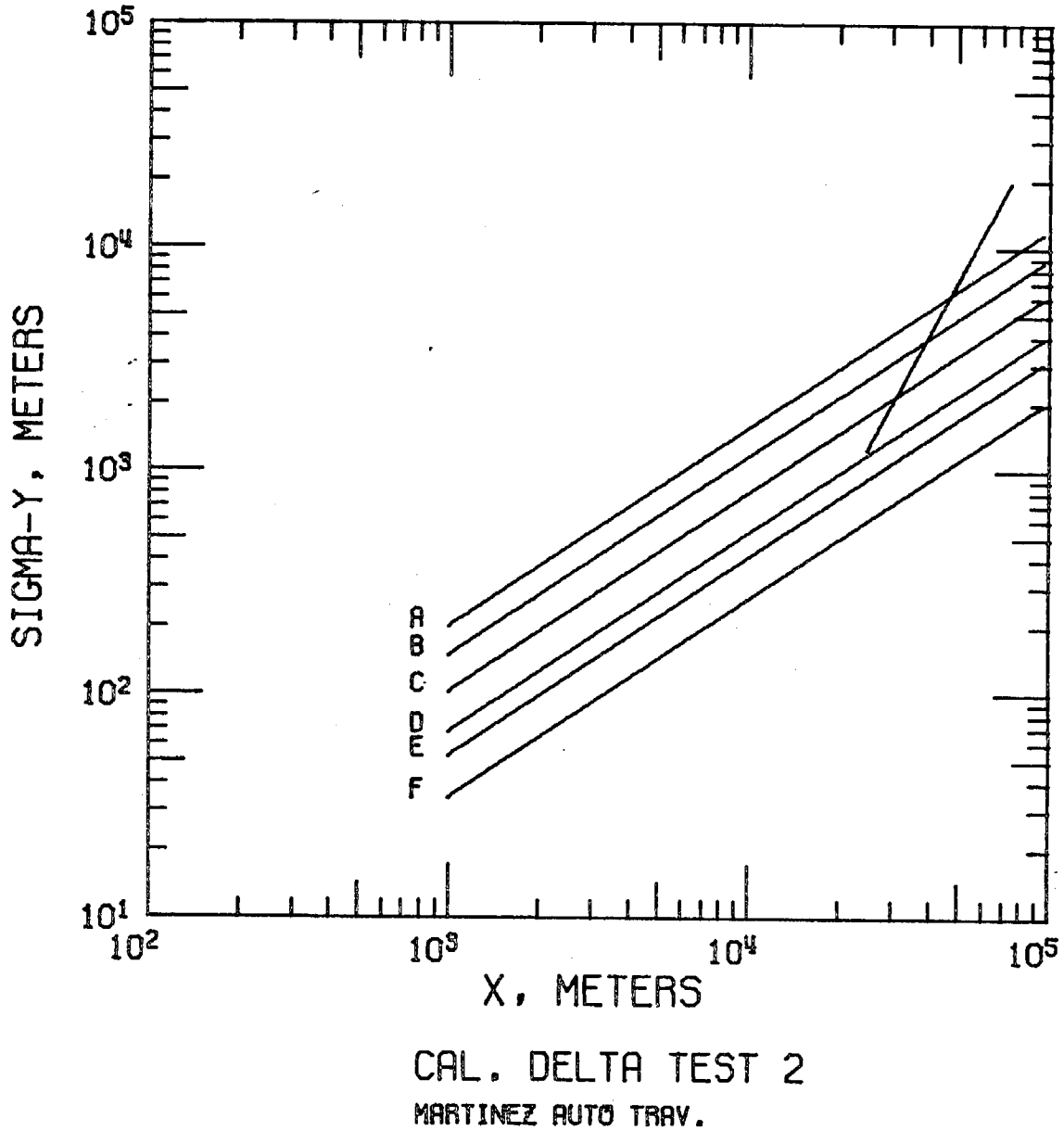

Figure 82. Comparison of horizontal dispersion of plumes emitted from Martinez with the horizontal dispersion of plumes associated with Pasquill atmospheric stability classes.

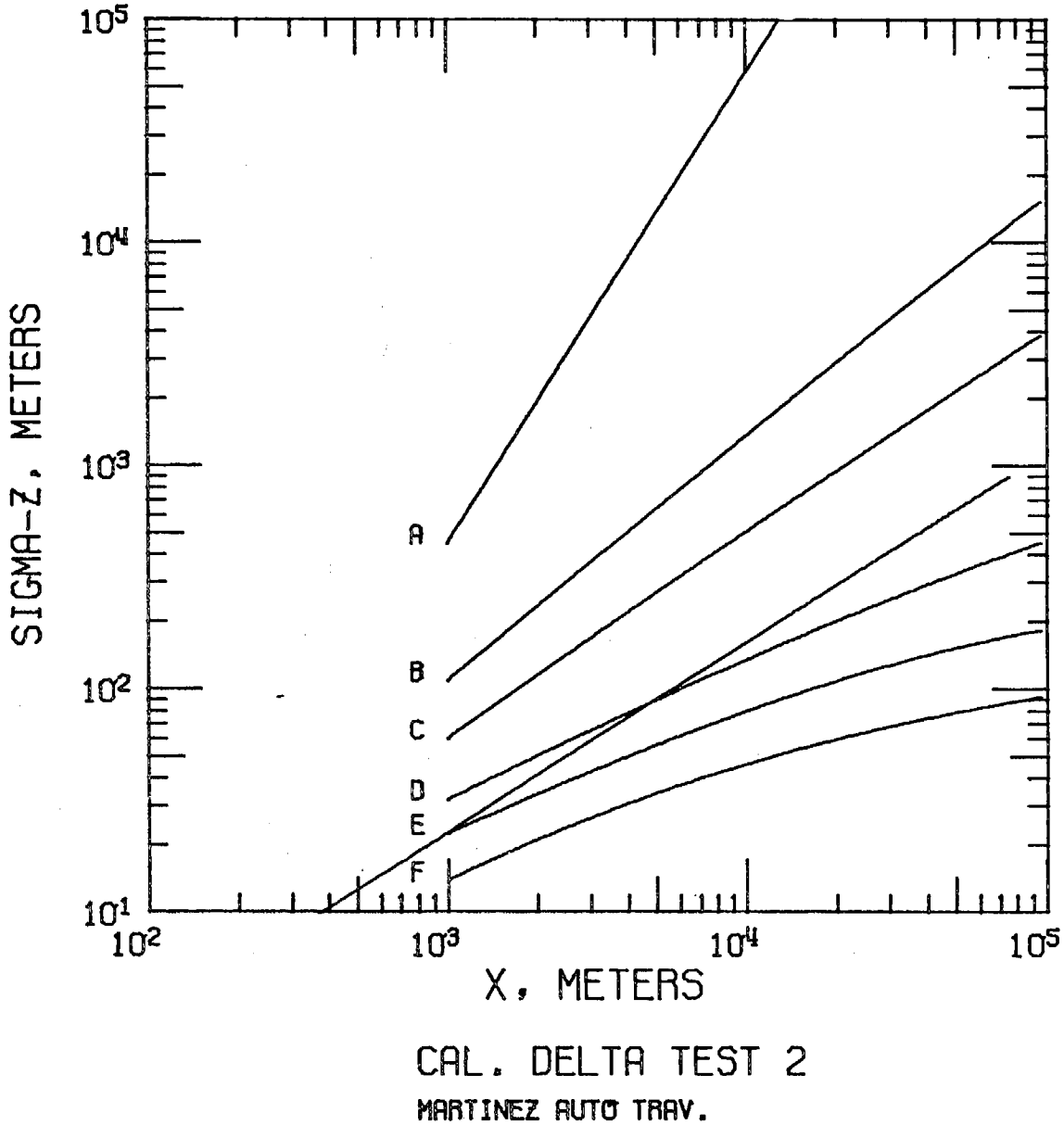

Figure 83. Comparison of vertical dispersion of plumes emitted from Martinez with the vertical dispersion of plumes associated with Pasquill atmospheric stability classes.

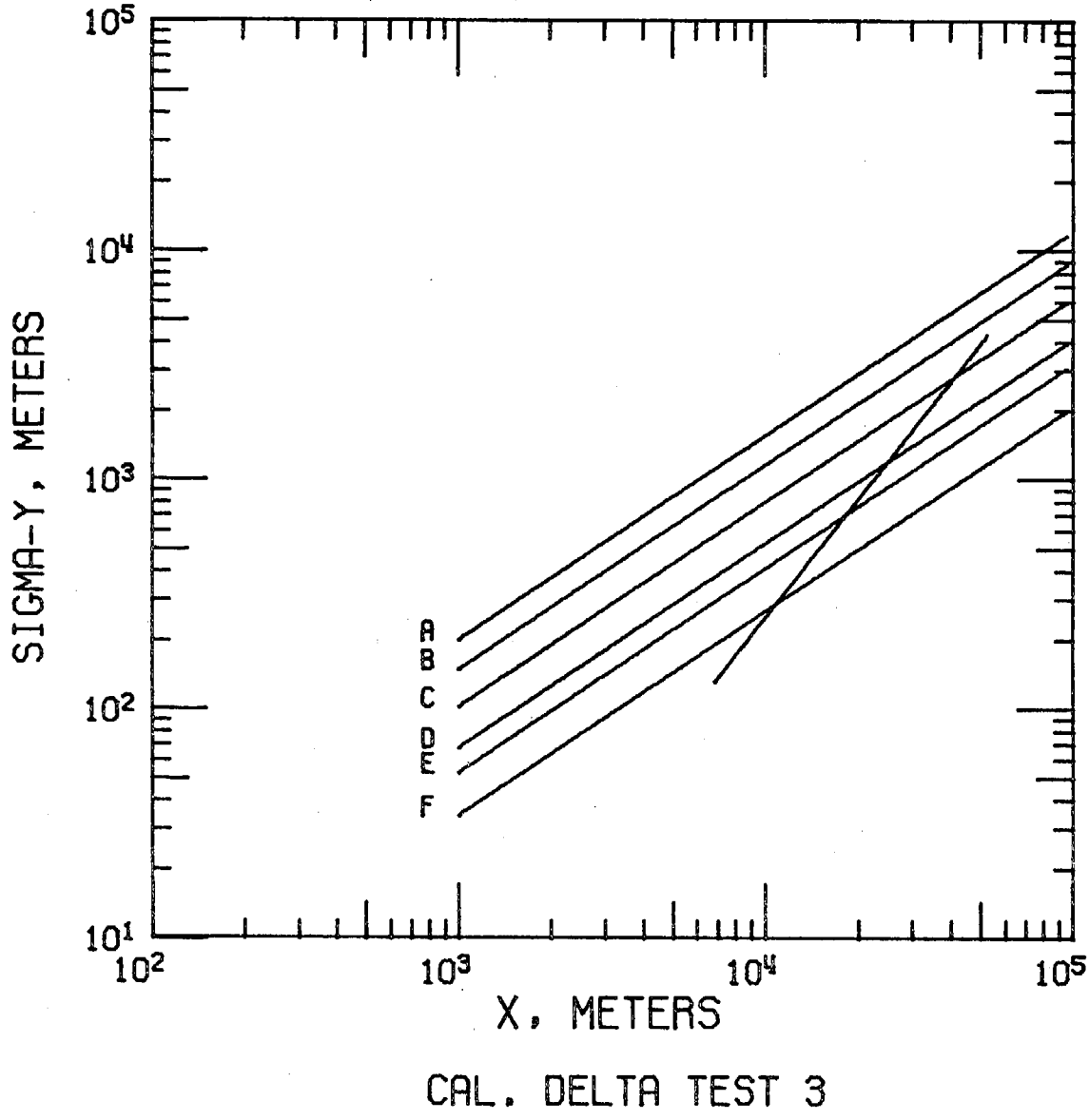

Figure 84. Comparison of horizontal dispersion of plumes emitted from the Dow site with the horizontal dispersion of plumes associated with Pasquill atmospheric stability classes.

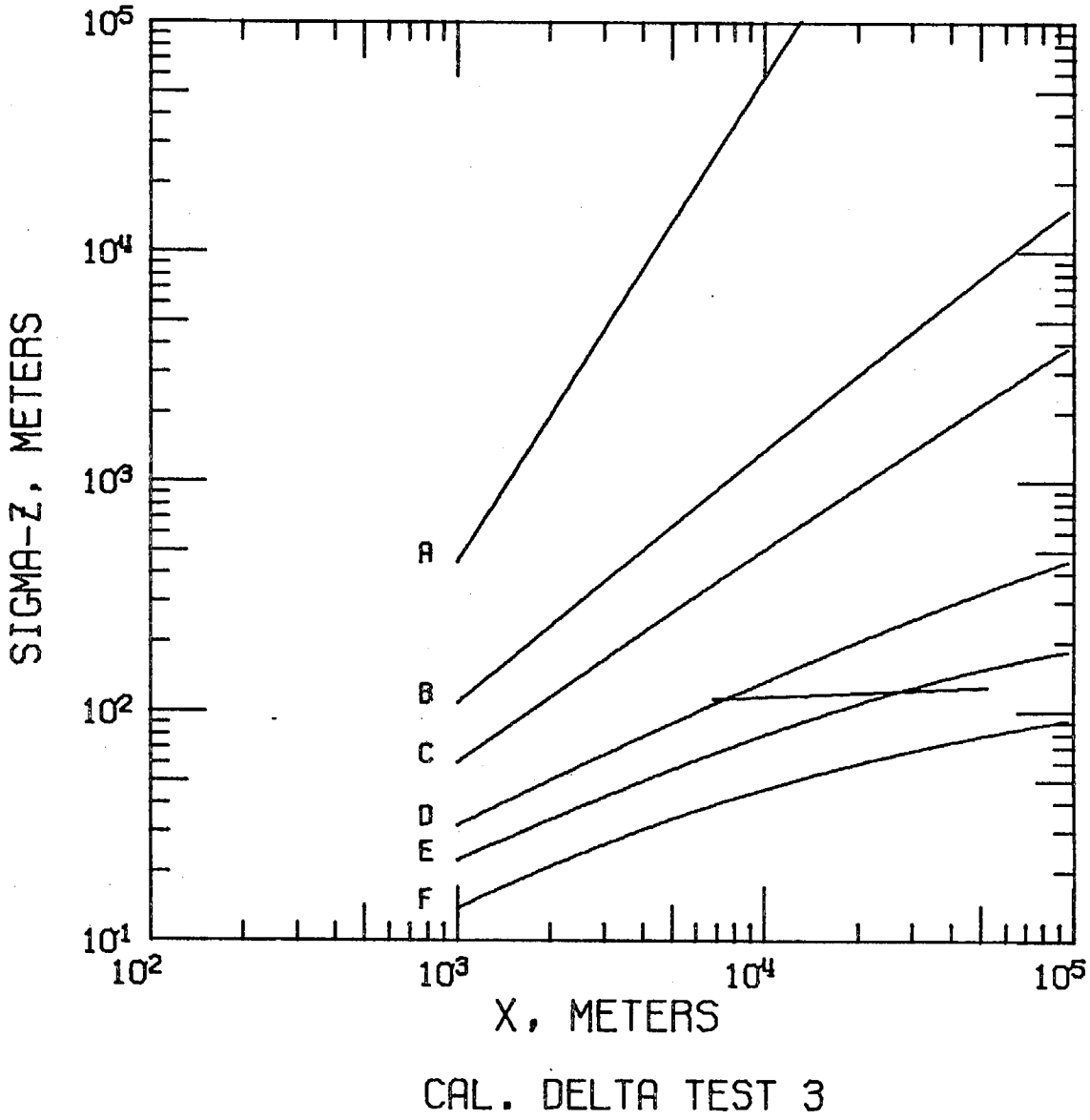

Figure 85. Comparison of vertical dispersion of plumes emitted from the Dow site with the vertical dispersion of plumes associated with Pasquill atmospheric stability classes.

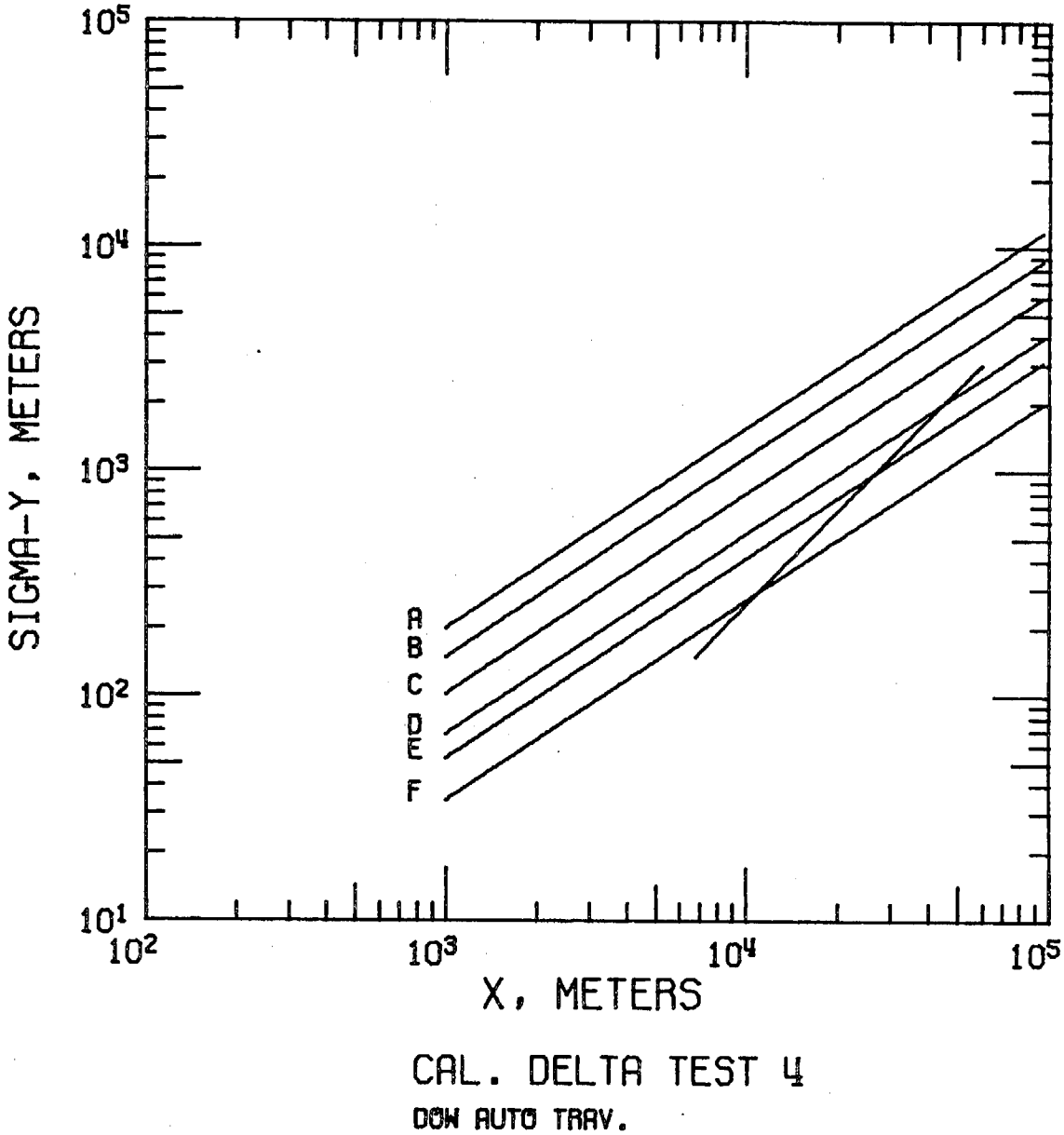

Figure 86. Comparison of horizontal dispersion of plumes emitted from the Dow site with the horizontal dispersion of plumes associated with Pasquill atmospheric stability classes.

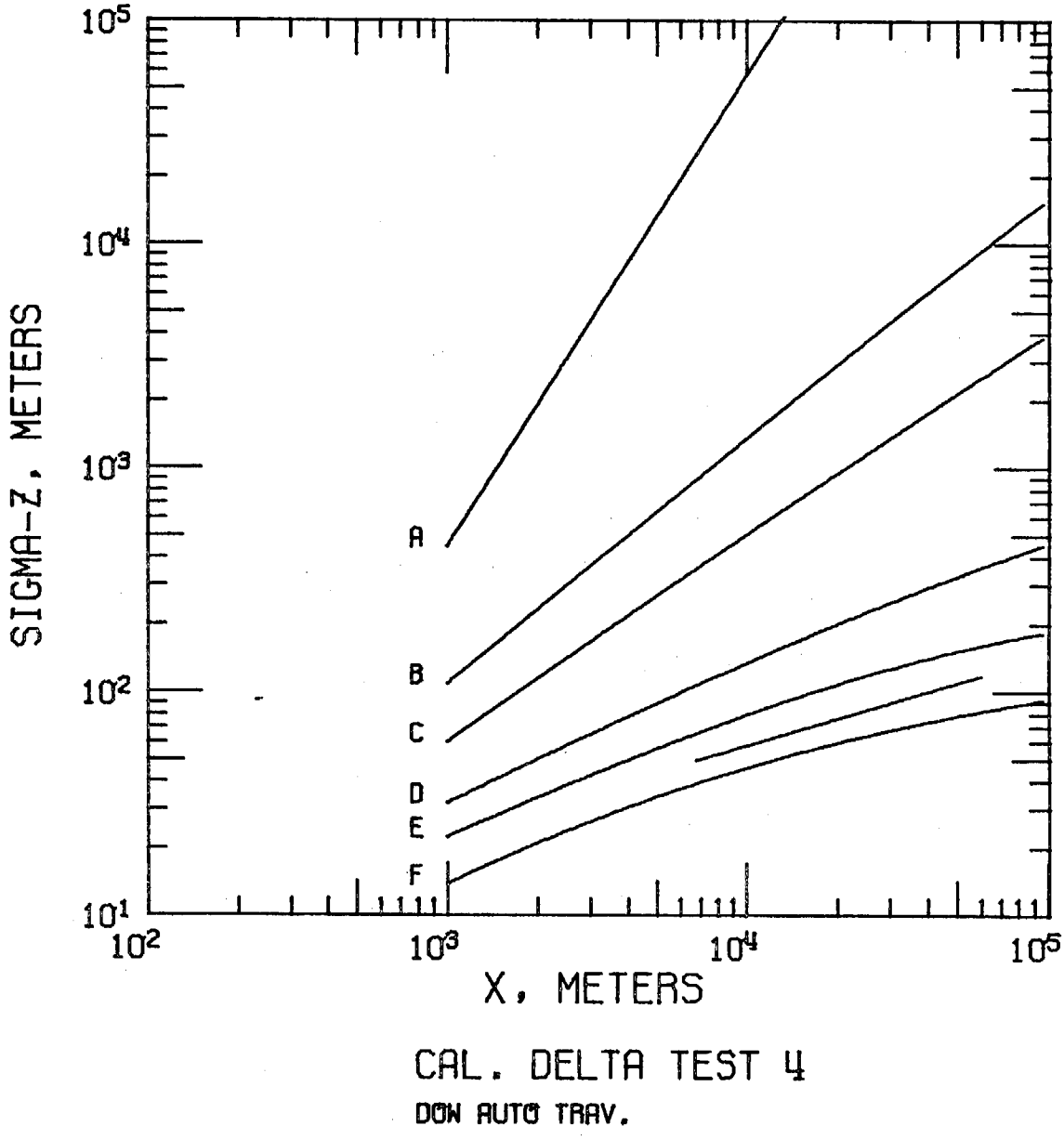

Figure 87. Comparison of vertical dispersion of plumes emitted from the Dow site with the vertical dispersion of plumes associated with Pasquill atmospheric stability classes.

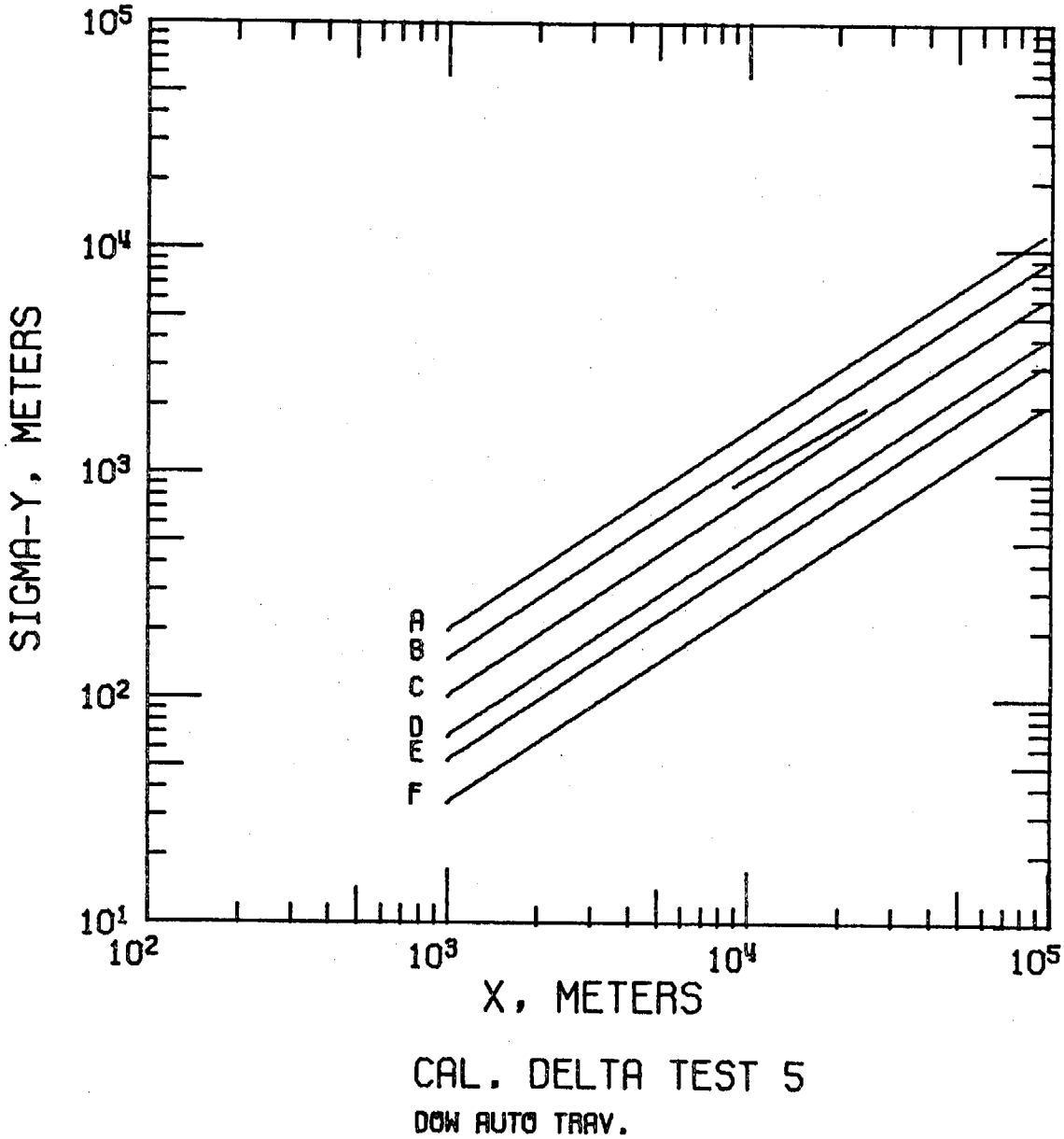

Figure 88. Comparison of horizontal dispersion of plumes emitted from the Dow site with the horizontal dispersion of plumes associated with Pasquill atmospheric stability classes.

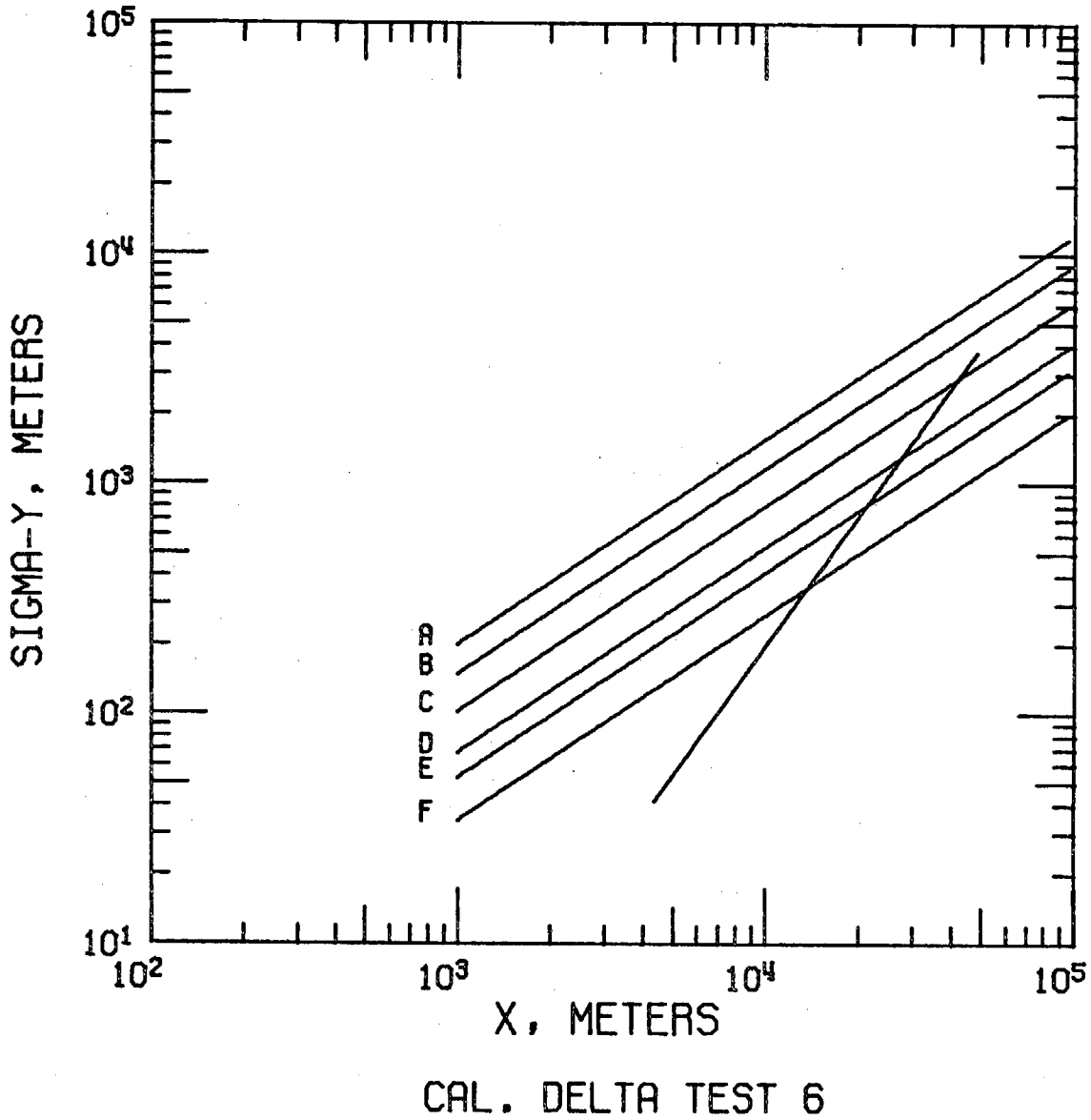

Figure 89. Comparison of horizontal dispersion of plumes emitted from the Dow site with the horizontal dispersion of plumes associated with Pasquill atmospheric stability classes.

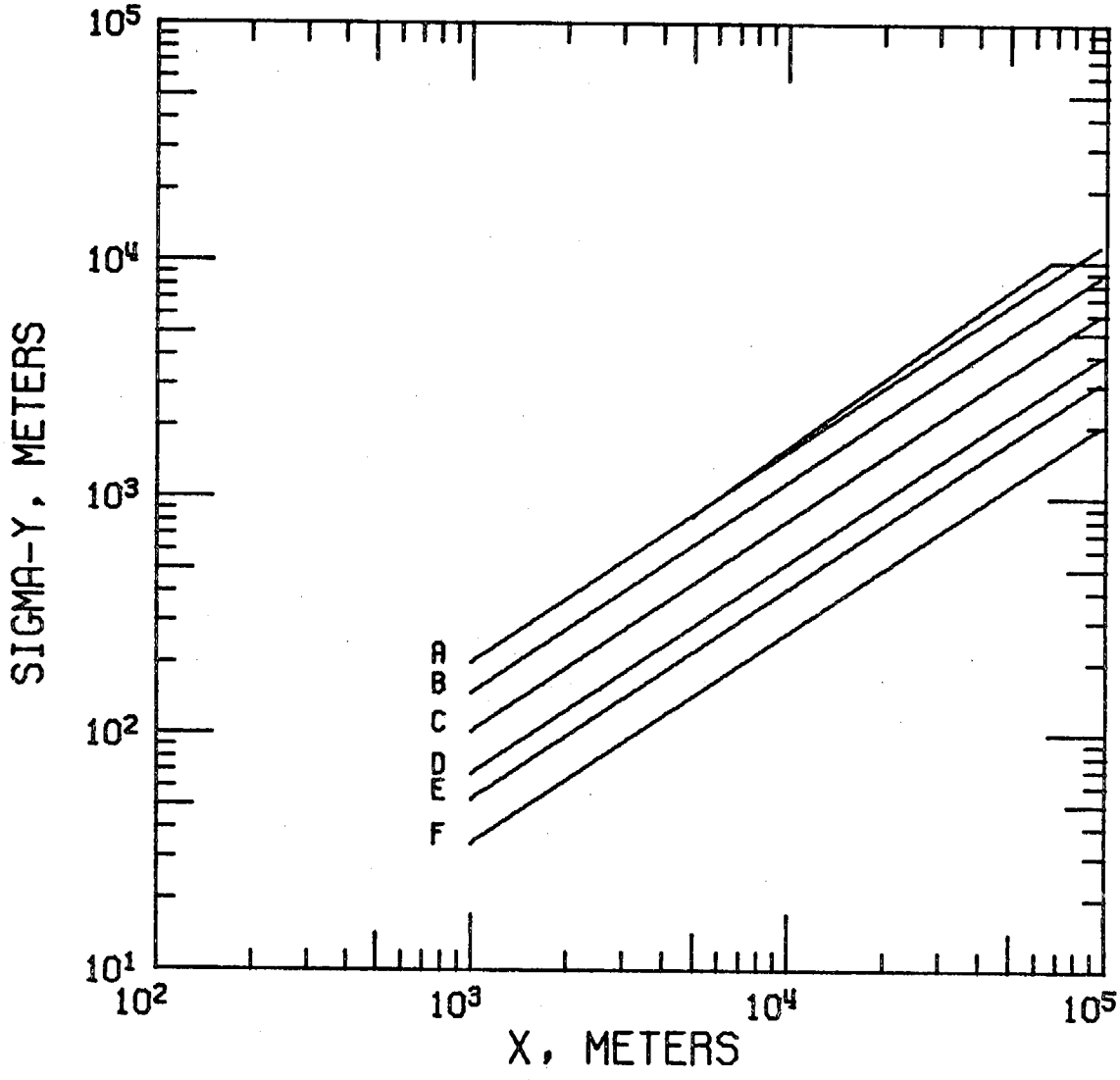

Figure 90. Comparison of horizontal dispersion of plumes emitted from Pinole with the horizontal dispersion of plumes associated with Pasquill atmospheric stability classes.

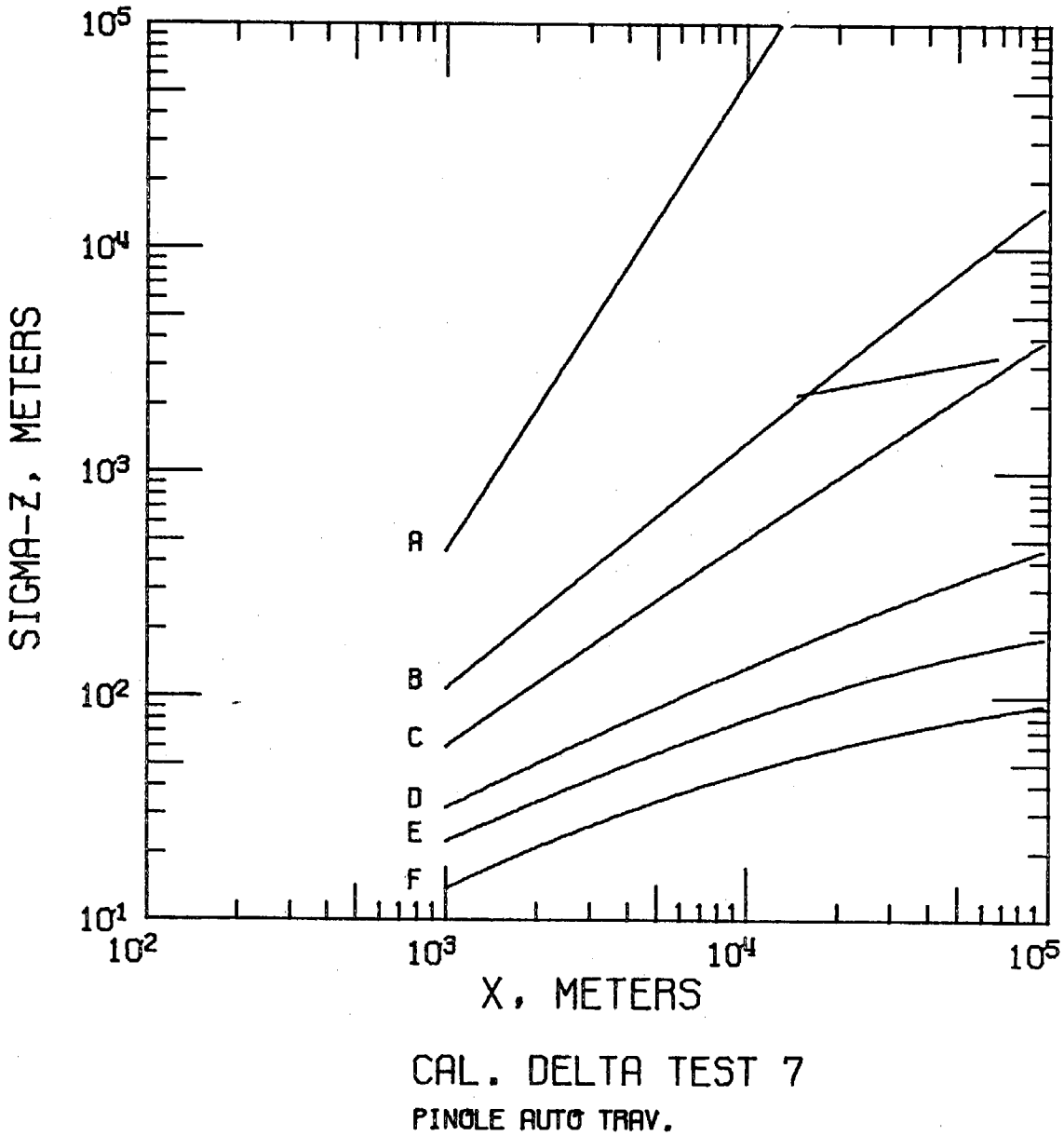

Figure 91. Comparison of vertical dispersion of plumes emitted from Pinole with the vertical dispersion of plumes associated with Pasquill atmospheric stability classes.

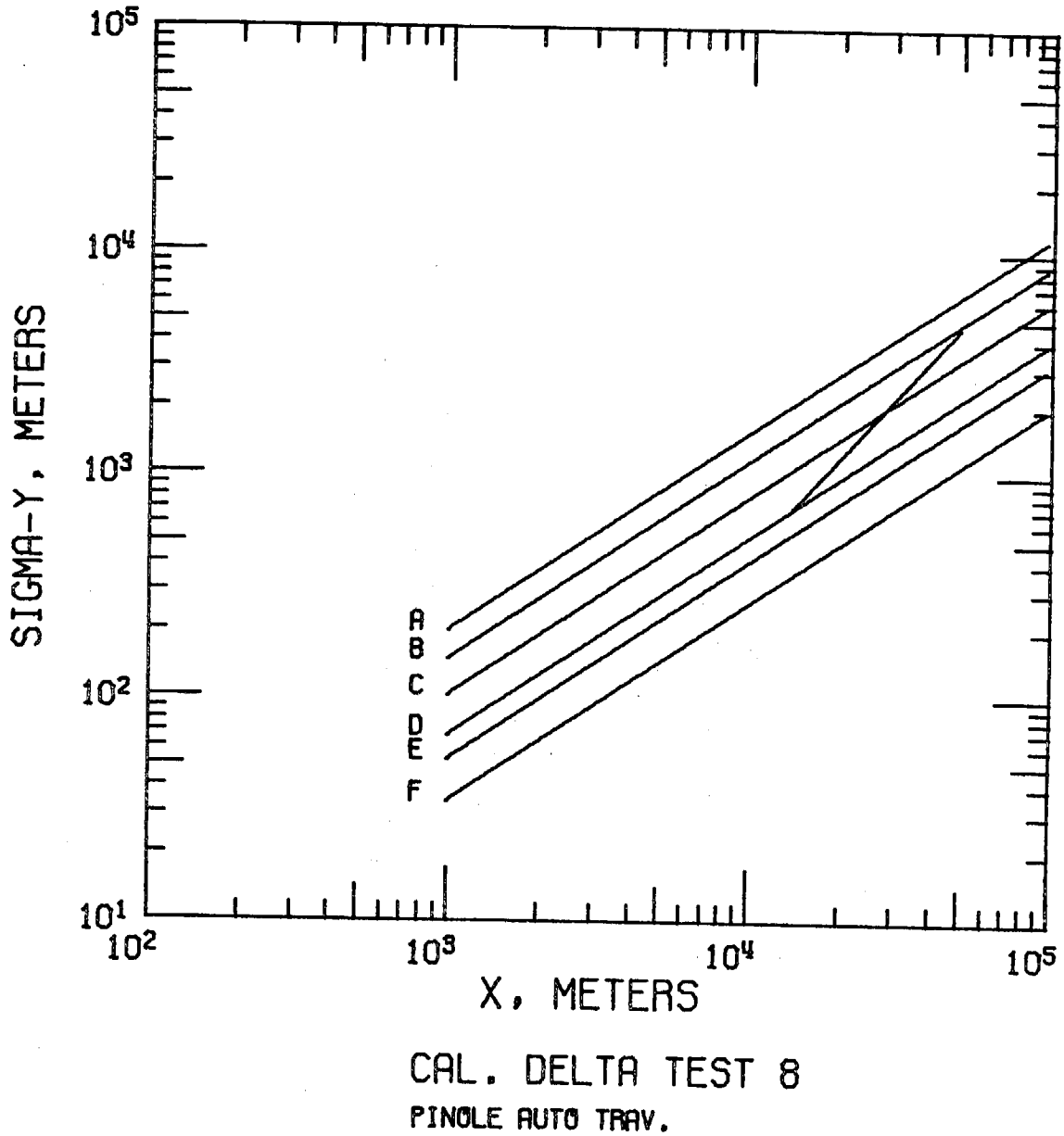

Figure 92. Comparison of horizontal dispersion of plumes emitted from Pinole with the horizontal dispersion of plumes associated with Pasquill atmospheric stability classes.

The dispersion coefficients corresponding to the dispersion curves for σ_y and σ_z from Turner (1970) are listed in Table 11. The horizontal dispersion curves from every test, except Tests 5 and 7, indicate that atmospheric stability decreases with increasing distance. Results from Test 1 show that conditions were comparable to class B immediately downwind at the Dow site, and less stable than class A at far downwind distances. This pattern is more obvious in Tests 2, 3, 4, 6 and 8. Conditions range from very stable near the source to very unstable at far downwind distances. These curves suggest that the strong jet of wind passing through the Carquinez Strait and over the Dow site has a very large effect on the dispersion of pollutants at close downwind distances from the source. Typically, the plumes crossing Highway 160, 10 km downwind of the Montezuma Hills, are very narrow; during the seven Dow releases, the plume centerlines observed in the automobile traverse data crossed Highway 160 within a 2.1 km crosswind zone (see Figure 118, Section 4.8 of this volume). However, the plumes observed crossing Highway 99, 50 km downwind of the Montezuma Hills, were relatively broad, and their trajectories crossed Highway 99 in a zone extending from Lodi to Tracy during the seven tests.

The slopes of the experimental horizontal dispersion curves are roughly a factor of 2 greater than the slopes of the corresponding curves given by Turner. Thus, the rate of spreading under the field test meteorological conditions was a factor of 2 greater than the dispersion associated with the classical Pasquill stability categories. However, the horizontal dispersion curves generally begin under more stable conditions than would be predicted from wind speed and insolation

considerations. Conditions during Test 1 were assumed to be Pasquill classes B-C; the horizontal dispersion curve for Test 1 ranges from class B near the source to class A far from the source. During Test 2, stability conditions were predicted to be Pasquill classes B-C; the horizontal stability according to dispersion data for the Dow releases ranged from class F near the source to class B far downwind. Stability conditions were assumed to be classes D-F for Tests 3 and 4; the stability conditions suggested by the horizontal dispersion curves ranged from more stable than class F, 7 km from the Dow site, to approximately class C at 50 km downwind. The horizontal dispersion curve from Test 6 begins under more stable conditions than class F at 5 km downwind, and ranges to class C conditions at 50 km downwind. The existing stability conditions were predicted to be class D conditions. Near the Dow site the atmosphere appears to be very stable; 50 km east of the Dow site, conditions approach those predicted from meteorological data.

Data from Test 5 for a Dow release and Test 7 for the Pinole release appear to follow the classical Pasquill curves. The predicted stability conditions during Test 5 were classes B-C; the experimental curve lies between classes B-C. The predicted conditions during Test 7 were B-C; the experimental curve is practically coincident with the Pasquill class A curve. Data obtained for Test 8 from Pinole indicated stability conditions to be B-C; the dispersion curve ranged from class D to class B.

The vertical dispersion data do not show the same stability pattern apparent in the horizontal data. Generally, the vertical dispersion curves follow the classical Pasquill curves. For Test 1, the experimental curve lies between the Pasquill class C and D curves; this is in

a range slightly more stable than the classes B-C predicted for the test. Classes D-F were assumed to exist during Test 4; the vertical dispersion curve lies between the curves for classes E and F. The scatter in the vertical dispersion data for Test 7 was rather large. The data points lie between classes A and D, and the best-fit line lies between classes B and C. Stability conditions during the day were predicted to be classes B-C. For Test 3 conducted at night, the vertical dispersion data suggest that vertical mixing was almost independent of the transport distance. This is in agreement with the results of the mass balance analysis for the nighttime test. Even after moving distances of 50 km, the plumes extended to approximately the same height as that found at 7 km.

The relative dispersive capabilities of the atmosphere among the four meteorological regimes are summarized in Figures 93 and 94 for Dow releases and in Figures 95 and 96 for Pinole-Martinez releases. The Dow horizontal dispersion data clearly show the effects of daytime heating upon the regional dispersion processes. The afternoon Sea Breeze curve ranges from class C near Dow to class B far downwind. The other daytime period and the evening and nighttime periods are characterized by a dispersion process which is more stable than the Pasquill class F, 7 km from the Dow site, and close to class C at 50 km downwind. The large difference between the Sea Breeze curve and the remaining curves at short downwind distances can be attributed to the increased vertical mixing which prevails during the sunny, warm afternoon period. During the tracer releases, aside from Test 5, average wind speeds at the Dow site ranged from 4.6 to 9.3 m/sec (10 to 21 mph). These high wind speeds account for the extremely stable conditions apparent in the dispersion curves at close downwind distances.

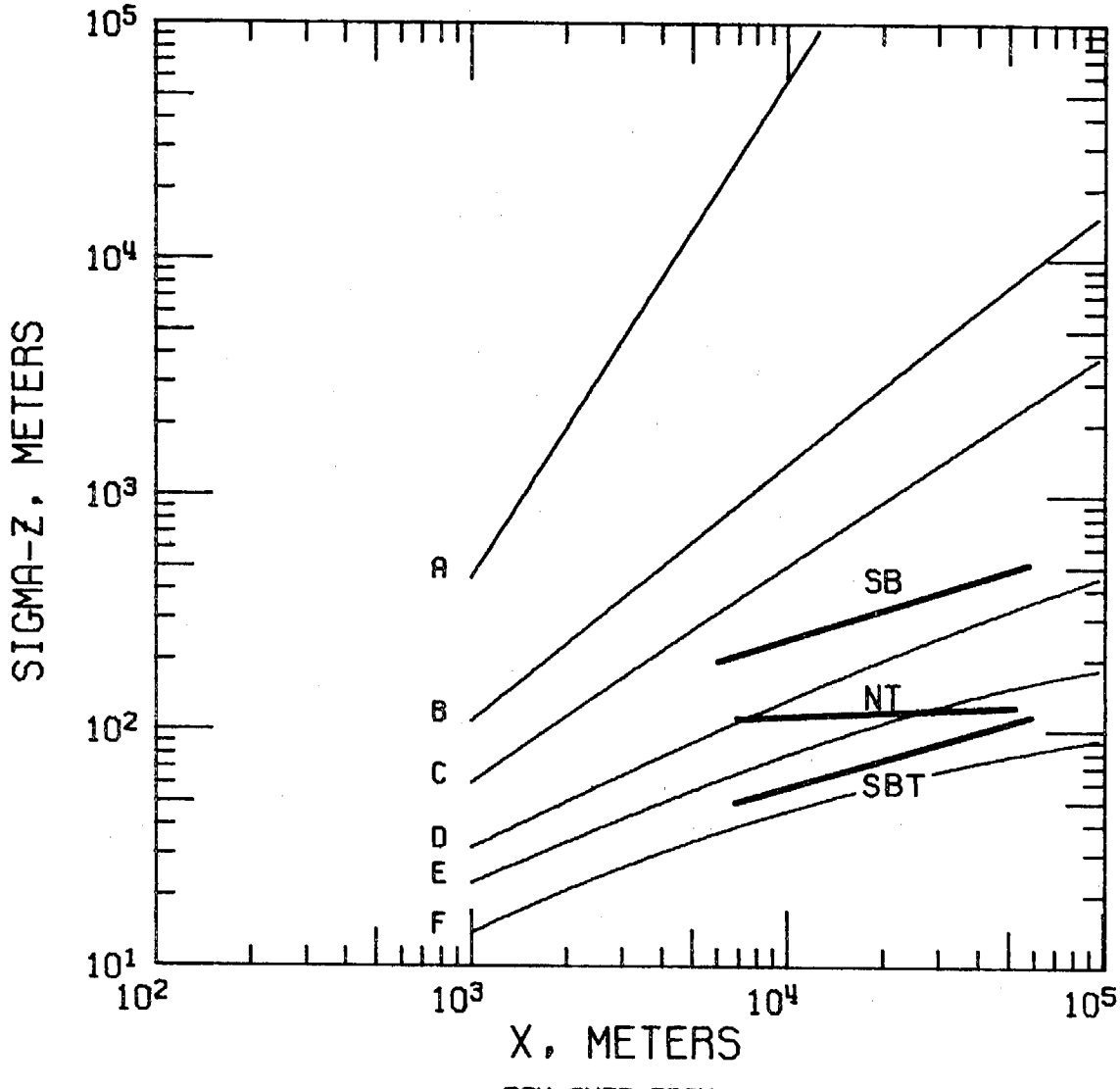

Figure 94. Vertical crosswind dispersion parameter, σ_z, as a function of distance downwind of the Dow site during Sea Breeze (SB), Sea Breeze Tail (SBT), and Nighttime (NT) conditions, and the vertical dispersion parameter associated with Pasquill atmospheric stability classes.

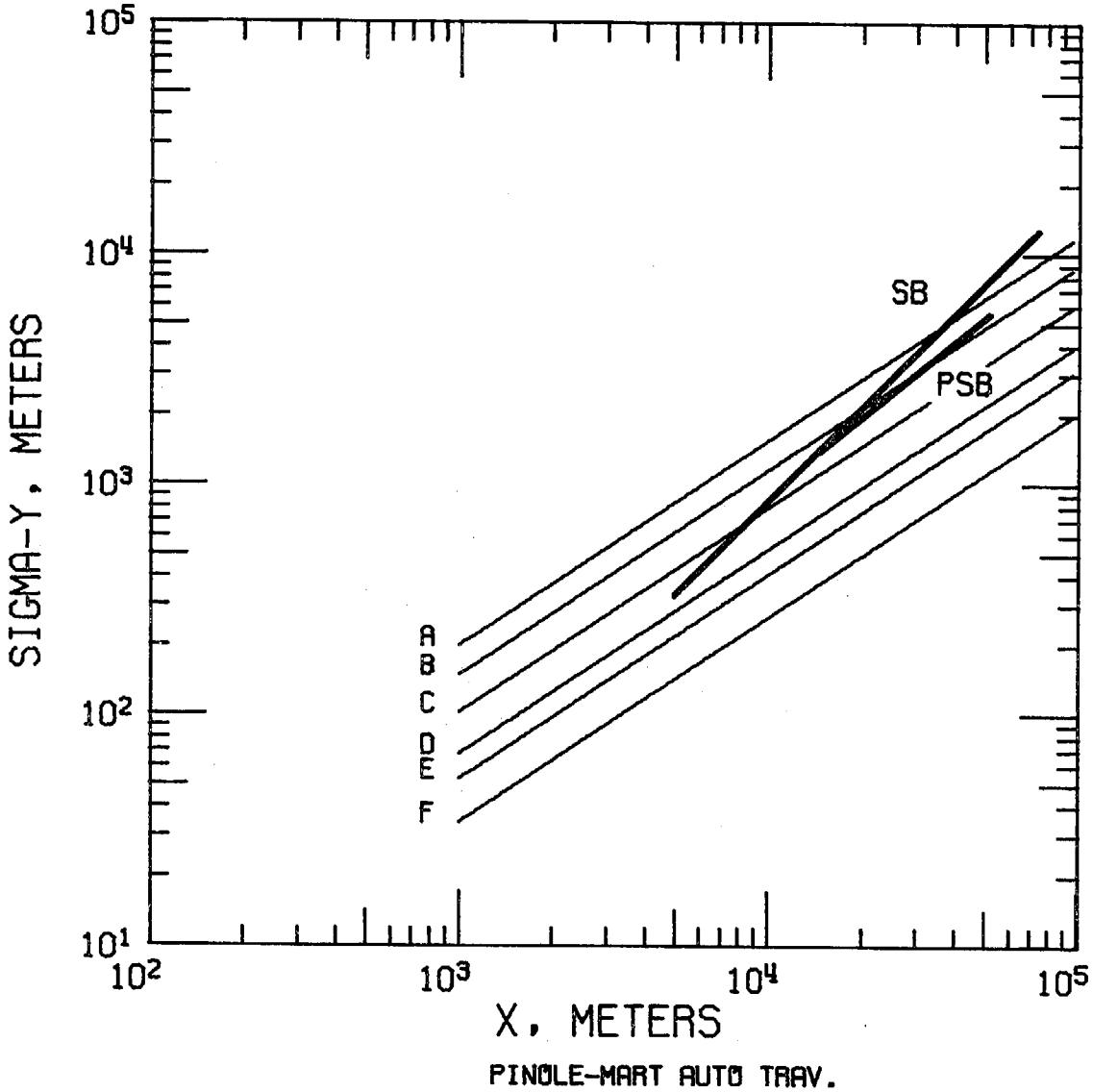

Figure 95. Horizontal crosswind dispersion parameter, σ_y, as a function of distance downwind for tracer releases from Pinole and Martinez during Sea Breeze (SB) and Pre-Sea Breeze (PSB) conditions, and the horizontal dispersion parameter associated with Pasquill atmospheric stability classes.

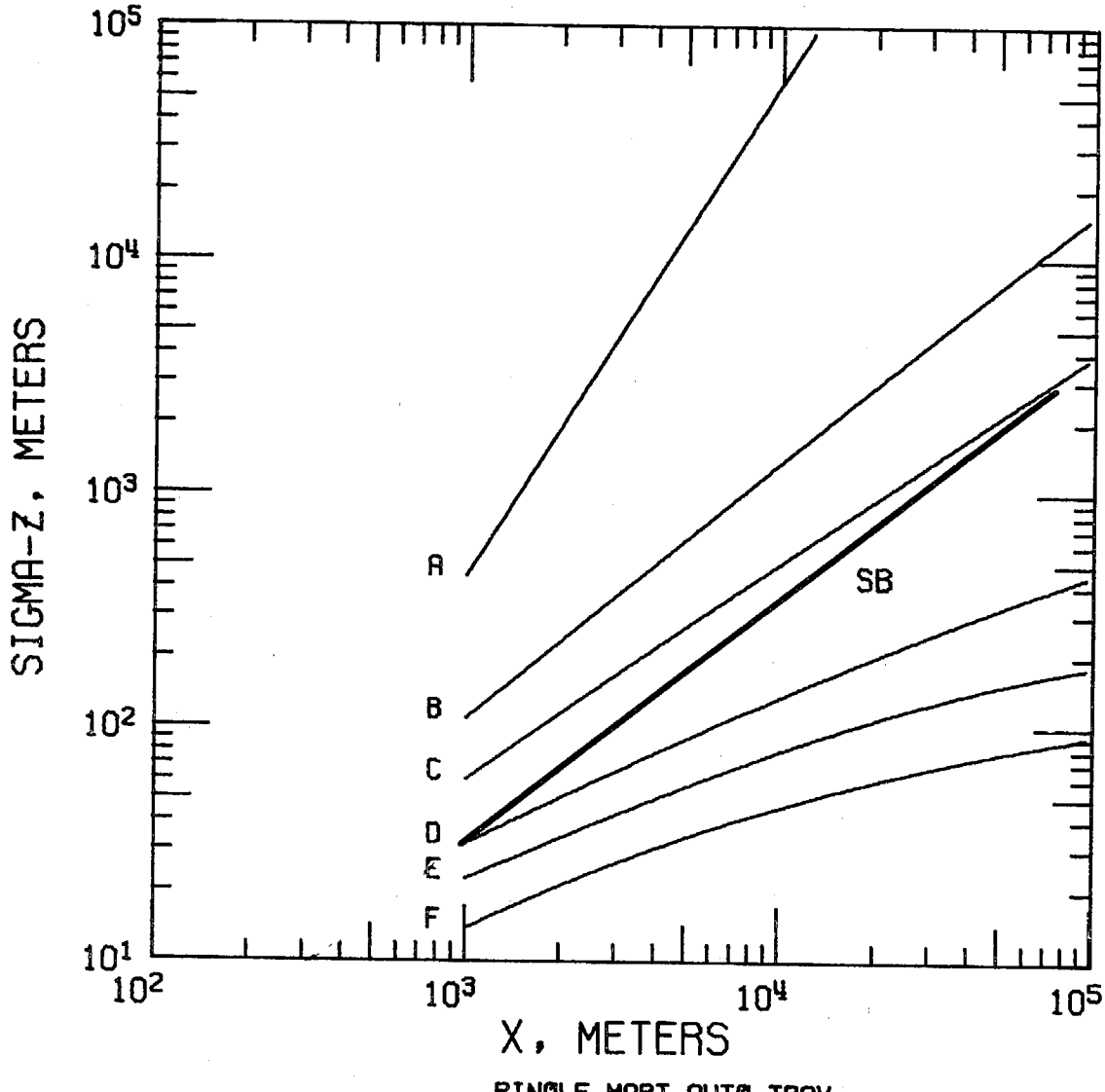

Figure 96. Vertical crosswind dispersion parameter, σ_z, as function of distance downwind for tracer release from Pinole and Martinez during Sea Breeze (SB) conditions, and the vertical dispersion parameter associated with Pasquill atmospheric stability classes.

The vertical dispersion curves for Dow releases are similar to the horizontal curves. Dispersion observed during Sea Breeze conditions is greater than that found during the other meteorological periods. However, for close downwind distances, the vertical dispersion data do not show the very stable nature of the atmospheric found in the horizontal dispersion curves. Under Sea Breeze and Sea Breeze Tail conditions, the vertical dispersion curves are approximately parallel to the curves associated with the Pasquill stability classes. Data obtained during the Nighttime period indicate that vertical dispersion is almost independent of the transport distance.

If one assumes that horizontal dispersion is only a function of changes in the horizontal wind field and vertical dispersion is only a function of the turbulent vertical heat exchange between the land and the atmosphere, then it appears that the dispersion processes near the Dow site are governed by a balance between the abnormally strong and steady winds and a relatively classical air-ground heat transfer. During the Sea Breeze period, the vertical mixing associated with the afternoon heating of the ground overrides the stabilizing effects of the steady winds. Stability conditions near the Dow site are reasonably close to those expected from insolation considerations. At other times, when the effects of heating are smaller, horizontal dispersion is sharply limited because of the steadiness and strength of the winds. However, during Sea Breeze Tail conditions when the land is cooling from the afternoon sun, vertical dispersion follows the classical Pasquill pattern. At night when wind speeds increase, horizontal and vertical dispersion near Dow are both very limited.

The dispersion data associated with the Pinole and Martinez tracer tests indicate that horizontal and vertical dispersion increased with distance at rates greater than those for Pasquill stability classes. This is similar to the pattern observed in the data obtained during the Dow releases. The horizontal dispersion curves obtained from Pre-Sea Breeze data is very similar to the curve derived from the Sea Breeze data. Both curves lie in the range of stability which was assumed to exist during the tests. The vertical dispersion curve indicates that conditions were one Pasquill class more stable than those predicted from the meteorology. It appears that strong and steady winds moving through the Carquinez Strait created a more stable atmosphere near the release points than was assumed to exist.

In summary, this analysis of the observed dispersion of the tracer indicates that the strong winds measured during the tracer tests generally cause horizontal dispersion to be limited near the release point. During the daytime, vertical dispersion follows the classical Pasquill dispersion curves; at night, vertical dispersion appears to be independent of downwind distance. The available data for Pinole and Martinez releases yield results which are similar to the results of the Dow dispersion analysis. At downwind distances of 50 km, the extent of horizontal dispersion under all periods approaches or exceeds that predicted from the meteorology using Pasquill stability classes.

It is very important to realize that these results are based on eight tracer tests covering a two-week period in September. We do not imply in

this section that these results are necessarily representative of typical or worst case meteorological conditions. However, as we noted in the description of the tracer tests, the wind patterns observed during the field study were generally similar to those which occurred most frequently according to Smalley (1957). Mixing depth patterns were similar to those attributed to typical conditions by Miller (1968). A more complete discussion of typical and worst case conditions which occur in the Delta region is presented in the MRI report concerning the field study.